TRIBOLOGY OF ORGANIC SELF-ASSEMBLED MONOLAYERS (SAMs) AND THIN-FILMS ON Si SURFACE

NALAM SATYANARAYANA

NATIONAL UNIVERSITY OF SINGAPORE

2007

TRIBOLOGY OF ORGANIC SELF-ASSEMBLED MONOLAYERS (SAMs) AND THIN-FILMS ON Si SURFACE

NALAM SATYANARAYANA
(*B. Tech, NIT, Warangal, India*)

A THESIS SUBMITTED

FOR THE DEGREE OF DOCTOR OF PHILOSOPHY

DEPARTMENT OF MECHANICAL ENGINEERING

NATIONAL UNIVERSITY OF SINGAPORE

2007

Preamble

This thesis is submitted for the degree of Doctor of Philosophy in the Department of Mechanical Engineering, National University of Singapore under the supervision of Dr. Sujeet Kumar Sinha. No part of this thesis has been submitted for any degree or diploma at any other Universities or Institution. As far as the author is aware, all work in this thesis is original unless reference is made to other work. Part of this thesis has been published/accepted and under review for publication as listed below:

Book Chapters

1) N. Satyanarayana, S. K. Sinha and M. P. Srinivasan, "Friction and wear life evaluation of silane-based self-assembled monolayers on silicon surface", *"**Life Cycle Tribology**" (**Editors: D. Dowson, M. Priest, G. Dalmaz and A. A. Lubrecht**), Tribology and Interface Engineering Series, No. 48, Elsevier Publishers, 2004, P. No. 821-826 (a part of Chapter 4)***.**

2) N. Satyanarayana, S. K. Sinha and M. P. Srinivasan, "Tribology of ultra-thin self-assembled films on Si: the role of PFPE as a top mobile layer" in a book titled, *"**The Role of Surfactants in Tribology**" (**Editors: G. Biresaw and K. L. Mittal**), Marcel Dekker publishers, USA*, in press (*Chapter 4*).

3) N. Satyanarayana and S. K. Sinha, "Tribology of ultra-thin polymer coatings on Si surface", ***"Polymer Tribology" (Editors: S. K. Sinha and B. J. Briscoe)***, Imperial College Press, London, 2007, to be submitted.

Patent

1) "Ultrahigh-molecular-weight polyolefin-based coatings with good wear resistance" A USA patent application filed on 3rd June 2006 (with S. K. Sinha, S. C. Lim and B. H. Ong), PCT Int. Appl. (2006), WO 2006130118 A1 20061207.

Journal Articles

1) N. Satyanarayana and S. K. Sinha, "Tribology of PFPE overcoated self-assembled monolayers deposited on Si surface", ***Journal of Physics D: Applied Physics 38 (2005) 3512-3522*** *(a part of Chapter 4).*

2) N. Satyanarayana, S. K. Sinha and B. H. Ong, "Tribology of a novel UHMWPE/PFPE dual-film coated onto Si surface", ***Sensors and Actuators A: Physical 128 (2006) 98-108*** *(a part of Chapter 5).*

3) N. Satyanarayana, N. N. Gosvami, S. K. Sinha, and M. P. Srinivasan, "Friction, adhesion and wear durability studies of ultra-thin PFPE overcoated 3-Glycidoxypropyltrimethoxy silane SAM coated on Si surface", ***Philosophical Magazine 87 (2007) 1-19*** *(a part of Chapter 4).*

4) N. Satyanarayana, K. S. K. Rajan, S. K. Sinha and L. Shen, "Carbon nanotube reinforced polyimide thin film for high wear resistance", ***Tribology Letters, 27 (2007) 181-188*** *(Chapter 6).*

5) N. Satyanarayana, S. K. Sinha and L. Shen, "Effect of molecular structure on friction and wear of polymer thin films deposited on Si surface", ***Tribology Letters, 28 (2007) 71-80*** *(Chapter 7).*

6) N. Satyanarayana, L.H. Goh, M. Minn and S. K. Sinha, "The effect of normal load and sliding velocity on the friction and wear of UHMWPE film on Si surface", to be submitted *(a part of Chapter 5)*.

Conference Papers (Peer Reviewed)

1) N. Satyanarayana and S. K. Sinha, "Tribology of PFPE overcoated self-assembled monolayers deposited on silicon surface: Effect of thermal treatment", ***WTC2005-64067, Proceedings of WTC 2005, World Tribology Congress III, Washington D.C., USA*.**

2) N. Satyanarayana and S. K. Sinha, "Tribology of ultra-thin polymer films covalently bonded to silicon surface: Effect of molecular structure", ***IJTC2007-44236, Proceedings of STLE/ASME International Joint Tribology Conference, IJTC2007, October 22-24, 2007, San Diego, California, USA***.

Conference Oral Presentations

1) N. Satyanarayana, C. C. Hing and S. K. Sinha, "Effect of bonding strength of self-assembled monolayers with Si substrate on wear resistance", ***Proceedings of the Nano Sikkim 2: Friction and Biotribology, International Conference conducted by International Nanotribology Forum (INF), 8th to 12th Nov '2004, India, Abstract Number: O-10.***

2) N. Satyanarayana and S. K. Sinha, "Enhancing tribological properties of self-assembled monolayers on silicon surface with the dip-coating of PFPE", ***Proceedings of the 1st International Conference in Advanced Tribology (iCAT), Singapore 1st-3rd Dec'2004, pp. B.24.***

3) N. Satyanarayana, H. C. Chen and S. K. Sinha, "Influence of bonding type of self-assembled monolayers with silicon substrate on tribological properties", ***Proceedings of the 1st International Conference in Advanced Tribology (iCAT), Singapore 1st-3rd Dec'2004, pp. B.25.***

4) N. Satyanarayana, N. N. Gosvami and S. K. Sinha "Micro- and Macro scale Tribological Properties of PFPE modified Self-assembled monolayers on Si surface", ***Proceedings of the International Conference on Materials for Advanced Technologies 2005 (ICMAT 2005), 3-8 July 2005, Singapore, Abstract Number: E-9-OR41.***

5) N. Satyanarayana and S. K. Sinha, "Effects of molecular structure on the tribological characteristics of polymer films covalently bonded to silicon surface", ***International Conference on Industrial Tribology (ICIT-2006), Bangalore, India, Nov 30-Dec 2, 2006, Abstract number: OS03-6.***

Conference Poster Presentations

1) N. Satyanarayana and S. K. Sinha, "Tribology of PFPE overcoated self-assembled monolayers deposited on silicon surface: Effect of thermal treatment", ***WTC2005-64067, World Tribology Congress III, Washington D.C., 12-16 Sep'2005, USA***

Acknowledgements

This dissertation would not have been completed without the contribution of many individuals, to whom I am deeply indebted. First, I would like to express my sincere gratitude to my supervisor, Dr. Sujeet Kumar Sinha, for giving me an opportunity to work with him as well as for his priceless guidance, encouragement and support through out my PhD. He has always been available whenever I needed any sort of help and many thanks for that. I would also like to express my gratitude to Assoc. Prof. M. P. Srinivasan for his guidance and advise regarding the deposition and characterization of organic thin films. I benefited a great deal through discussions with him and his team members (Zhigang, Feng Xiang and Puniredd). I also like to express my sincere thanks to Prof. Seh Chun Lim for his direct and indirect help in many aspects for the completion of my PhD.

I am grateful to the Material Science Lab staff, Mr. Thomas Tan Bah Chee, Mr. Abdul Khalim Bin Abdul, Mr. Ng Hong Wei, Mrs. Zhong Xiang Li, Mr. Maung Aye Thein and Mr. Juraimi Bin Madon for their support and assistance for many experiments. I am also grateful for the help provided by the staff in other labs and in particular Nano-Bioengineering (Ms. Satin), Nano-Biomechanics (Ms. Eunice and Mr. Hairul), Manufacturing Lab, Workshop and Chemical Engineering Labs (Dr. Yuan and Ms. Sam). I would like to thank Ms. Shen Lu of A*-STAR IMRE, Singapore for her help in getting access to Nano Indenter XP and conducting several tests.

I would like to thank all my colleagues in the lab for their numerous helps and friendship (Nitya, Minn, Robin, Sharon, Eugene, Chwee Sim, Murali, Hassan, Kong Boon, Sandar and many others). I would like to thank all my friends Srinu, Sekhar,

Mohan, Subhash, Ugandhar, Pardha, Rajan, Dr. Bharath and Dr. Venugopal and many others for their numerous helps and constant support. I also would like to thank all Brahma Kumaris and Brahma Kumars in Singapore Raja Yoga Center for their causeless love, support and blessings.

Finally, I want to thank my family for their support and encouragement, and most of all, my wife, Latha, for having courage, patience and stamina to live through a virtual reality marriage for the past 4 years, and raising one wonderful son (Uday) in my virtual absence. No words are sufficient to express my gratitude and thanks for her support and understanding.

Last but not least I would like to dedicate this dissertation to almighty GOD, point of light, SHIVA.

Table of Contents

Summary

Silicon (Si), which is an important structural material for many microsystems (such as micro-electromechanical systems or MEMS), suffers from several surface related tribological issues such as high friction, adhesion and wear during sliding and occasional contacts. Currently, tribology related failures are the main limitations in the development of high life-cycle microsystems. Bare Si surface (without suitable modification) shows high coefficient of friction (0.5-0.6) and generates wear particles within few cycles of sliding. The reasons for this behavior are the hydrophilic nature of its surface and brittleness of the silicon oxide layer which is inevitably present on Si. Apart from its poor tribological performance, Si is a popular material for microsystems (or MEMS) applications because of its high strength, low residual stress and matured fabrication technologies to produce micro-components. Therefore, it is very essential to improve the tribological performance of Si in view of increasing demand for new technologies (MEMS, NEMS and nanotechnology applications). Hence, in this thesis, we propose and investigate low friction and wear-resistant coatings based on organic SAMs and polymeric films for Si surface.

Mainly two approaches are explored: (1) overcoating an ultra-thin layer of perfluoropolyether (PFPE) onto different self-assembled monolayers (SAMs); (2) development of polymer thin-films with enhanced tribological properties. The composite SAM/PFPE layer has demonstrated very high wear life on the Si surface in sliding contact compared to traditionally used only SAM coating. It is shown that PFPE, which forms nano-scale liquid-like layer, provides essential lubrication and works better with a hydrophilic SAM (such as 3-aminopropyltrimethoxysilane (APTMS) or 3-

glycidoxypropyltrimethoxysilane (epoxy SAM)). Further in this research, coating procedure has been developed for the deposition of a novel ultra-thin film (with exceptional wear-durability) of ultra-high molecular weight polyethylene (UHMWPE) on Si surface. The presently developed highly hydrophobic UHMWPE film has demonstrated low coefficient of friction and very high wear durability. Overcoating of PFPE onto UHMWPE film further enhanced the wear life of pristine UHMWPE film. It has also been demonstrated that the addition of filler materials such as CNTs shows excellent improvement in the wear-durability when they are added to the polymer films. We further elucidate the effect of molecular structure of the polymer film on the friction and wear and have shown that the polymer film with linear molecular structure shows low friction and high wear durability than those containing bulky side groups. The mechanisms responsible for high wear-durability of selected films are explained from their microstructure, chemical, physical and mechanical properties.

List of Tables

List of Figures

List of Notations

AFM: Atomic force microscopy

APTMS: 3-Aminopropyltrimethoxysilane

CNT : Carbon nano tube

CSM: Continuous Stiffness Measurement

Epoxy SAM: 3-Glycidoxypropyltrimethoxysilane

FDTS: 1H, 1H, 2H, 2H-perfluorodecyltrichlorosilane

FE-SEM: Field Emission- Scanning Electron Spectroscopy

FTIR: Fourier Transform- Infrared Spectroscopy

HDPE: High density polyethylene

L-B: Langmuir-Blodgett method

LDPE: Low density polyethylene

LFM: Lateral Force Microscopy

LIGA: A German acronym for lithography, electroplating and molding

MEMS: Micro-electro-mechanical systems

MPa: Mega Pascal

MWCNT: Multi walled CNT

NEMS: Nano-electro-mechanical systems

NMP: N-methyl 1, 2- pyrrolidone

OTS: Octadecyltrichlorosilane

PAA: Polyamic acid

PDMS: Polydimethylsiloxane

PE: Polyethylene

PEEK: Poly ether ether ketone

PEMs: Polyelectrolyte multilayers

PFPE: Perfluoropolyether

PI: Polyimide

PMMA: Polymethylmethacrylate

PS: Polystyrene

PTFE: Polytetrafluoroethylene

RMS- Root mean square roughness

SAM: Self-assembled monolayer

SEM/EDS: Scanning Electron Microscope equipped with X-ray Energy Dispersion Spectroscopy

Si_3N_4: Silicon nitride

SFA: Scanning Force Apparatus

SWCNT: Single walled CNT

ToF-SIMS: Time of Flight-Secondary Ion Mass Spectroscopy

UHMWPE: Ultra-high-molecular-weight polyethylene

XPS: X-ray photoelectron spectroscopy

Chapter 1

INTRODUCTION

1.1 History of Tribology and its significance to Industry

Tribology is defined as the study of friction, wear and lubrication. It is the science and technology of two interacting surfaces in relative motion, in a given environment. Friction and wear are often undesirable (though they are essential and helpful in few applications) phenomena resulting from sliding and rolling surface contacts. Friction is defined as the resistance offered to the sliding while wear is defined as the surface material removal phenomenon. Low friction and low wear are desirable, in many applications, to increase the life or durability of components in relative motion. The word "tribology" was derived from the Greek word "tribos" meaning rubbing. Even though the term "tribology" is new, its applications spans a period similar to that of recorded history [Dowson 1998].

The realization of tribology dates back to 3500 BC when the wheel was invented to reduce friction in translationary motion. The Egyptians in 1880 BC used sledges to transport large statues and used water to lubricate the sledges. Leonardo da Vinci (1452-1519), was the first to state that the coefficient of friction is the ratio of friction force to normal load. Amonton in 1699 experimentally found that the friction force is directly proportional to the normal load and is independent of the apparent area of contact. These two observations are popularly known as Amonton's laws of friction. A third law stated as, the friction force is independent of velocity for ordinary sliding speeds, has been experimentally observed and proposed by Charles Augustine Coulomb which is frequently included with those of Amonton's laws.

Tribology has grown over the years as an engineering discipline keeping pace with other technical developments in industrialized world. Today, this area of knowledge is receiving ever-increasing attention due to the fact that machines with greater precision and smaller tolerances are being designed and built, whose performance is critically dependent upon the nature of the surface of interacting components whether in lubricated or dry conditions. Friction and wear are major concerns in practically all modern mechanical machines. A few examples are internal combustion and aircraft engines, automobiles, gears, cams, bearing, and seals. The invention of new characterization techniques such as SFA [Tabor and Winterton 1969 and Israelachvili and Tabor 1972] and AFM/LFM [Binnig et al 1986 and Mate et al 1987] and the advanced technical applications such as magnetic storage devices, MEMS/NEMS, nanotechnology have led to further developments in tribology and opened the doors to the new field of tribology known as micro-tribology/nano-tribology involving the study of friction and wear at very small length scales [Bhushan 1991]. The present thesis has explored the area of micro-tribology in the context of improving the tribological properties (especially friction and wear durability) of Si surface which has large industrial application (for example lubrication for small components used in MEMS).

1.2 Modern Aspects: Nanolubrication

Nanolubrication is the study of ultra-thin lubricants (thickness in the range of few to several nanometers). The applications of nanolubrication include hard-disk drive and MEMS components. The components of these devices need a lubricant layer of few nanometers to reduce friction, stiction (unintentional adhesion of compliant

microstructure surfaces) and wear. Therefore, a part of the present thesis is devoted to the development and testing of several nano-lubricants needed for MEMS components with an aim of investigating the mechanisms responsible for low friction and high wear durability of ultra-thin films. Hence, we will first discuss the lubrication challenges in MEMS components and then present our objectives and methodologies used for the development of nano-lubricants and other films with relatively higher thickness.

1.2.1 Micro electro mechanical systems (MEMS)

MEMS are the machines fabricated by the integration of miniaturized mechanical components with microelectronic components. MEMS extend the benefits of microelectronic fabrication to sensing and actuating functions [Muller et al 1990, Sze 1994, Bryzek et al 1994 and Madou 1997]. Recently, several MEMS devices have been commercialized or are being considered for many commercial products such as accelerometers, gyroscopes, optical switches, medical devices, pressure sensors, digital micro-mirror displays etc [Chau and Sulouff 1998, Bernstein et al 1993, Yeow et al 2001 and Cao et al 2001].

Historically, integrated-circuits (ICs) have been formed from silicon and silicon based materials. As a consequence, polycrystalline silicon is the most commonly used structural material for MEMS today. Though silicon is a good structural material for the micron-scale [Petersen 1982] the inherent mechanical design of MEMS devices brings a new level of complexity to their production and reliability compared to standard integrated circuits. Various micro-fabrication techniques such as bulk as well as surface micromachining and LIGA (a German acronym for lithography, electroplating and

molding) are used to produce the MEMS components [Madou 1997]. Surface micromachining is the most common method for MEMS fabrications which involves the deposition, patterning and etching of thin films [Howe 1988 and Muller 1990]. Surface micromachining allows for the production of sophisticated microstructures with parallel fabrication and high fabrication yield.

1.2.2 Reliability Issues in MEMS

Though MEMS are becoming commercially attractive through the development of the technologies such as LIGA, surface and bulk micromachining, there are a number of reliability issues that need to be addressed. The devices must be tested for reliable operation in a variety of environments before commercialization. We briefly provide an overview of major reliability issues in MEMS.

1.2.2.1 Stiction

Stiction is defined as the unintentional adhesion of compliant microstructure surfaces when restoring forces are unable to overcome interfacial forces (such as capillary, chemical, van der Waals and electrostatic attractions). The surface and interfacial forces play an important role because of the large surface-to-volume ratio and microscopic length scale of MEMS components [Mastrangelo 1997, Tas et al 1996, Rymuza 1999, Maboudian 1998, Maboudian and Howe 1997, Komvopoulos 1996, Bhushan 1998 and de Boer and Mayer 2001].

In the context of MEMS, stiction is primarily of two types: (1) release stiction and (2) in-use stiction. The adhesion of surface-micromachined structures to the underlying

substrate after the final sacrificial layer etch is called release stiction and it is caused primarily by liquid capillary forces. Various successful methods which have reduced the release stiction are texturing the surfaces to reduce contact area [Alley et al 1993], changing the water meniscus shape [Abe et al 1995], use of a supercritical fluid [Mulhern et al 1993 and Dyck et al 1996], freeze sublimation drying [Guckel et al 1990], polymer support [Webb 2005, Wallace et al 1996 and Mastrangelo 1997] and other dry-release methods [Mastrangelo and Saloka 1993, Orpana and Korhonen 1991, Kozlowski et al 1995, Forsen et al 2004, Miller et al 1996 and Suh et al 2005]. In-use stiction is the permanent adhesion of two surfaces during operation or storage and it may eventually lead to device failure. Microstructure surfaces may come into contact intentionally in applications where surfaces impact or shear against each other or unintentionally through acceleration or electrostatic forces. In-use stiction can be reduced by either physical and/or chemical modifications of surfaces. In the case of physical modification approach, the surfaces are roughened to reduce the effective contact areas [Komvopoulos 1996 and Alley et al 1993] whereas chemical modification approach includes, deposition of fluorocarbon films [Mastrangelo 1997 and Man et al 1997], treating Si surface with NH_4F or HF to create hydrophobic, non-polar Si-H bonds [Houston et al 1995 and 1997], deposition of self-assembled monolayers (SAMs) [Srinivasan et al 1998 (a)] etc.

Surface forces play an important role in MEMS because of the small length scale involved and virtually every type of MEMS device is susceptible to either release or in-use stiction.

1.2.2.2 Wear

Wear occurs due to the movement of one surface over another and is defined as the removal of material from a solid surface by some kind of mechanical action. In high shear locations, micromachines can suffer from substantial wear, in addition to stiction problems [Tanner et al 1999 (a), Williams 2001, Wang et al 2002, Senft and Dugger 1997]. Even though Si is a good structural material for the microscale (because of its high Young's modulus and low density), it is not a good tribological material because it shows high adhesion, stiction and wear without suitable surface modification [Gardos 1998]. Because of small contact areas even moderate actuation forces cause wear when contacting surfaces undergo sliding because of the generation of enormous contact pressures. For example, the hubs on microgears have shown wear debris after about few hundred thousand cycles [Tanner et al 1999].

Unlike stiction, the mechanism for wear in microdevices is not very well understood. Few studies have been found involving the characterization of wear in MEMS components, which are presented here. Flater et al [2006] have carried out the friction and wear studies using a polycrystalline silicon nanotractor device which simulates the actual MEMS interface. They found that the nanotractor device fails through interfacial seizure due to wear processes at the sliding interface and have not commented on the wear mechanism. They also identified that the surface roughness does not strongly affect wear properties. This study has also identified that a monolayer coating of (tridecafluoro-1,1,2,2-tetrahydrooctyl) tris (dimethylamino)-silane ($CF_3(CF_2)_5Si(N(CH_3)_2)_3$) has shown certain improvement in the wear resistance of MEMS surface. Eapen et al [2006] have carried out wear studies of MEMS electrostatic

motors, both in air and vacuum with and without lubrication films (hydrocarbon layers). Their main focus was to understand the wear mechanism in vacuum in comparison with that in air. Basically, the MEMS (modified and unmodified) have shown low wear life in vacuum than in air and there are many differences in the morphology of wear debris (of size ~1-10 μm) generated while the amount of wear debris depends on the specific lubricants used. The wear debris generated in air are in the form of long cylindrical rolls which acted like bearings and reduced friction and wear (humid air led to the formation of long cylindrical rolls due to the oxidation of Si grains (debris) generated), whereas those generated in vacuum are in the form of agglomerates of platelets which led to further wear due to their abrasive nature. Finally, this study has suggested that the wear mechanisms are different in air and in vacuum and hence the lives of the components are also different. Tanner et al [1999 (a)] have carried out experiments on surface micromachined microengines driving load to determine the fundamental relation between the operational drive frequency (microengine speed) and the life time of the microengine and associated wear mechanisms. They reported that the life cycles of the microengine depend on the frequency (linear relation), and, the primary wear process involves a combination of mechanisms; the initial wear particles result from surface degradation and adhesion and these trapped wear particles cause abrasive wear by third body wear process. Tanner et al [1999 (b)] further studied the relation between the environmental humidity and the life time of the micro engine. They identified that humidity was a strong factor in the wear of rubbing surfaces in polysilicon micromachines. They showed that the volume of wear debris generated was a function of the humidity; low humidity led to

high wear volume. The surface hydroxides formed at higher humidity levels acted as a lubricant and hence reduced the wear.

All of the above studies conclude that the primary mechanisms of wear in MEMS are adhesion (one surface pulling sections of another due to surface bonding), abrasion, corrosion and surface fatigue. Further, wear depends on the environmental conditions that the device experiences during storage and service as well as the details of the mechanical contacts. The wear resistance of the MEMS has been improved to some extent by the use of SAMs. Recently, some hard coatings such as Al_2O_3 and TiO_2 formed by atomic layer deposition were proposed as wear resistant coatings for MEMS, but they may face additional challenges from process integration. Therefore, further research is needed to develop wear resistant coatings that can be deposited using economical processes which are compatible with MEMS processing techniques.

The present section where we explained the reliability issues in MEMS is closed with a popular quotation made by (late) Professor David Tabor from Cambridge University: “God made solids, but the surfaces are the work of the devil”, which clearly explains the complexity of the surfaces and their critical role in tribology.

1.3 Research objectives

The objectives of the present thesis can be summarized as the development of ultra-thin films (SAMs and polymer thin films of composite and hybrid nature) on Si surface (with the aim of low friction and high wear durability) and the evaluation of their tribological properties. The underlying goal of all the studies presented here is to identify the mechanisms responsible for good tribological properties (especially wear durability)

of organic ultra-thin films which may be helpful in the development of new lubricants for Si based micro-components.

1.4 Research Methodology in the present thesis

To accomplish the above-mentioned objectives, we have carried out deposition of several organic ultra-thin films (SAMs and polymer films) and evaluated their tribological properties. In the SAMs area, we have developed a method of overcoating them with PFPE which has greatly enhanced the wear durability of SAMs. In the polymer films area, we have developed a novel method to obtain ultra-thin layers of UHMWPE which have shown exceptional wear durability when overcoated with PFPE. We also investigated the influence of the addition of CNT as a filler material to the polymer film which has helped to increase the wear durability. Finally, in a specific study, we have studied the effects of the molecular structures of the polymers on the wear durability of their films.

As an introduction, the whole work in this research is explained below with brief motivation while the corresponding results and discussion will be explained in detail in the coming chapters:

- *Tribological properties of PFPE overcoated SAMs*

In this part, we aim to investigate the effect of overcoating an ultra-thin film of PFPE on various SAMs (self-assembled monolayers) (both polar and non-polar SAMs). The tribological properties such as coefficient of friction and wear durability are investigated.

Many SAMs can reduce coefficient of friction and stiction to great extents, but the wear resistance achieved by these monomolecular layers is not sufficient to provide long life to the high velocity moving MEMS components [deBoer and Mayer 2001]. These monolayers do not demonstrate high wear durability either because there is no mobile portion of the lubricant or because of some molecular properties which are not well understood. Once wear initiates, the molecules are easily removed from the contact area and there is no replenishment in these layers due to the solid nature of the SAM molecules. Therefore, we propose the concept of PFPE (bound+mobile) overcoating onto SAMs (bonded) coated Si as a means to enhance the wear durability [Satyanarayana and Sinha 2005, Satyanarayana et al 2007 (a)]. We hypothesize that the mobile PFPE helps in the lubrication of the contact and replenishment into the worn regions and hence enhances the wear durability considerably.

- *Tribology of a novel UHMWPE/PFPE dual-film coated onto Si surface*

The aim of this approach is to provide ultra-thin coating of a polymer (UHMWPE) on Si surface by a simple dip-coating process and to evaluate its tribological properties. Some polymers (for example UHMWPE) are highly wear resistant in bulk form, however their films have rarely been tried due to the difficulty in coating them on to a substrate. Further, the mechanism of enhancing the wear durability of UHMWPE film by overcoating with an ultra-thin layer of PFPE is presented.

- *Carbon Nanotube Reinforced Polyimide Thin-Film for High Wear Durability*

The motivation for this study is the aim of enhancing the wear durability of a particular polymer thin film by introducing fillers. It has been identified in our literature study that the addition of filler materials such as short carbon fiber, graphite, PTFE,

MoS_2, CNTs, nano-particles (such as nano-TiO_2 particles) etc effectively reduces the wear of bulk polymers (both thermoplastic and thermoset polymers) [Friedrich et al 2002, Zoo et al 2004 and Cai et al 2004]. Therefore, it is important to study the effect of the addition of filler materials to a polymer film on its wear durability characteristics. Hence, we have selected SWCNT as a potential filler material for PI (polyimide) film on Si to enhance its wear durability.

- *Influence of molecular structure of the polymer films (covalently bonded to Si surface) on their tribological properties*

We focused on the study of the effect of molecular structure of the polymer films (which are covalently bonded to Si surface) on their tribological properties, an understanding of which, we believe, will have implications in the area of tribology of polymer thin films. To accomplish this objective, we selected two polymer films: PE and PS which are covalently bonded to Si surface through a reactive SAM (APTMS) which acts as an intermediate layer. The PE molecule has linear chain with C_2H_4 groups connected to each other whereas the PS molecule has similar backbone structure as that of PE but contains bulky benzene groups in place of one of hydrogen. Therefore the objective of the present study is to investigate the effect of having a bulky benzene group at the side of the linear chain on tribological properties (especially friction and wear durability).

1.5 Structure of the thesis

The present thesis consists of a total of eight chapters. The literature survey involving the developments in ultra-thin film lubrication is explained in Chapter 2. All

experimental characterization techniques used in the present thesis (physical, chemical, mechanical and tribological) are explained in Chapter 3. Chapter 4 consists of the results and discussion on PFPE overcoated SAMs where we will demonstrate how an ultra-thin layer of PFPE greatly enhanced the wear durability of SAMs. The development of the coating procedure for a novel UHMWPE film and its tribological properties are discussed in Chapter 5. The effect of the addition of SWCNTs to PI on its tribological properties is explained in Chapter 6. Chapter 7 consists of the results and discussion on the study involving the influence of molecular structure of the polymer films (covalently bonded to Si surface) on their tribological properties. Finally, the thesis will close with brief summary and final specific conclusions (Chapter 8) with some suggestions for future work (Chapter 9).

Chapter 2

Literature Review

2.1 Self-assembled monolayers (SAMs)

SAMs are defined as the ordered molecular assemblies that are formed spontaneously by the adsorption of a surfactant with a specific affinity of its head group to a substrate [Ulman 1991]. They are usually prepared from solution, although some systems can be prepared from vapor as well. Both preparation routes, i.e. from solution and vapor, allow for coating of arbitrary shape and are not restricted to only planar geometries. Figure 2.1 is a schematic diagram, showing various constituents of a SAM molecule (head group, chain and surface terminal group).

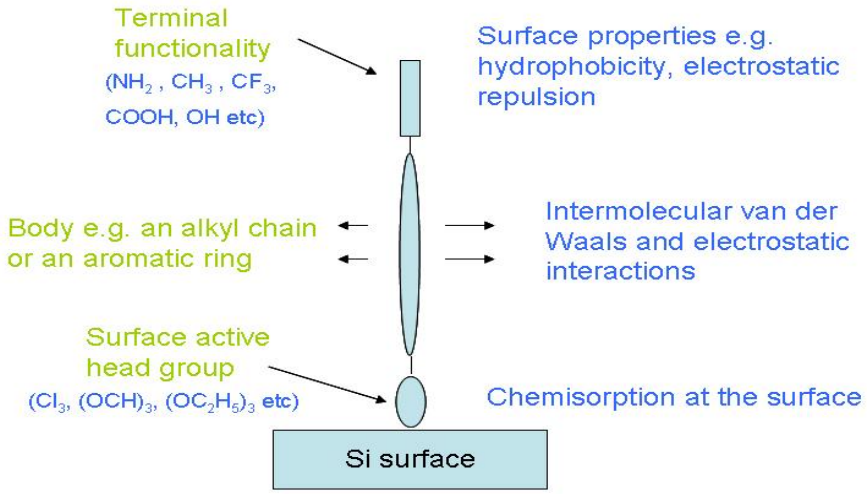

***Figure 2.1**: Representation of various parts of the SAM molecule and their primary functions with some examples of surface active head groups and terminal functional groups.*

As sketched in Figure 2.1, SAMs consist of three building blocks: a head group that binds strongly to a substrate by covalent bond, a surface terminal (tail) group that constitutes the outer surface of the film, and a spacer chain (body or backbone chain) that connects

the head and the surface terminal groups. The two essential requirements of a SAM to control hydrophobicity, adhesion, friction and wear are good adhesion to the substrate and a non-polar terminal group [Satyanarayana et al 2004 (b) and Satyanarayana and Sinha 2005]. For strong adhesion/attachment of the SAM molecules to the substrate, the head group of the molecular chain should contain a polar end group, which must form chemical bonds with the specific surface chemical functionalities. Moreover, molecular structure and any crosslinking would have significant influence on the friction and wear phenomena. Prior to the SAM deposition, the substrate surface should have high surface energy (hydrophilic) so that there will be a strong tendency for molecules to adsorb onto the surface. To achieve strong bonding between the organic molecules and the substrate surface, the surface should be highly functional with polar groups (such as hydroxyl groups) and dangling bonds (generally unpaired electrons). The interactions between the molecular chains are van der Waals or electrostatic type with energies in the order of <10 kcal/mol. In practice, the SAM molecules are not perpendicular to the substrate and they are tilted at an angle to the surface and the tilt angle depends on various factors such as head group, substrate and spacer group. For example, alkane-thiolates adsorbed on Au shows a tilt angle of 30-35^{o} to the surface normal [Ulman 1996].

SAMs are usually produced by immersing a substrate in a solution containing a precursor that is reactive to the substrate surface, or by exposing the substrate to a vapor of the reactive chemical species [Ulman 1991]. Figure 2.2 shows a typical procedure involved in the formation of SAMs from solution. For simplification, the molecules are shown as vertically aligned but they may align with some tilt angle as explained above.

The spacer chain of SAM is mostly alkyl chain ($-C_nH_{2n+1}$), or made of a derivatized alkyl group (for example aromatic groups).

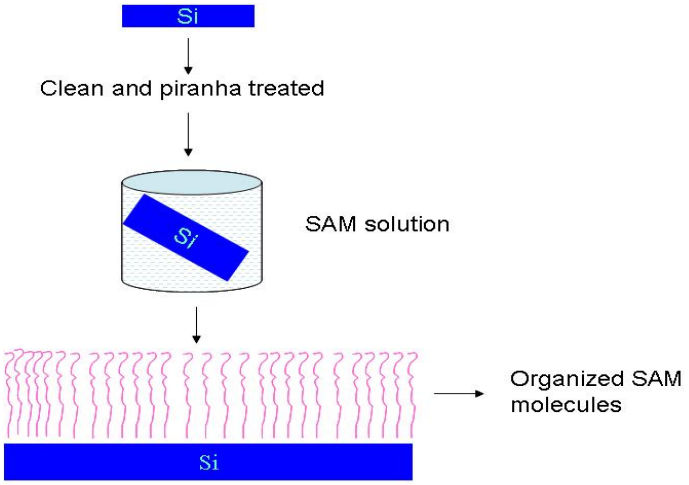

***Figure 2.2**: The procedure involved in the formation of self-assembled monolayers.*

By having different terminal groups at the surface, the film surface may be made to attract (hydrophilic) or repel (hydrophobic) water molecules. A non-polar methyl ($-CH_3$) or trifluoromethyl ($-CF_3$) group is commonly used for a hydrophobic film to achieve low surface energy. For a hydrophilic film, the commonly used surface terminal groups are alcohol (-OH) or carboxylic acid (-COOH) groups. The most commonly used surface active head groups are thiol (-SH), silane (e.g. trichlorosilane $-SiCl_3$), and carboxyl groups (-COOH). The substrates routinely used are gold, silver, platinum, steel, copper, hydroxylated surfaces of SiO_2 or Si, Al_2O_3 on Al, glass and hydrogen terminated single crystal Si (H-Si). Hydroxylation of oxide surfaces is important to make them hydrophilic. The hydroxylation of bulk Si, poly-Si or SiO_2 film surfaces may be done by treating them with a piranha solution (a mixture of, by volume, 70% H_2SO_4 and 30% H_2O_2) at 60-80^oC for 30-60 min. The thickness of a particular SAM film can be controlled by varying the

length of the hydrocarbon chain. For individual organic molecules to pack together and provide a better ordering, a substrate for a given SAM molecule should be selected such that the cross sectional diameter of the spacer chains of the molecule is equal to or smaller than the distance between the anchor groups attached to the surface [Bhushan 2004 (a)].

Many literatures have been reported on SAMs. The two important SAMs which have been extensively studied are alkyl-silane SAMs on Si [DePalma and Tillman 1989, Ruhe et al 1993, Srinivasan et al 1998 (a), Cha and Kim 2001, Ren et al 2002, Sung et al 2003] and alkyl-thiol SAMs on Au [Lio et al 1997, Bhushan and Liu 2001 and Liu et al 2001 (a)].

2.2 Polymer Films on Solid Surfaces

2.2.1 Introduction

The properties of the objects can be dramatically improved by the application of thin coatings to the surface of materials as they allow control of the interaction of a material with its environment. The beneficial usages of thin coatings have been known to the man for several thousand years. Approximately 7000 years ago lacquer (generated from tree sap) was used as a protective coating for wooden objects in China. Lacquers and varnishes have been applied to homes and ships for decoration and as protective measures against adverse environmental conditions by the early Greeks and Romans, as well as the ancient Asian cultures in China, Japan and Korea. In today's industrial applications, the range of coatings extends much beyond the simple decoration and protective aspects, and functional coatings have become an enabling technology in a vast

variety of different high-tech areas such as: computer chips, hard-disk manufacturing, MEMS/NEMS components, biomedical as well as aviation applications.

2.2.2 Polymer Coatings: From First Principles to High-Tech Applications

For a large number of chemical and physical processes, the bulk properties of a material as well as the surface properties (such as micro-structure, composition etc) determine the performance of the entire system. Therefore, coatings consisting of thin organic films are frequently applied to the surfaces of many solids to control their interaction with the environment. Thin polymer films onto a surface can control various interfacial properties such as friction, wear, adhesion, adsorption of molecules from the surrounding environment, or wetting ability with water or other liquids.

Three advanced applications of the ultra-thin polymer layers are explained below to emphasize the importance of developments in this fascinating field of polymer films. First example involves the protection of hard-disk surface by the coating of an ultra-thin polymer layer of perfluoropolyether (PFPE) [Bhushan 1996]. By the application of the PFPE film of 2-4 nm thickness the tribological properties are greatly improved, the wear is reduced, and the mean time to failure of the disk is greatly prolonged. The second application involves the use of ultra-thin polymer layers to reduce the stiction (unwanted adhesion) and wear in the MEMS components. Procedures have been developed to coat ultra-thin polymers such as fluorocarbon based polymers onto MEMs components which reduces stiction and wear. The third application involves the use of few nanometers thick polymer layer onto blood-explosed implant materials or sensors so that the adhesion of the blood cells onto these surfaces can be mitigated.

2.2.3 Surface-coating Techniques

Depending on the type of interactions between the polymer molecules and solid surfaces, coatings can be either physically adsorbed or chemically tethered. These interactions between the polymer molecules and surfaces greatly enhance the performance of these coatings.

Many of technologically important coating techniques rely on the physical interaction between the deposited molecules and the substrate, including [Advincula et al 2004]:

- printing/droplet evaporation
- spray coating
- spin coating
- dip-coating
- doctor blading

A common feature of all the above deposition techniques is that the molecules are adsorbed from solution and solvent evaporates during the coating process. If the deposition conditions are appropriately selected, layers with well-defined thickness and good homogeneity can be obtained without major effort. Some of the above processes such as dip-coating and spin-coating allow the deposition of extremely thin film coatings (starting from just few nanometers thickness), but essentially there is no upper limit to film thickness achievable, if suitable conditions are applied. The above techniques are somewhat empirical in nature as certain parameters are difficult to predict a priori, for example, the evaporation of solvent etc.

More sophisticated techniques involving the polymer films with physical interactions are: Langmuir-Blodgett technique, the adsorption of monomolecular layers of homo- and block copolymers from solution and Layer-by-Layer deposition where multilayer stacks of oppositely charged polyelectrolytes are deposited onto a charged substrate. These techniques have better control of the internal structure of the films and have high precision with regard to the thickness of coatings. With the exception of Langmuir-Blodgett technique, all other techniques do not require any complicated set-up and are quite simple. As the molecules are attached to their substrate by physical interactions, the forces holding them at the surface are rather weak.

Under unfavorable conditions, the physisorbed polymer layers can be subject to destruction by the so called "Big Four Ds" [Advincula et al 2004]:

- desorption during solvent exposure;
- displacement by molecules which have stronger interaction with the surface;
- dewetting (for films above the glass transition temperature);
- delamination (for films below T_g)

Therefore, efforts have been turned towards the development of chemisorbed polymer layers to enlarge the application capabilities of these films. A current technique for the preparation of well-controlled surface layers is the use of small molecules with reactive head group so that chemical bonding between these molecules and the surface can be achieved. The recent development in this field is the formation of polymer "brushes" where the polymer molecules have reactive end groups attached at the end of the chain so that after chemisorption the polymer molecules assemble in the form of brush bristles. As the research is progressing for the development of a variety of films

using this technique, the applications of these films are yet to be tested in several technical fields.

2.3 Tribology of Polymeric Solids

This section reviews the progresses made in the area of friction, wear and lubrication of polymers in their bulk form. The classical theories of friction and wear mechanisms of polymers and their films are summarized.

2.3.1 Introduction

Tribological applications of polymers and their composites have been increasing because of several technical and economical reasons. The polymers have several advantages over other materials such as self-lubricity, light weight, corrosion or oxidations resistance, non-toxic nature and ease with which the near-net shape is manufactured. Despite the listed advantages, there are many challenges for their effective and economic use for some specific tribological applications. For example, low friction does not always necessarily lead to low wear and the wear rate can be extremely high for a slight increase in the contact pressure or sliding speed.

The science and engineering of polymer tribology is still in the process of development whereas the understanding of the polymer film tribology started only very recently. As there are no generalized tribological mechanisms in the case of polymer films, only the friction and wear mechanisms of polymer solids are reviewed here and anticipating that these will be helpful in the understanding of friction and wear processes in the case of polymer films to a large extent. The tribological performances of polymers

depend upon a large number of factors which add complexity and the data must be interpreted very carefully to explain the associated friction and wear mechanisms in a tribological process involving polymers.

2.3.2 The mechanisms of polymer friction

The frictional energy in the case of polymers is dissipated by two major processes [Bowden and Tabor 1986]: (1) the ploughing actions of the asperities of a harder surface and (2) the dissipation in overcoming the adhesive interactions between the two surfaces in the absence of sharp asperities. This two term non-interacting model is well described by the interfacial friction as shown in Figure 2.3. In a particular friction event of a polymer, the surface roughness of the hard counterface and the shear properties of the polymer decide the dominant energy dissipation mechanism.

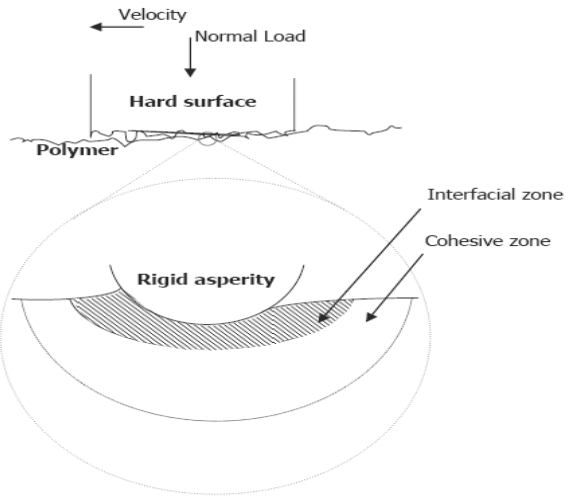

***Figure 2.3**: The two-term model of wear process, reproduced from Briscoe and Sinha [2005], with kind permission from John Wiley & Sons Ltd, UK. The distinction between the cohesive and interfacial wear processes arises from the extent of deformation in the softer material by rigid asperity of the counterface.*

2.3.2.1 The Ploughing Term-Brief Summary

The ploughing component of friction arises from the plastic flow and fracture induced sub-surface deformation depending upon the polymer's mechanical response under the contact conditions. The ploughing component of the friction force has been modeled for elastomers by considering the elastic work done and the fraction which is dissipated. According to this model, the friction force is expressed as a function of the elastic work done [Bowden and Tabor 1986]:

$$F=\beta\varphi \qquad (1)$$

Where β is the fraction of the energy lost in frictional hysteresis work and φ is the elastic work done in deforming the polymer per unit sliding distance. This analytical model has application in scratch deformation, in the computation of scratch hardness, where a conical or a spherical indenter is used to model the asperity interaction. The above analysis which only uses elastic energy loss by hysteresis has a main problem that it significantly underestimates the actual ploughing friction force.

2.3.2.2 The Adhesion Term- Brief Summary

When two bodies are brought close together, the nature and strength of the adhesion forces depends on the electrostatic and van der Waals forces, and, in the presence of polar atoms, on the dipole interactions and hydrogen bonding. All these forces are short range and thus operate at real contact areas. The adhesion associated with static friction and dynamic friction at the interface is related to the shear and deformation of a very thin layer of the polymer which is directly in contact with a counter surface. The

properties of this thin layer evolve during the sliding process due to changes in the interfacial temperature.

In the case of elastomeric polymers, the frictional work is done in moving waves of attachment on the surface of the polymer. This type of behavior involves contact adhesion and de-adhesion (energy loss) as the wave forms forward. These waves are known as Schallamach waves. The visco-elasticity of elastomers and their ability to extend giving large local recoverable strains lead to the above mentioned behavior. In the case of non-elastomeric polymers, the waves of attachment either do not exist or exist at molecular scale which are difficult to detect using a normal optically visualized tribological test. If the strength of the polymer is stronger than the strength of the adhesive forces, true sliding takes place. In such sliding process, the frictional energy is dissipated through the shear of a very thin zone (of few nanometers thickness) of the polymer at the interface. The frictional energy dissipation mainly takes place either in the transfer film (which may be deposited on the smooth counterface) or in a very thin layer of the polymer which is in direct contact with the counter surface.

The shear strength of the shearing layer at constant velocity and temperature is related to the contact pressure, p as [Briscoe and Evans 1982]:

$$\tau = \tau_o + \alpha p \qquad (2)$$

where τ_o and α are constants. As the frictional force is the product of the shear strength of the interface and the real area of contact, Equation (2) can be written as

$$\mu_a = \tau_o/p + \alpha \qquad (3)$$

In equation (3), as the pressure increases for higher load conditions, the first term on the right-hand side becomes very small and hence Equation (3) may be further approximated as

$$\mu_a \sim \alpha \qquad (4)$$

2.3.3 Wear

2.3.3.1 Semantics and Rationalizations

As stated in the Introduction chapter, wear is defined as the removal of material from a solid surface by some kind of mechanical action and it is measured in terms of the mass, or volume, loss from a moving or eroding contact. Several events such as mechanical forces, frictional work, impact forces, cavitation forces etc induce damage in the contact members. As a result of these events (some or all) the surfaces lose mechanical cohesion and debris is produced.

The wear of polymers can be classified as shown in Figure 2.4.

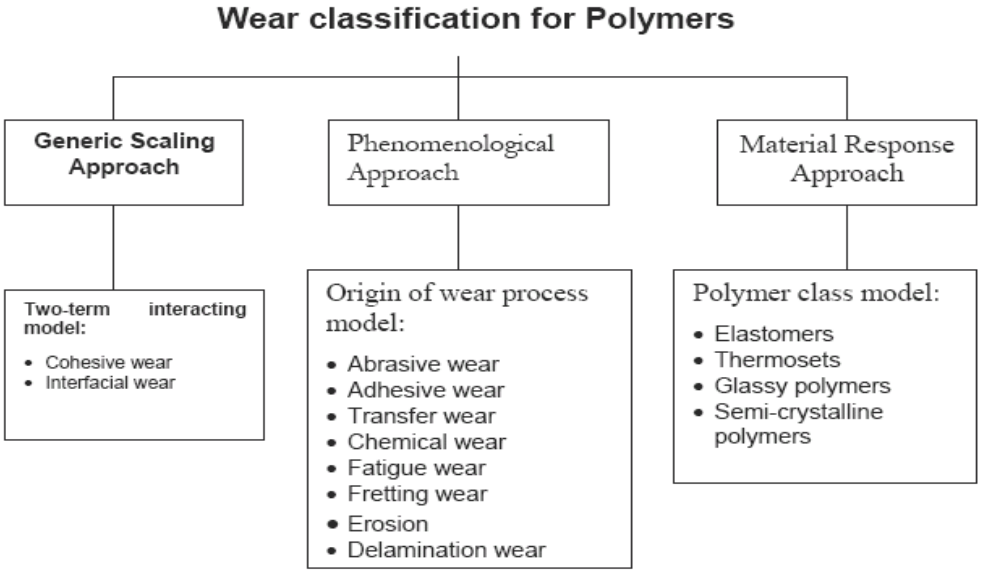

***Figure 2.4**: Classification of wear of polymers and associated approaches used in classification (reproduced from Briscoe and Sinha [2005], with kind permission from John Wiley & Sons Ltd, UK).*

First classification involves the generic scaling approach which emerges from the accepted value of the two-term non-interacting model of friction. According to this model, the friction is of two kinds: interfacial and bulk (ploughing). The wear caused by these frictional processes is classified as cohesive and interfacial wear. The second classification (phenomenological approach) consists of abrasive, adhesive, transfer, chemical, fatigue, fretting, erosion and delamination wear processes. In the third approach, the wear is divided according to the material response. According to this approach, the polymers are distinguished as elastomers, thermosets, glassy polymers and semi-crystalline polymers as having unique wear behavior.

The wear mechanisms classified based on generic scaling responses and phenomenological approaches are explained in detail below. The wear mechanisms in the case of particular polymers are not explained to simplify the wear mechanisms.

2.3.3.2 Wear Classification Based on Generic Scaling Responses

I Cohesive Wear

Cohesive wear, defined as the combination of adhesive and abrasive interactions, consists of ploughing and sub-surface damage. This classification was apparent from the success of the two-term non-interacting model of friction. In the case of cohesive wear, the associated energy is dissipated by adhesive and abrasive (subsurface) interactions. In another way, the cohesive wear is related to the bulk mechanical failure property. This definition is supported by the Ratner-Lancaster correlation which provides an interrelationship between the abrasive wear and tensile toughness [Ratner et al 1964] and

the correspondence between fatigue life and wear life in the case of abrasion of elastomers [Briscoe 1981].

II Interfacial Wear

This class of damage or wear consists of the other part of two-term model (the adhesive part) and this mode does not readily correlate with accessible bulk failure properties. The scheme of interfacial wear processes is shown in Figure 2.5. As a result of interfacial wear, a highly oriented film forms at the counterface, which may reduce the coefficient of friction but may increase the wear rate. PTFE is the classical example in the unfilled form [Pooley and Tabor 1972]. In the cases of glassy polymers (either uncross-linked or cross-linked), the transfer layer formed during interfacial wear may be a degraded polymer which may not show a reduction in the friction.

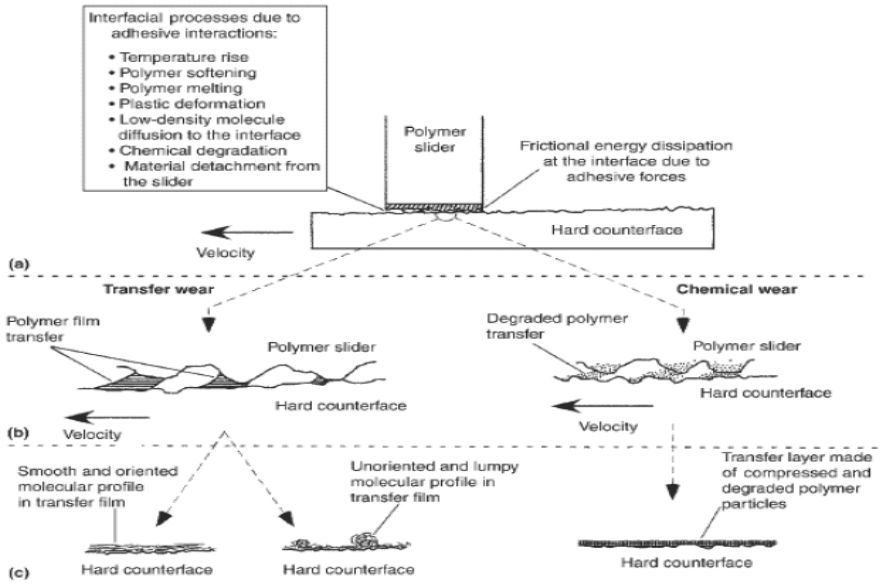

Figure 2.5*: Schematic description of the interfacial wear process (reproduced from Briscoe and Sinha [2005], with kind permission from John Wiley & Sons Ltd, UK).*

2.3.3.2 Phenomenological Classification of Wear Damages

I Abrasive Wear

Abrasive wear is the common name for a cohesive wear as explained above on the basis of two-term friction model. There are at least two types of abrasive wear based on the type of the interfaces: two-body and three-body abrasive wear. In the case of two-body wear, only two surfaces (the polymer and the mating counterface) are involved in the wear process whereas in the case of three-body wear, the hard debris or foreign particles trapped between the two surfaces are involved in the wear process which may further increase or decrease the rate of wear, by several orders. Sometimes the loose debris particles may form strong and tenacious thin films on either of the two mating surfaces which may drastically change the nature of the interface. This is the main wear mechanism in polymer composites sliding against hard metallic surfaces.

The abrasive wear was related to the quasi-static bulk mechanical properties by Ratner et al [1964] and Lancaster [1969] as:

$$V = \frac{(K\mu W v)}{(HSe)} \qquad (5)$$

Where V is the wear volume, K is proportionality constant, μ is the coefficient of friction, W is the normal load, v is the sliding velocity, H is the hardness of the polymer, S is the ultimate tensile stress and e is the % elongation to break. The above equation (5) was validated experimentally by Ratner and Lancaster and many other researchers who have observed a linear relation between V and $\frac{1}{Se}$ [Ratner et al 1964, Briscoe 1981 and Shipway and Ngao 2003]. The above equation resembles the classical Archard's wear

law [Archard 1953], however, the abrasive wear for polymers is dependent upon a combination of bulk properties.

II Adhesive Wear

Adhesive wear is nothing but the interfacial wear as explained earlier. The formation of an interfacial transfer film on the hard counterface is the most important phenomenon in adhesive wear. The adhesive and rheological properties of the interfacial layer or film influence the wear rate and the friction coefficient. If the film is more adhering and tenacious, it may reduce the wear rate by several orders in the steady state stage when a polymer is slid against a hard but smooth thermally conducting counterface. Several polymers have been studied for their adhesive wear properties using smooth metallic counterface and among many such polymers, PTFE and PE have shown low friction and low adhesive wear properties. In the case of PTFE, there is an extensive molecular reorientation in the direction of sliding which reduced the coefficient of friction because of an easy slip between the aligned molecule chains.

III Chemical Wear

The material removal process as a result of extensive chemical reactions between the mating materials and the environment is known as chemical wear. It has been suggested that some chemical reaction is essentially present in almost all tribological interactions. There are four main reasons to promote a tribo-chemical reaction in polymer-metal interaction: (1) elevated interfacial temperature at which polymers can melt, ions can be pulled out or some chemical reaction (such as oxidation) can take place,

(2) catalytical actions of the exposed clean metal surface, (3) the actions of the fillers in either catalyzing the reaction or in actually taking part in making reaction products and (4) contribution from the mechanical straining of the materials which can result in the enhanced chain scission of the molecules. For example, Briscoe et al [1974] and Pratt [1964] have observed a reaction between PTFE and Pb (lead) in the presence of bronze or CuO which results in the formation of a strong adhering PTFE film in porous bronze bearings.

IV Fretting Wear

Fretting involves movements of two adjacent surfaces with small amplitude of the relative displacement and often at high frequencies. Bulk polymers or polymer coatings have often been used to counter fretting problems in metal components. The debris particles strongly influence the fretting damage of the polymer surfaces, and the counterface wear debris formation and crack nucleation and growth are the two competing phenomena in the case of fretting damage. Vincent et al [1992] have introduced the concept of fretting map to rationalize different material responses in fretting and have observed that the wear debris generation increases as the displacement amplitude is increased and as the normal load is decreased. If the normal load is increased crack formation takes place rather than wear debris generation. It has been observed that the fretting wear is high if there is a combination of linear and torsional motion at the contact [Briscoe et al 1998 (b)]. The environment (for example, humidity) also plays a significant role on the fretting life of the majority of polymeric contacts.

V Fatigue Wear / Rolling Wear

Fatigue failure occurs as a result of cyclic or random changes in the stress levels below the fracture strength of the materials. The fatigue failure phenomenon as a result of cyclic sub-surface variation is known as fatigue wear. Such variations in the surface stresses induce sub-surface cracks which finally propagate to the surface producing a chip or flake of the wear debris. In the rolling contacts such as bearing and gear applications, the contact stress varies during the operation and lead to fatigue wear. In the recent years, the use of the polymers as the gear materials increased because of the commercial manufacture of many high-temperature engineering polymers that have a combination of excellent strength and toughness properties and due to the advantages of polymers over other materials such as self-lubricity, non-contaminant and low unit product cost. In a study by Stolarski [1992 and 1993], PEEK has shown superior fatigue wear resistance when compared to Nylon 6,6 and acetal while acetal was better than nylon 6,6. Among many polymers, PEEK has shown superior fatigue wear resistance properties because of its good high temperature and better strength properties and moreover, the additions of fibers to PEEK have further improved its fatigue wear resistance.

2.4 Tribology of Polymer Films

This area is in its early development stage and only very few studies have focused on the development of tribology and the underlying mechanisms of friction and wear in the case of polymer films. One property that is well established is that the effect of the interactions between the polymer molecules and the solid surfaces. The physically adsorbed polymer layers show low wear resistance when compared to the chemically

adsorbed polymer films [Luzinov et al 2001]. The SEBS (poly [styrene-b-(ethylene-co-butylene)-b-styrene]) copolymer has shown very high wear durability when they are chemisorbed onto epoxy-terminated SAM than when physisorbed onto unmodified Si surface.

2.5 Current Developments in Nanolubrication (or MEMS lubrication): Friction and wear durability data of L-B films, SAMs and polymer films

Ultra-thin organic molecular layers have been proposed as the lubricants for Si based MEMS systems [Komvopoulos 1996, Rymuza 1999 and Bhushan et al 1995 (a)]. The lubricant layers, generally, can be formed by two methods: (1) the L-B method and (2) the Self-assembly method [Ulman 1991].

2.5.1 Langmuir-Blodgett monolayers (L-B monolayers)

L-B monolayers were the very early organic films which were considered and studied for the boundary lubrication purposes on metal surfaces such as cadmium, copper, platinum, steel [Rabinowicz and Tabor 1951], mica [Bailey and Pratt 1955 and Briscoe and Evans 1982] and Si surfaces [Novotny and Swalen 1989]. L-B films were effective in reducing the friction and wear of metallic surfaces [Rabinowicz and Tabor 1951] and Si surface [Novotny and Swalen 1989].

Using L-B method, a monolayer film can be deposited on a flat surface using a single molecular type. This technique utilizes the ability of the surfactant molecules to pack closely at an air-liquid interface with an ordered monolayer structure. When a substrate is moved through the water-air interface, a monolayer can be transferred during

emersion (retraction or upstroke) or immersion (dipping or downstroke). A monolayer usually will be transferred during retraction when the substrate surface is hydrophilic, and the hydrophilic head groups interact with the surface. On the other hand, if the substrate surface is hydrophobic, the monomer will be transferred during the immersion, and the hydrophobic alkyl chains interact with the surface. Over the years, many molecules have been studied, such as fatty acids, silanes, thiols, phospholipids and polymeric films. However the drawbacks of L-B method are, firstly it is difficult to uniformly coat the non-polar molecules or high molecular weight polymers, and secondly, since they are bonded with the weak van der Waals forces, the durability of these monolayers is less. Moreover L-B technique cannot be used for three dimensional surfaces and is mainly concerned with flat surfaces [Bhushan et al 1995 (b) and Ando et al 1989]. Therefore, because of these limitations, L-B monolayers can hardly find applications in MEMS components, eventhough some L-B layers are very effective in reducing friction and wear to some extent.

2.5.2 Alkyl-based Self-Assembled monolayers (SAMs)

Since L-B films do not provide higher wear resistance, SAMs have been proposed as prospective candidates for robust molecular lubricants [DePalma and Tillman 1989, Bhushan et al 1995 (a), Ruhe et al 1993, Colton 1996 and Horrison and Perry 1998]. These nanometer thick monolayers have been introduced in the 1980s for surface modification through chemical adsorption of functional organic molecules with the formation of chemical bonds between reactive end groups and surfaces [Ulman 1991]. As explained in Section 2.1.1, the two important SAMs which have been extensively

studied are alkyl-silane SAMs and alkyl-thiol SAMs which bind to oxides of Si/metals and gold, copper and Ni surfaces respectively. Since Si is the base material for MEMs components, alkyl-silane SAMs have been extensively studied to apply them as lubricants for MEMs components. These SAMs have shown higher durability than the classic physisorbed monolayers and decreased the friction coefficient for MEMS components to very low values (< 0.1). One of the important technological advantages of these SAMs is that self-assembly processes are compatible with wet-chemistry processes in the micro fabrication industry. Therefore, much attention has been paid recently to SAMs because of easy preparation and their excellent properties such as extremely low thickness (few nano-meters), steady chemical and physical properties and good covalent bonding with the substrate. Moreover, the properties of the SAMs can be widely varied by changing the chain length [Ruhe et al 1993], chemical nature [Bhushan and Liu 2001 and Liu et al 2001], terminal group chemistry [Kim et al 1997 and 1999] and degree of cross linking within the layer, which makes them more attractive than the physisorbed L-B films [Ulman 1991].

Much has been reported on the tribological properties of SAMs, especially of silane SAMs, which can combine with Si-based materials. Most of the work available in the literature has been conducted using AFM/FFM, which simulates single asperity surface interactions [Bliznyuk et al 1998]. Only few research results are currently available on the continuous sliding configuration (such as pin-on-disk) which simulates the actual rotating parts of MEMs, moving at much higher velocities than those achievable in AFM.

By preparing silane SAMs on silicon surface, the coefficient of friction (COF) is reduced from 0.5-0.6 to 0.1, as has been reported by many groups [Zarrad et al 1995 and Mino et al 1993] using reciprocating tribometer and from 0.15 to 0.018 reported by Tsukruk et al [1996] using Frictional Force Microscopy (FFM).

The effect of increasing the chain length of silane SAMs on tribological properties such as friction and wear has also been extensively studied [Ruhe et al 1993, Nakano et al 2003, Xiao et al 1996 and Lio et al 1997]. Ruhe et al [1993] found that the initial dynamic coefficient of friction was independent of the length of the alkyl silane chains while the wear life extended as the chain length of the SAMs increased. They relate this behavior to the higher flexibility of the longer chains which can dissipate more mechanical energy by the shearing process than the short chain molecules and to the stronger intermolecular interactions [Ruhe et al 1993]. Similar findings have been reported for methyl terminated thiols on gold surface [Nakano et al 2003]. Nanotribological investigations involving the study of the effect of chain length of silane SAMs on friction have shown that friction is higher with short chains when compared to longer chains [Xiao et al 1996]. Figure 2.6 shows experimentally observed variation of the frictional force and elastic modulus with respect to the film thickness of molecular layers [Horrison and Perry 1998 and Guo and Zhao 2006]. The reasons for this behavior are first, the increase in the energy dissipation modes, and second, the increased disorder with shorter chains [Lio et al 1997].

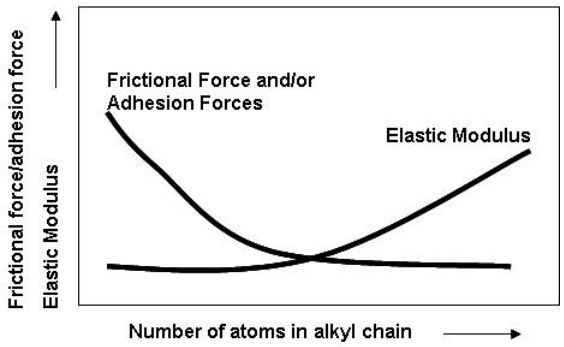

***Figure 2.6**: Generalized trends for the variation of frictional and adhesion forces and elastic modulus with increase in the film thickness of molecular layers.*

Kim. et.al [1997 and 1999] have systematically studied the effect of the surface terminal group chemistry on frictional properties and found that introduction of a small percentage of bulky groups such as CF_3 and CH_2 $(CH_3)_2$ in place of CH_3, dramatically increased the frictional forces. They infer this behavior to the more amount of resistance offered to the shearing by these bulky terminal groups*.

Silane SAMs have been deposited onto MEMs components and micro motors and their effect on the performance of the components has been evaluated [Deng et al 1993, Srinivasan et al 1998 and Dugger et al 2000]. Deng et al [1993] have observed that OTS coating onto flange-bearing polysilicon micromotor significantly reduced the wear and the flange frictional force/torque by a factor of about 1.5 and showed a relatively stable rotor speed and minimum operating voltage during a nine month testing period. Srinivasan et al [1998] have demonstrated that OTS coating onto polycrystalline silicon microstructures can reduce the adhesion by more than three orders of magnitude over the standard oxide-coated structures and that the FDTS coating also reduced the adhesion by four times. Dugger et al [2000] have observed that OTS coating onto a micromachined

* The size of the F atom is bigger than the H atom and hence CF_3-SAM offers more resistance than CH_3-SAM and shows high friction.

structure made from polysilicon has slightly reduced the coefficient of friction and increased the sliding duration by a factor of three when compared to that for unlubricated structures. These studied have demonstrated that SAMs coating improves the tribological performance of MEMS components.

Among the alkyl silane SAMs, OTS SAM is the most widely studied SAM and is regularly used in the industry as anti-stiction and anti-friction organic modifier [Bliznyuk et al 1998 and Alley et al 1995]. This SAM has shown completely hydrophobic property, lower coefficient of friction and reasonable wear resistance when compared to other SAMs with different terminal groups such as azide (N_3) and CF_3 [DePalma and Tillman 1989 and Lander et al 1995].

The above studies have shown that some of the silane SAMs are efficient in reducing the coefficient of friction, work of adhesion and stiction values, but their wear resistance is not sufficient to provide long life to the high velocity moving MEMS components [DeBoer and Mayer 2001].

In addition to the lower wear resistance, for silane SAMs, there are another difficulties arising from the coating process itself. The SAM solution must be freshly prepared and conditioned appropriately just before each coating. This is required because of its sensitivity to the atmospheric humidity and the tendency of the SAM molecules to polymerize [Maboudian et al 2002]. Therefore, great care and control are needed while preparing the silane SAM solutions and during deposition. This problem is partly being solved by the vapor deposition methods [Ashurst et al 2003].

Because of the difficulties of low wear life and and bulk polymerization of OTS SAMs, other alkyl silane SAMs has been proposed which are also covalently bonded

with Si surface. Some of these monolayers are dichlorodimethylsilane (DDMS, $Cl_2Si(CH_3)_2$) [Ashurst et al 2001 (a) and Kim et al 2001], dichlorodipropylsilane (DDPS, $(C_3H_7)_2SiCl_2$) and dichlorodiethylsilane (DDES, $(C_2H_5)_2SiCl_2$) [Kim et al 2001]. Because of less number of reactive Cl atoms, these SAMs have shown lower tendencies to polymerize and are less sensitive to the atmospheric humidity. When compared to OTS SAM, these SAMs have shown comparable anti-stiction properties with improved film quality. However, the wear resistance of these monolayers has not been investigated and it is expected that these monolayers may not show higher wear resistance than OTS SAM, because they have similar thicknesses and molecular flexibilities as those of OTS SAM molecules. SAMs such as 1-Octadecene ($C_{16}H_{33}CH=CH_2$) [Ashurst et al 2001 (b)] which is bonded through Si-C bonds with substrate, alkoxyl monolayers which are bonded through Si-O-C bonds with the substrate [Major et al 2003], n-isooctane and n-octylamine bonded through Si-O and Si-N bonds with the substrate [Zhu and Houston 1999] have been investigated and proposed as alternatives to the conventional OTS SAM which binds with the Si through Si-O-Si bonds. All these SAMs have shown comparable anti-stiction properties with OTS, however, their wear durability data are not available.

2.5.3 Functional SAMs

Functional SAMs, with reactive chemical groups at the surface, are formed by chemisorption of molecules with two reactive ends [Lee et al 1994]. These SAMs are similar in microstructure to the conventional SAMs and the difference being the presence of reactive groups at the surface instead of the non-reactive terminal groups such as CH_3, CF_3 etc. These SAMs with reactive surface groups can be used for the grafting of other

organic molecules, polymers, nanoparticles, dendrimers, biomaterials and other inorganic materials. These SAMs act as glue or intermediate layer for other molecules to be grafted onto the Si surface. Many functional SAMs have been fabricated with carboxyl, hydroxyl, amine, acrylate, sulfate, epoxy and other chemical groups [Lee et al 1994, Nuzzo and Allara 1983, Beake and Leggett 2000, Cant et al 2003, Agarwal et al 1997 and Elender et al 1996].

The general formula of the functional SAMs is R_n SiX. It has two functional groups R and X. The functional group X (examples such as ethoxy, methoxy, thiol etc) is attached to substrates such as Si, Au etc. while the other functional groups R (examples such as amino, sulfate, carboxyl, epoxy, hydroxyl and vinyl etc) are used to attach to an organic resin etc. Therefore, by the use of these functional SAMs, a variety of polymers, organic resins, nanoparticles can be bonded to the model surfaces such as Au and technologically important semiconductor materials such as Si etc.

Generally, the frictional force increases proportionally to the adhesive interactions if capillary contribution is eliminated [Noy et al 1995, Marti et al 1995, Beake and Leggett 2000 and Tsukruk et al 1998]. Since the adhesive forces are higher for these functional SAMs, the friction coefficients are much higher for these SAMs and are typically in the range 0.1-0.5 with some even reaching a value upto 1-2 [Satyanarayana and Sinha 2004]. Therefore, these functional SAMs are not used as the molecular lubricants rather they are used as molecular "glues" for adhesion promotion to subsequent layers of SAMs.

2.5.4. Grafted Polymer Layers

Formation of molecularly thick layers from adsorbed macromolecular chains has been used to modify/improve surface properties [Tsukruk et al 2002 (b), Muller et al 2003, and Bouhacina et al 1997]. These polymer layers can be adsorbed both physically and chemically. But the physically adsorbed polymer layers form weakly bonded films which show lower stability, low wear resistance and they dewett the substrate at elevated temperatures [Fleer et al 1993, Yerushalmi-Rozen et al 1994 and Luzinov et al 2001]. For example, physically adsorbed SEBS (poly [styrene-b-(ethylene-co-butylene)-b-styrene]) polymer films on Si surface has shown lower durability when compared to those SEBS films which are covalently adsorbed onto Si substrate [Luzinov et al 2001]. Therefore, chemical attachment of polymer layers to the substrate improves the stability and prevents dewetting at elevated temperatures. Hence, several techniques have been developed to chemically bind the polymer films to Si substrate. Introducing the chemical functional groups as either terminal reactive ends or multiple reactive centers into flexible polymer chains helps to chemically bind the polymer layers to the substrate. Many a times, we need to have functional groups on the Si surface to chemically bind with the polymer films. These reactive functional groups on the Si surface can be obtained by the deposition of the functional SAMs which have been explained in Section 2.2.3. This technique involving the addition of polymer chains onto the substrate is called "Grafting-To" approach. The limitation of this technique is that only very small amount of the polymer (typically less than 5 mg m^{-2}) can be immobilized on the substrate, because of the reason that once a dense layer is formed, it will hinder further reaction of the polymer molecules with the substrate. Therefore, an improved method has been introduced

recently, which is termed as "Grafting-from" technique, in which polymer layers have been obtained by the in-situ polymerization at the surface using a photo initiator SAM [Prucker and Ruhe 1998]. By this technique we can bind higher amounts of polymers. The polymer films formed by this technique have yet to be tested for their applications in tribology.

2.5.4.1 Specific examples of polymer films tested for their tribological properties

In this section, we will review literature results on the tribological properties of polymer thin films.

Kitoh and Honda [1995] have observed that the sputtered PI film of 20 nm thickness on Si surface has shown better abrasion resistance than sputtered PTFE film on Si. Sidorenko et al [2002] have shown that a trilayer architecture, consisting of poly (methacrylate) layer on SEBS polymer chemisorbed onto Si via epoxy SAM, has shown good wear durability characteristics. The trilayer architecture on Si has shown a wear durability of 3300 cycles at a contact pressure of 1.2 GPa when sliding against a 3 mm diameter steel ball using an oscillating friction and wear tester whereas the OTS SAM layer has failed within 900 cycles under the same testing conditions [Sidorenko et al 2002]. Liu et al [2002] have shown that the PDMS films spin-coated on hydrophilic surfaces (hydroxilated Si or vinyl terminated Si) have shown higher wear durability whereas PDMS films spin-coated on hydrophobic surfaces (methyl terminated Si) have shown very low wear durability and the authors concluded that good chemical interactions between PDMS film and the substrate led to better anti-wear properties. Sakata et al [2005] have shown that PMMA brush formed on Si wafer immobilized with

2-bromoisobutylate has shown better anti-wear properties, tested in a reciprocating sliding test against to stainless steel ball at a normal load of 0.49 N, when compared to the spin-coated PMMA film on bare Si which was attributed to the end-grafted structure of the polymer brush. In a recent study, Sun et al [2006] have shown that chemisorption of PI films on Si via reactive polymer layer (polyglycidyl methacrylate, PGMA) has shown a wear durability of 25,000 cycles at a normal load of 0.5 N in a reciprocating sliding test against 3 mm diameter steel ball at a sliding velocity of 20 mm s^{-1} whereas the same PI film on Si, without the intermediate reactive polymer layer, has failed within 800 cycles under the same testing conditions. This study demonstrated the importance of the chemical bonding between the polymer film and the Si surface (which is often achieved by means of reactive SAM/polymer layers) for better anti-wear properties.

2.5.4.2 Research strategy on polymer thin films used in the present thesis

From the above literature review on the tribology of polymer thin films, it is clear that this area needs further research in view of both fundamental research and technological applications. Therefore, polymer thin films are surely a promising research area and may be able to provide good lubrication to durable MEMS and other microsystem devices. Moreover, scientifically, no fundamental principles are available which will guide in selecting a polymer thin film with particular desired properties. It is also understood that researchers are successful in obtaining several ultra-thin polymer films with the desired functionalities only recently and many of such new polymer films have to be tested for their applicability to solve tribological problems in many technological applications.

Therefore, three different types of studies are conducted in the present thesis (in addition to the work on PFPE overcoating onto SAMs) (as listed below) to explore the fascinating and yet complicated field of polymer thin films. The motivation behind each study and the overview of the objectives are explained in the respective chapters.

(a) Development of ultra-thin films of UHMWPE

(b) The influence of the addition of CNTs (filler material) on the wear durability of polymer thin films

(c) The effect of the molecular structure of the polymer films on their tribological properties

The above strategies are part of the overall objectives and methodologies as mentioned in Section 1.3 and 1.4.

Chapter 3

Experimental procedure

In the present chapter we will describe various common experimental methods used for physical, chemical, mechanical and tribological characterizations of the films developed in this research. Details of the materials used, film deposition and sample preparation are given in respective chapters for easy reference.

3.1 Surface Characterization and analysis

3.1.1 Contact angle measurement

Contact angle is sensitive to the chemical nature of the top molecular layer and the measurement of contact angle is relatively simple, inexpensive and a popular technique for characterizing the wettability of surfaces. Water (polar) is the main liquid that is commonly used to measure the contact angle, however, other liquids such as formamide (polar), hexadecane (non-polar), diiodomethane (non-polar) etc are also used to measure their respective contact angles. The contact angle technique is indeed a quick method to qualitatively determine whether or not the target film is being properly coated onto the substrate. Contact angle of a liquid on a substrate is the angle between the liquid/solid interface and liquid/vapor interface as shown in Figure 3.1. The contact angle of a solid-liquid-vapor system is governed by the solid-liquid, liquid-vapor and solid-vapor interfacial forces of the system (as evident from Figure 3.1). For a liquid drop resting on a surface at thermodynamic equilibrium with its saturated vapor, the sum of the interfacial surface tensions must be zero at the solid-liquid-vapor contact point. Thus, the contact angle can be obtained from Young's equation [Adamson 1990]:

$$\gamma_{LV} \cos \theta = \gamma_{SV} - \gamma_{SL}$$

where θ is the contact angle and γ_{LV}, γ_{SV} and γ_{SL} are the liquid-vapor, solid-vapor and solid-liquid surface tensions respectively.

Figure 3.2 shows the images of the liquids on two selected surfaces to show the distinction between the hydrophilic and hydrophobic surfaces. Figure 3.2 (a) shows the hexadecane contact angle on bare Si (hydrophilic surface) and Figure 3.2 (b) shows the water contact angle on OTS SAM (hydrophobic surface).

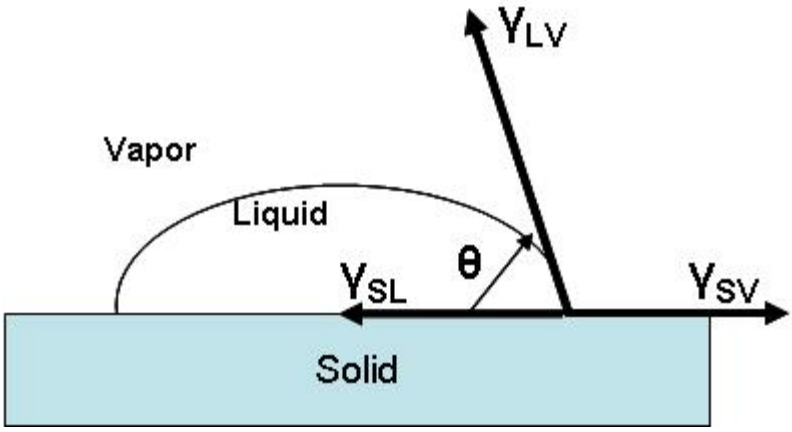

***Figure 3.1**: The representation of contact angle between the liquid/solid and liquid/vapor interface.*

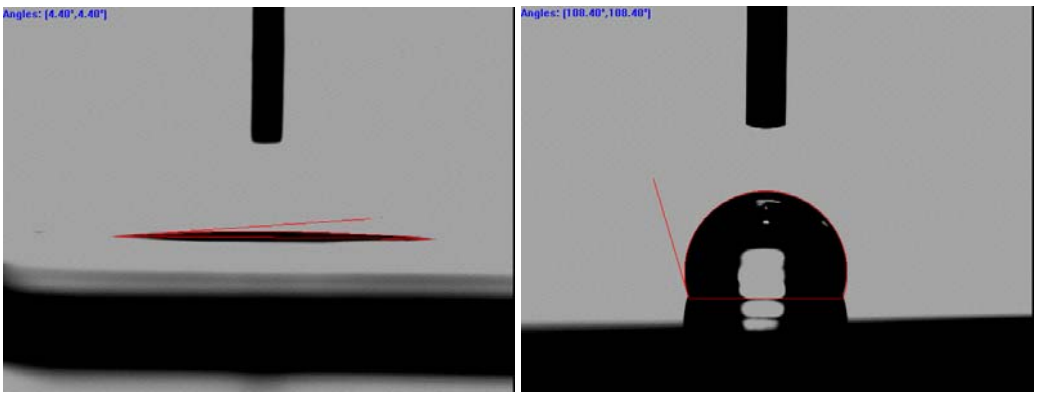

(a) (b)

***Figure 3.2**: (a) Hexadecane contact angle on bare Si surface (~4.5^o, hydrophilic) and (b) Water contact angle on OTS SAM on Si surface (~108^o, hydrophobic).*

In the present research, the static (equilibrium) contact angles for distilled water on the unmodified and modified surfaces were measured with VCA Optima Contact Angle System (AST Products, Inc. USA). A water droplet of 0.5 to 1 μl was used for contact angle measurement. At least 5 to 6 replicate measurements, for three different samples, were carried out and an average value was taken. The variation in the water contact values at various locations of a sample is within $\pm 2^{o}$. The measurement error was within $\pm 1^{o}$.

3.1.2 Topography measurements with Atomic Force Microscopy (AFM)

In AFM imaging, a tip is brought close to the surface where the tip interacts with the surface through many interfacial forces, which in turn causes the tip to deflect. A laser beam focused on the tip is reflected from the tip into a photodiode array to measure the deflection of the tip. Primarily, AFM can be operated in two modes to measure the topography (contact mode and tapping mode) [Digital Instruments MultiMode™ Instruction Manual 1997]. In the contact mode AFM, the tip rasters the surface while the deflection is maintained constant via a feedback loop. In the tapping mode AFM, the tip is oscillated at its resonance frequency (on the order of 300 kHz), while scanning the sample surface. The reflected laser beam operates a sinusoidal signal in the photodiode array, whose amplitude depends on the surface topography. As the oscillating tip is rastered over the surface, the tip is deflected by its interactions with the surface and causes a change in the measured amplitude. The tip in the contact mode AFM is dragged across the surface and hence may sometimes be able to damage/alter the surface features whereas the tapping mode is gentler and cannot lead to any modification of the surface

features. Hence, tapping mode AFM is routinely used for topography studies of ultra-thin films (especially organic thin films).

The tip geometry plays an important role in determining the actual topography of the thin film or any surface. Variations in tip structure may cause variations in AFM images. Typically, a sharp tip would provide an accurate representation of the surface topography. If the tip is blunt the surface topography is going to be erroneous. For example, if the tip is blunt and the surface features of the sample (to be imaged) are such that the dimensions of the surface features are smaller than those of the apex of the tip, then instead of tip imaging the sample surface features, the sample surface features image the tip surface. Additionally, the mechanical properties of the cantilever are important in controlling the performance of the AFM imaging, for example, the spring constant and the resonance frequency are of particular importance. A small spring constant is desired to effectively detect small forces and a high resonance frequency is required to make the tip insensitive to vibrations and mechanical noise.

The surface topography of SAMs and polymer films modified Si substrates, in the present research, was investigated using Digital Instruments Multimode^{TM} AFM (Veeco, USA). Tapping mode was used for imaging using a silicon tip and all images were collected in air. The set point voltage used was 1-2 V and the scan rate was 1 Hz.

3.1.3 Ellipsometry

Ellipsometry is a surface analysis tool that provides information about the refractive index and the thickness of surface confined films. When plane-polarized light interacts with a surface at a particular angle, it is resolved into s-polarized (parallel) and

p-polarized (perpendicular) components. These two components are reflected from the surface in different ways, both components change their amplitude and phase. Elliptically polarized light results when the reflected s- and p-polarized light is combined. Ellipsometry uses this phenomenon to estimate the thickness of a film between two phases (the substrate and air) by measuring the ratio, r, between the reflection coefficients of the p- and s-polarized light, r_p and r_s, respectively.

$$r=r_p/r_s= \tan \Psi \exp (i\Delta)$$

where tan Ψ is the ratio of magnitudes of the parallel and perpendicular components and Δ is the phase shift between these two components. As ellipsometry is measuring the ratio (or difference) of two values rather than the absolute value of either, it is very accurate, reproducible and robust. Using a least-squares minimization (iterative procedure) unknown optical constants and/or thickness parameters are varied, and Ψ and Δ values are calculated using the Fresnel equations [Tompkins 1993]. The calculated Ψ and Δ values, which match the experimental data best, provide the optical constants and thickness parameters of the sample.

In the present research, the thicknesses of certain films (SAMs and ultra-thin polymer films) were measured by using variable-angle spectroscopic ellipsometry (VASE, J.A.Woollam, Co., Inc). The measurements were carried out at the wavelengths ranging from 400 to 1000 nm with the resolution of 10 nm and geometries of φ=65, 70 and 75^0, where φ is the angle between the sample normal and the incoming laser beam. The thickness of the films was evaluated by using WVASE 32 software (J.A.Woollam, Co., Inc) by applying the effective medium approximation. The refractive index values used for different film materials are listed in the respective chapters. At least 3 to 4

replicate measurements, for at least 3 samples, were carried out and an average value is reported. The error in the thickness measurement was within $\pm 3A^0$.

3.1.4 Fourier Transform-Infrared Spectroscopy (FTIR)

FTIR is an analytical technique to identify organic (and in some cases inorganic) materials. This technique measures the absorption of infrared radiation by the sample material versus wavelength. The infrared absorption bands identify molecular components and structures. When a material is irradiated with infrared radiation, absorbed IR radiation usually excites molecules into a higher vibrational state. The wavelength of light absorbed by a particular molecule is a function of the energy difference between the at-rest and excited vibrational states. The wavelengths that are absorbed by the sample are characteristic of its molecular structure.

An interferometer is used in the FTIR spectroscopy to modulate the wavelength from a broadband infra-red source. A detector measures the intensity of transmitted or reflected light as a function of its wavelength and provides an interferogram, which must be analyzed with a computer using Fourier transforms to obtain a single-beam infrared spectrum. The FTIR spectra are usually presented as plots of intensity versus wavenumber (in cm^{-1}) where the wavenumber is the reciprocal of the wavelength. The intensity can be plotted as the percentage of light transmittance or absorbance at each wavenumber.

FTIR spectra for UHMWPE and PI films on Si were obtained in air using a Bio-Rad FTIR model 400 spectrophotometer using transmission mode. Each spectrum was collected by accumulating 16 scans at a resolution of 4 cm^{-1}. The spectra were collected

from at least 5 to 6 replicate points and they were found to be identical at all points of measurement. Bare Si, after piranha treatment, was used for background scan.

3.1.5 X-ray Photoelectron Spectroscopy (XPS)

The chemical state of the sample surface after modification was studied by XPS. XPS gives information about the atomic composition of the surface and is especially sensitive to the local chemical environment of an atom. In the XPS measurement, x-rays are usually generated either by Mg or Al source and directed to the sample surface. The x-rays cause a core electron to be emitted from the sample. The kinetic energy of this electron is detected with an electron multiplier and is equal to the difference between the energy of the x-ray (1253 eV for Mg, 1486 eV for Al) and the binding energy of the electron. In the present research, XPS measurements were made on a Kratos Analytical AXIS HSi spectrometer with a monochromatized Al Kα X-ray source (1486.6 eV photons) at a constant dwell time of 100 ms and pass energy of 40 eV. A photoelectron take-off angle of 90^{o} (with respect to the sample surface) was used to obtain the core-level signals. All binding energies (BE) were referenced to the C1s hydrocarbon peak at 284.6 eV.

3.1.6 ToF-SIMS (Time of Flight- Secondary Ion Mass Spectroscopy)

Time of Flight Secondary Ion Mass Spectrometry (ToF-SIMS) is a surface analytical technique used to obtain elemental and molecular chemical data (static SIMS), and concentrations of impurities in semiconductors and metals (dynamic SIMS). All elements (including hydrogen) are detectable by SIMS.

In the SIMS analysis, the sample surface is bombarded with a beam of primary ions which generates secondary products. The bombardment of primary ions produce cascade of atomic collisions within the solid (after transferring some of their energy to the lattice atoms), resulting in the emission of electrons, neutral species, atoms, molecules, atomic ions and cluster ions. These atoms and clusters are called secondary ions and they can be analyzed by time-of-flight mass spectrometry. In the ToF analyzer, the ejected secondary ions are accelerated with a common energy, but at different velocities depending on the particle mass. Due to the differences in these velocities, larger ions move through the analyzer slower than the smaller ions. The travel time of the secondary ions through the analyzer determine their mass. SIMS is a surface-sensitive analysis method, since only the secondary ions generated in the outermost 10 to 20 Å region of a sample surface can overcome the surface binding energy and escape the sample surface for detection and analysis.

In the present research, ToF-SIMS measurements were conducted using ION-TOF GmbH, Germany. Positive secondary ion mass spectra were measured using a 25 keV Ga primary ion beam at a total ion dose of 10^{12} ions cm^{-2}.

3.1.7 SEM observation of polymer films

JEOL JSM-5600 LV SEM (scanning electron microscope) equipped with EDS (energy dispersive spectroscopy) was used to investigate the surface morphology of the polymer films studied in the present research.

3.1.8 Measurement of thickness of the polymer films using laser profilometer

A non-contact confocal laser profilometer (NanoFocus μScan®, NanoFocus AG, Germany) was used for measuring the thickness of PI films on Si surface (Chapter 7). The sample surface with half area coated with polymer film and other half uncoated was subjected to the thickness measurement (Figure 3.3). The laser profilometer measures the thickness (with a resolution of 100 nm) from the step height at the edge of the film (Figure 3.3). Laser profilometer has been used in the literature to measure the thickness of many such films [Pavoor et al 2004 and Jang and Kim 1996].

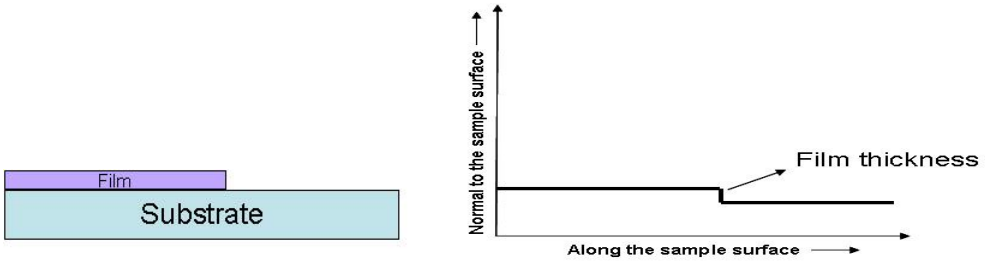

***Figure 3.3**: Schematic diagrams representing the principle involved in the measurement of the film thickness using laser profilometer.*

3.1.9 Adhesive Force Measurements using AFM

Since 1989, AFM has been used as a tool for studying surface interactions by means of force-distance curves and a great deal of work has been carried out on both theoretical and experimental aspects [Binnig et al 1986 and Cappella and Dietler 1999]. Theoretically, AFM is able to measure force-distance curves on any kind of surface, with high lateral (1 A^o) and vertical (0.1 A^o) displacements and force (1 pN) resolutions. The study of force-distance curves provide a good understanding of the physics of contact and hence of all the phenomena related to AFM imaging techniques.

A typical force-distance curve (a plot of tip-sample forces versus tip-sample distance) is shown in Figure 3.4, which is experimentally obtained for bare Si.

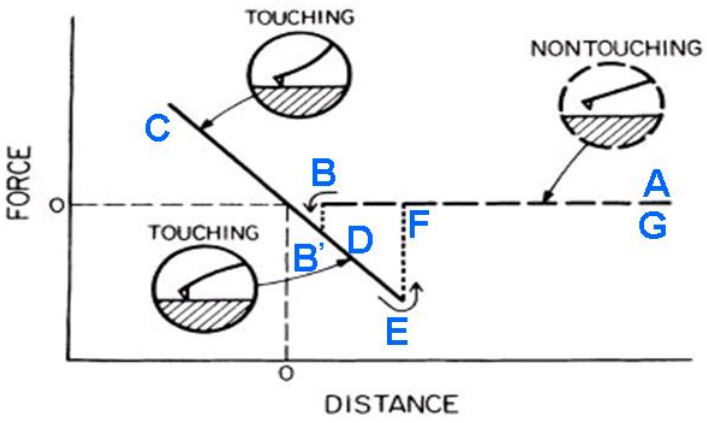

***Figure 3.4**: The representation of a typical force-distance curve with illustrations of corresponding tip-sample interaction at various positions on force-distance curve.*

At the start of the force-distance curve measurement, the tip and the specimen are far away and the cantilever is in its rest position. PZT tube controls the vertical movement of the cantilever and the specimen is stationary. Therefore, as the voltage is applied to the Z-electrode of the PZT tube, the cantilever moves towards the tip. From A to B in Figure 3.5, there is no change in the force as the sample and the tip have not come into contact. As the tip approaches the sample surface, at point B (when the tip is in close proximity to the specimen) the force becomes attractive. The cantilever bends towards the specimen and the attractive force increases gradually until point B' where the tip and the sample are in intimate contact and the force becomes repulsive. As the tip is further pressed against the sample, the sample pushes the cantilever back through its original position entering the repulsive region (or loading portion) of the force curve. The force reaches maximum at point C where the PZT tube extension is maximum and afterwards the PZT tube starts to retract (unloading portion). As the PZT tube retracts, the force between the tip and sample decreases. At point D the tip is still in contact with the specimen and remains in contact even with further PZT tube retracting because of the adhesion force between the

two. The cantilever suddenly detaches from the specimen at point E when the cantilever force exceeds the adhesive force. Further withdrawal of the tip (F to G) does not affect the force as the tip is not in contact with the specimen. It has to be noted that the loading and unloading curves do not coincide due to the thermal drift and hysteresis effect.

In the present research, a commercial AFM (Molecular Imaging Corporation, USA) was used for measuring adhesive forces. Commercially available Si_3N_4 cantilevers/tips were employed for the measurements with a tip radius of 15-20 nm. The measurements were carried out in air at a relative humidity of ~16-18% and at room temperature (~21^oC). The spring constant of the cantilever used was 0.36 Nm^{-1}, as provided by the supplier. The normal spring constant was also obtained experimentally by using a standard method of measuring their frequency in vacuum [Cleveland et al 1993] and the experimental values coincided well with the manufacturer's specifications. The stiffness values of the cantilevers of similar dimensions show a maximum error of 5%. The force versus distance measurements were performed at 10-20 different locations on each sample and the curves shown in this thesis are typical for each modification and an average adhesion force value is reported.

3.1.10 Tribological Characterization of SAMs and polymer thin films on Si surface

Friction and wear durability tests were carried out using a commercial micro tribometer (UMT-2, Universal Microtribometer, Center for Tribology, USA) which can be operated in both ball-on-disk and ball-on-plate modes (Figure 3.5).

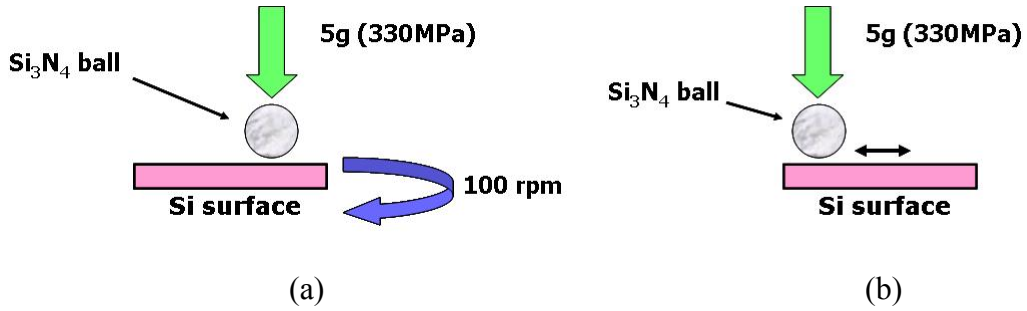

(a) (b)

***Figure 3.5**: The contact configuration in (a) ball-on-disk sliding test (disk rotating) and (b) ball-on-plate sliding test (disk reciprocating).*

For all the samples, the coefficient of friction and wear durability measurements are carried out using ball-on-disk mode using a 4 mm diameter Si_3N_4 ball (roughness R_{RMS}=4 nm) at a rotational speed of 100-200 rpm giving a sliding speed of 0.021-0.042 ms^{-1} at a wear track diameter of 4 mm and at normal loads of 5-7 g which give a contact pressure of approximately 330-370 MPa (calculated using the Hertzian Contact Model). Si_3N_4 ball is used as the counterface because it is very hard when compared to Si and inert towards organic species. Even though the typical contact pressures in MEMS are in the range of less than one to a few MPa [Lumbantobing et al 2004 and Williams and Le 2006], the present wear durability tests are conducted at 330-370 MPa to shorten the time duration of the wear tests. A lubricant that can perform well at high pressures is also expected to show satisfactory performance at lower pressures. All tests were performed in a class-100 clean booth in ambient atmosphere at room temperature (23^{o}C) and a relative humidity of ~70%. In the present thesis, the initial coefficient of friction reported is the value obtained after 4 s of sliding (i.e. after 6-12 sliding cycles) i.e. after stabilization of the sliding process. After careful review of various definitions (or criteria) used for wear durability in the literature for similar sliding tests [Eapen et al 2002 and Ruhe et al 1993], the wear durability in the present research was defined as the number of cycles after

which the coefficient of friction exceeded a value of 0.3 or a visible wear scar appeared on the sample, whichever happened earlier. The average wear durability data reported in the present thesis was calculated from the data obtained from at least three different samples utilizing at least two different tracks on each sample. It is worth noting that the wear durability of a particular film can change if the above definition is altered, however, the above definition serves the purpose of comparing wear durability of different films.

The SEM (JEOL JSM-5600 LV) was used to observe the worn surfaces after appropriate number of sliding cycles.

As evident from the literature review presented in Chapter 2, much of the work on ultra-thin lubrication has been carried out using AFM/LFM. Even though AFM measures the friction very accurately on a localized point, it does not represent actual surface contacts of a microsystem such as MEMS. The reasons for this behavior are, firstly, the AFM tip gives a point contact (extremely small contact areas) whereas in MEMS components, the surface contact areas are much larger; secondly, the sliding speeds achievable in AFM (maximum achievable speeds are few tens of μms^{-1}) are extremely low compared to the speeds required for Microsystems (~200-300 mms^{-1} [Williams and Le 2006]). The contact pressures involved in AFM measurements are several tens to hundreds of GPa (because of extremely fine AFM tip) which are much larger than any anticipated nominal pressure applied in practice [Williams and Le 2006]. Moreover, long-term wear durability tests are not feasible using AFM. Therefore, in the present research, we employed a ball-on-disk tribometer which has realistic sliding contact area (with track width in the range of few hundred microns) and high sliding velocity.

3.1.11 Nano-mechanical property characterization of polymer films using Nanoindentation

MTS Nano Indenter® XP (MTS Corporation, Nano Instruments Innovation Center, TN, USA) was used for measuring elastic modulus and hardness of polymer films with a CSM technique. A small and sinusoidally varying signal is imposed in the CSM technique in addition to a DC signal, for driving the motion of the indenter. The data are obtained by analyzing the response of the system using a frequency-specific amplifier. In the CSM method, the contact stiffness can be measured at any point along the loading curve and not just at the point of unloading as in the conventional measurement. The equipment will provide the hardness and elastic modulus values calculated from the CSM stiffness data (acquired during the indentation experiment) using the analytical expressions developed by Oliver and Pharr [1992]. Therefore, in the CSM method, the hardness and modulus values are determined as functions of indentation penetration depth with a single indentation load/unload cycle. The load and displacement resolutions in the CSM technique are 50 nN and < 0.01 nm respectively. A triangular pyramid diamond indenter (known as Berkovich indenter) was employed for all nanoindentation tests. The average hardness and elastic modulus values are calculated from the data of a total of 5 indentations made on different random surface locations. Typical indentation load vs displacement curves are obtained, in certain films, at an applied load of 250 μN and the hardness and elastic modulus are computed using Oliver and Pharr [1992] method.

The NanoIndenter XP was also used for the nano-scratch tests on some polymer films. Conical diamond tip with a cone angle of 90^{o} and 1 μm radius was used for the

scratching. For each sample, a scratch length of 200 μm at an increasing normal load, from 10 μN to 250,000 μN, was made at a scratch velocity of 1 μm s^{-1}. The scratches were then imaged using SEM to understand the scratch resistance of polymer films.

Chapter 4

Tribology of PFPE overcoated Self-assembled monolayers (SAMs) deposited on Si surface

4.1 Background

As already emphasized in the literature survey presented in the Chapter 2, SAMs cannot provide high wear durability either because there is no mobile portion of the lubricant or because of some molecular properties which are not well understood. Once wear initiates, the molecules are easily removed from the contact area and there is no replenishment in these layers. The worn particles often also act as a third-body and thus accelerate the process of wear of the film and the substrate. Therefore, researchers have realized the importance of the incorporation of mobile molecules into ultra-thin organic films (such as polymer films) which will give self-repairability due to the migration of mobile molecules into the sliding contact, leading to high wear life [Ahn et al 2003]. This concept has been well studied for magnetic hard disk lubrication. For hard disk lubrication, a combination of both bonded and mobile PFPE on DLC (diamond like carbon) surface has shown higher wear durability than only either bonded or mobile PFPE [Katano et al 2003, Chen et al 2001 and Sinha et al 2003]. Katano et al [2003] have observed that the dual lubricant layers (based on PFPE) on hard-disk surface, which consists of a bonded layer with a strong polar end group and a mobile layer with a weaker polar end group, show higher wear durability than mono lubricant layer. Recently, Eapen et al [2002] have studied the MEMS lubrication utilizing the concept of using both

bonded and mobile portions of PFPE which have shown good improvement as far as wear durability is concerned.

Therefore, we propose the concept of PFPE (bound+mobile) overcoating onto SAMs (bonded) coated Si (Figure 2.4) as a means to enhance the wear durability [Satyanarayana and Sinha 2005 and Satyanarayana et al 2007 (a)]. The concept of utilizing the mobile PFPE to enhance wear durability of SAMs with different functional groups or polymer films has not been tried in view of MEMS lubrication. Julthongpiput [2003] proposed this concept of PFPE overcoating to enhance the wear resistance of epoxy nanocomposite polymer bilayers, however, the results are not available. Similar concept of overcoating a mobile hydrocarbon-based lubricant onto chemically bound monolayers onto Si based MEMS component has been used to enhance wear durability by Eapen et al [2005]. We do not attempt to compare our results with those of Eapen et al [2005] as the top mobile layer and monolayer films that they used are quite different when compared to our study. It is worth noting that both studies were carried out independently during the same period of time.

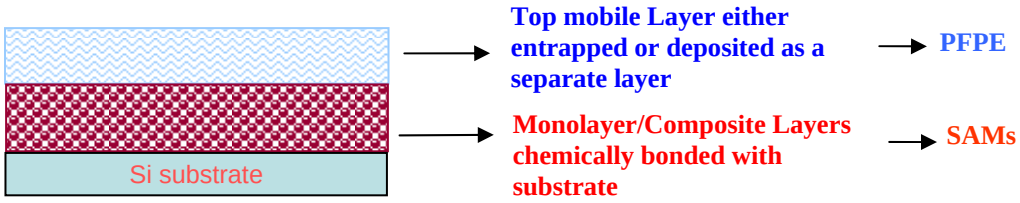

Figure 4.1: *The lubrication scheme of PFPE overcoating. Note that the thickness and pattern of the rectangular boxes have no significance.*

In the present study, we have focused on the effect of overcoating PFPE onto a single monolayer of SAM. Three different SAMs (OTS, APTMS and epoxy SAM) are used,

among which OTS is hydrophobic with methyl surface terminal groups whereas APTMS and epoxy SAMs are hydrophilic with amine and epoxy terminal groups respectively, to elucidate the effect of the surface functional group on the final tribological properties after overcoating with PFPE. PFPE is selected as the top layer because of its properties such as low surface tension, chemical and thermal stability, low vapor pressure, high adhesion to the substrate and good lubricity [Liu and Bhushan 2003]. The aim of the present study is mainly to investigate the influences of the PFPE overcoating (mobile and partially bonded) on the wear durability of SAM layers. The PFPE overcoated SAM surfaces are then subjected to strong shearing conditions in contact sliding to evaluate wear characteristics. Their tribological properties are finally compared with bare Si and SAM coated surfaces without PFPE overcoat.

4.2 Materials

Polished single crystal silicon (100) wafers of 4 inch diameter (obtained from Engage Electronics Pte Ltd, Singapore) were used as the substrate for SAMs coating. These Si wafers were appropriately cut into smaller pieces and then used for the surface modification and characterization.

OTS, APTMS and epoxy SAMs were obtained from Aldrich and were used for the preparation of SAM solution in toluene, without further purification. Zdol 4000 PFPE obtained from Solvay Solexis, Singapore (molecular weight 4000 g mol^{-1}, monodispersed, containing OH terminal groups) was used to coat the SAM and bare Si.

The chemical formulae of the three SAMs and PFPE used are as follows:

OTS:

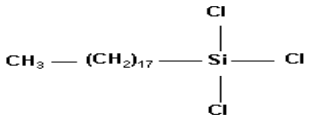

APTMS:

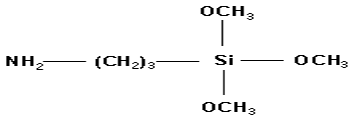

Epoxy SAM:

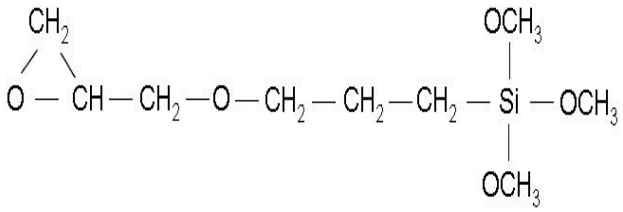

PFPE Z-dol 4000:

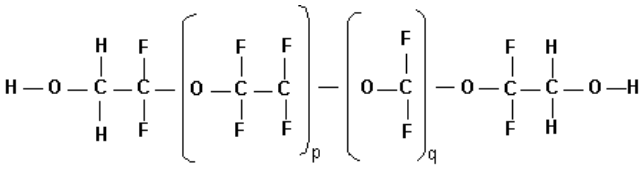

The ratio of p/q in PFPE is 2/3. Hydrofluoropolyether solvent (H-Galden ZV, obtained from Ausimont Inc, Singapore) was used for the preparation of PFPE solution, without further purification. Acetone (99.5%), methanol (99.8%), toluene (99.5% anhydrous) and distilled water were also used for various rinsing purposes during sample preparation.

4.3 Sample preparation

4.3.1 Cleaning and piranha treatment of Si surface

Si substrate was first ultrasonically cleaned with soapy water and distilled water followed by rinsing with acetone for 10 min in order to remove any foreign

particles/contaminants present on the surface. The cleaned samples were then hydroxylated by immersing in a piranha solution (a mixture of 7:3 (v/v) 98% H_2SO_4 and 30% H_2O_2) at 60-70 ^oC for 50-60 min. The objectives of piranha treatment are hydroxylation and removal of any organic/inorganic contaminants present on the surface. The Si surface was very smooth after piranha treatment (rms roughness is 0.3-0.5 nm). The samples were thoroughly rinsed with distilled water and acetone (after piranha treatment) and finally dried with N_2 gas.

4.3.2 Preparation of SAMs

The cleaned and piranha treated samples were subsequently immersed into the respective SAM solutions of APTMS or OTS with 3 mM or 5 mM concentrations, respectively, and were held for 5-6 h. A concentration of 1 vol% and a deposition time of 16 h were used for epoxy SAM formation. The depositional procedure for epoxy SAM is similar to that reported by Luzinov et al [2000] except that the present deposition was carried out in ambient atmosphere at 25 ^oC and a relative humidity of 70%. After the SAM deposition, the samples were sequentially rinsed with toluene and methanol to remove any physisorbed SAM molecules and were finally dried with N_2 gas.

Figure 2.2 shows the graphical representation of the procedure involved in the formation of SAMs by liquid process.

4.3.3 Dip-coating of PFPE onto SAMs

The custom built dip-coating machine was used to coat the PFPE onto SAMs. H-Galden was used as the solvent for PFPE and a concentration of 0.2 wt% was used. The

substrates were dipped in PFPE solution for 60 s and then withdrawn at a constant speed of 2.1 mm s^{-1}. PFPE was also coated onto Si after piranha treatment and used for comparison with PFPE coated SAMs. After PFPE coating, the samples were subjected to tribological tests without any delay to eliminate the aging effect at room temperature. To study the effect of thermal treatment on physical, chemical and tribological properties, the PFPE coated samples were heated at 150 ^{o}C for 2 h in air.

The amount of PFPE bonded (or un-bonded) to the SAM or Si surfaces is estimated from the atomic percentage of F (obtained using XPS) before and after rinsing with H-Galden. Such rinsing removes only the mobile portion (un-bonded) of PFPE whereas the chemically bonded portion remains firmly attached to the substrate. The effect of thermal treatment on the extent of bonding was also investigated by measuring the amount of PFPE bonded (or amount un-bonded).

4.4 Experimental procedures

The characterizations such as water contact angle measurements, AFM topography, ellipsometry and XPS are used to characterize the physical and chemical properties of the modified samples. For the measurement of thickness using ellipsometry, the refractive index values used for SiO_2, APTMS, OTS and epoxy SAMs and PFPE are 1.46 [Luzinov et al 2000], 1.45 [Clear and Nealey 2001], 1.424 [Aldrich® 2006], 1.429 [Luzinov et al 2000] and 1.3 [Ruhe et al 1996] respectively. The adhesion force of the selected samples is measured using AFM. Tribological properties such as coefficient of friction and wear life are measured using the micro-tribometer. All these characterization techniques have been explained in Section 3.1.

4.5 Results

4.5.1 Water contact angle results

Table 4.1 shows the water contact angles of bare Si, SAM surfaces before and after PFPE overcoating and thermally treated films.

Table 4.1*: Water contact angle values and coefficient of friction data of various surfaces studied. The variation in the water contact angles and coefficient of friction is within ±2 and ±0.05, respectively.*

Material	Water contact angle, degrees	Coefficient of friction
Bare Si	12	0.6
Si/PFPE-as lubricated	66	0.17
Si/PFPE-thermal treatment	112	0.13
Si/OTS	108	0.19
Si/OTS/PFPE-as lubricated	114	0.15
Si/OTS/PFPE-thermal treatment	110	0.13
Si/APTMS	50	0.5
Si/APTMS/PFPE-as lubricated	114	0.2
Si/APTMS/PFPE-thermal treatment	112	0.13
Si/epoxy SAM	52	0.6
Si/epoxy SAM/PFPE-as lubricated	81	0.1
Si/epoxy SAM/PFPE-thermal treatment	107	0.17

The water contact angle values of bare Si, OTS, APTMS and epoxy SAM surfaces are 12^o, 108^o, 50^o and 52^o, respectively, which suggests that OTS is hydrophobic whereas other surfaces are hydrophilic. The water contact angles of bare Si, OTS, APTMS and epoxy SAM surfaces immediately after PFPE overcoating are 66^o, 114^o, 114^o and 81^o respectively whereas thermal treatment after PFPE overcoating has shown the contact angle values as 112^o, 110^o, 112^o and 107^o, respectively. The observed differences in

water contact angle values after PFPE overcoating (and with post thermal treatment) suggest that the final wettability depends on the chemical as well as physical interactions between the SAM molecules and PFPE molecules and in turn suggests that PFPE interacts differently with different SAMs. Hydrophobicity (i.e. low surface energy) is one of the important criteria that are required for MEMS components because it can alleviate the problem of stiction arising from the capillary forces [Mastrangelo 1997 and Maboudian and Howe 1997] and the present results suggest that the PFPE coated surfaces may find applications as anti-stiction films in MEMS. Even without a SAM film, bare Si with PFPE coating and heat-treatment can provide water contact angle which is slightly higher than that of Si/OTS.

4.5.2 AFM topography results

AFM topography images of bare Si and three SAM surfaces before and after PFPE overcoating are shown in Figure 4.2 whereas the corresponding roughness values of these images are listed in Table 4.2. Table 4.2 suggests that the surface has become smoother after PFPE overcoating on all SAM surfaces with the exception of bare Si in which case the surface roughness has increased. The PFPE layer on SAM surfaces and bare Si is smooth and featureless (with the exception of epoxy SAM surface) except with few islands present at some random locations on the surface. PFPE overcoating in the case of epoxy SAM has shown the island structure which is similar to that of pristine epoxy SAM except that the PFPE layer is smoother than the epoxy SAM layer. PFPE overcoating onto epoxy SAM has marginally reduced the roughness from 0.74 nm to 0.45 nm. The present topography results suggest that PFPE overcoating onto SAMs makes the

surface more smooth (Table 4.2) which could be due to the flexible and linear PFPE molecules filling up the valleys present on the surface texture of the SAM.

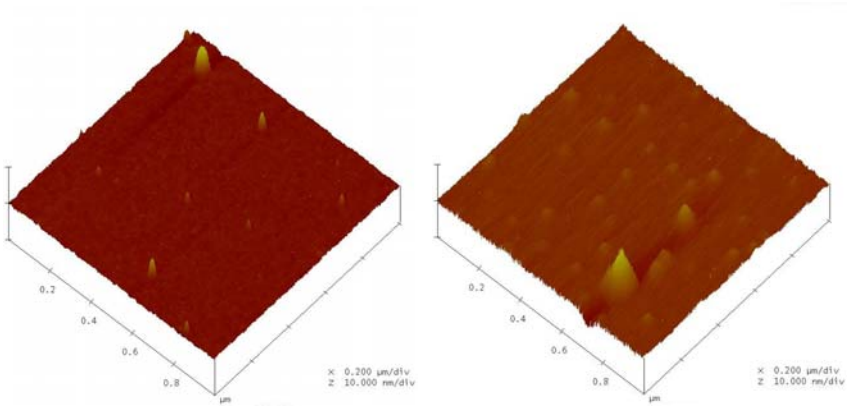

(a)

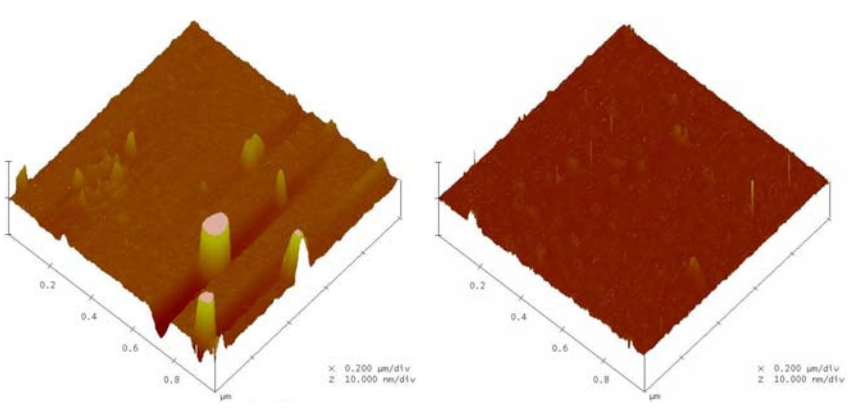

(b)

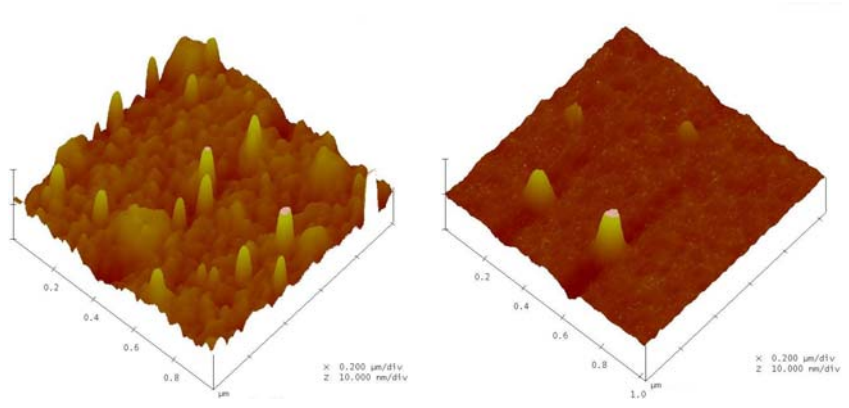

(c)

(Figure 4.2 continue to the next page)

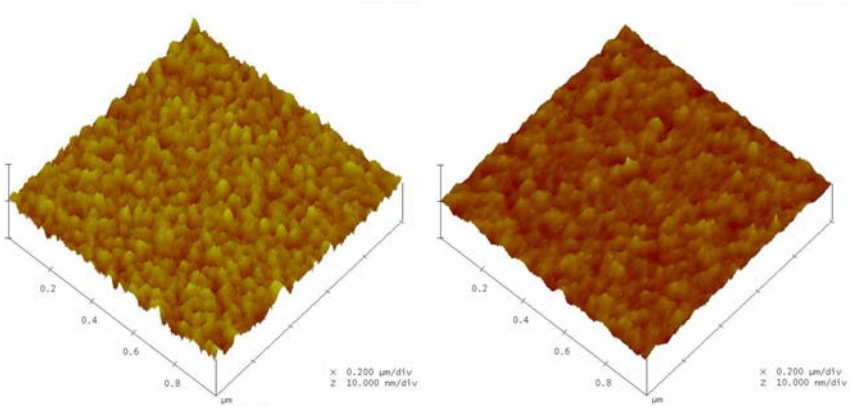

(d)

Figure 4.2: *AFM images of (a) Bare Si, (b) Si/OTS, (c) Si/APTMS and (d) Si/epoxy SAM, before (left image) and after coating with PFPE (right image). The vertical scale is 10 nm in all images.*

Table 4.2*: Surface roughness values obtained from AFM over 1 µm x 1 µm.*

Sample	Roughness, nm
Bare Si	0.31
Si/PFPE	0.638
Si/OTS	1.957
Si/OTS/PFPE	0.3
Si/APTMS	1.7
Si/APTMS/PFPE	1.048
Si/epoxy SAM	0.74
Si/epoxy SAM/PFPE	0.45

4.5.3 Thickness results

The silicon oxide, after piranha treatment, has shown a thickness of ~2 nm whereas OTS, APTMS and epoxy SAMs have shown thickness values as 2.9 nm, 4.1 nm and ~7 nm respectively. The thickness of silicon oxide and OTS SAM are in good agreement with those values reported by Clear and Nealey [2001]. In the case of APTMS and epoxy SAMs, the present thickness values are slightly higher than the corresponding

theoretical monolayer thicknesses which are attributed to the formation of multilayers because of the high humidity in the ambient condition. Similar formation of multilayers has been observed by Zhang and Srinivasan [2004] and by Luzinov et al [2000] in the cases of APTMS and epoxy SAMs respectively. As-lubricated PFPE film on bare Si and APTMS SAMs has shown a thickness of 1.7 nm whereas in the cases of OTS and epoxy SAMs, it has shown thickness values of 1.6 nm and 1.4 nm, respectively.

4.5.4 XPS results

The purposes of XPS characterization are, to confirm the successful deposition of the target film, to investigate the chemical state of SAM molecules before and after PFPE overcoating, and, to study the chemical interactions between SAM and PFPE molecules. For example, the amount of PFPE bonded with the SAM molecules before and after thermal treatment can be obtained from XPS data. The wide scan spectrum of bare Si and SAMs modified Si is shown in Figure 4.3 (a) whereas wide scan spectrum of PFPE overcoated SAMs and Si is shown in Figure 4.3 (b). The wide scan spectrum shown in Figure 4.3 (a) qualitatively confirms the successful formation of respective SAMs on Si. For example, the N1s peak appeared for APTMS SAM (originated from amine groups of APTMS molecules), confirms its successful formation and also the presence of F1s peaks on all PFPE coated surfaces support the presence of PFPE molecules.

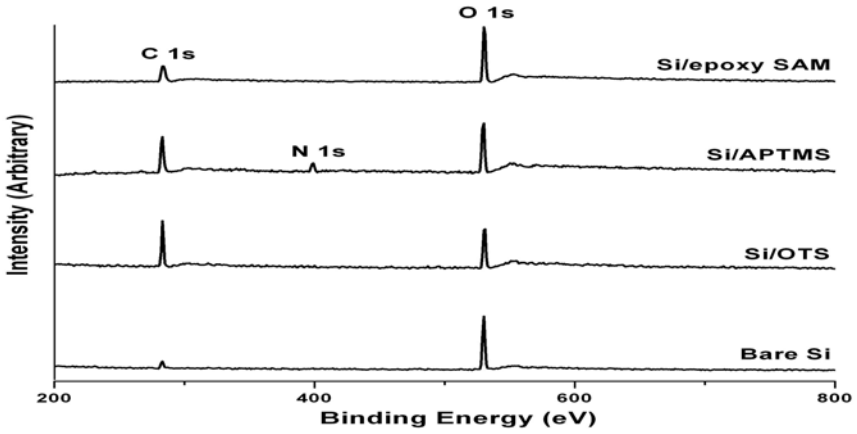

(a)

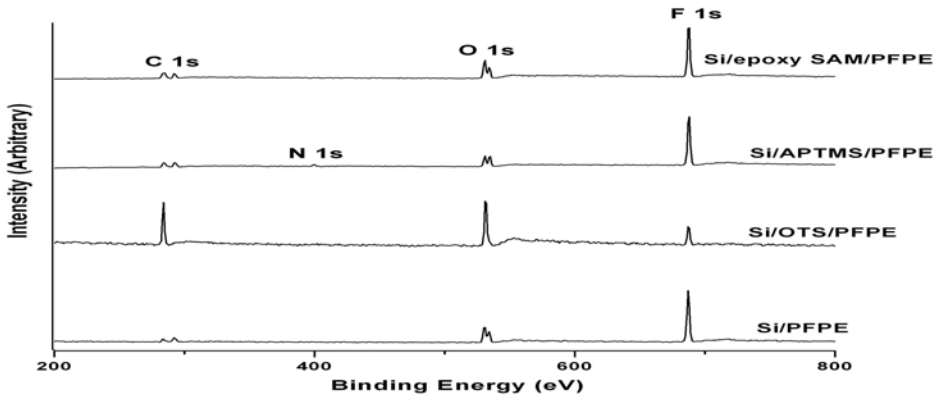

(b)

Figure 4.3: *(a) Wide scan spectrum of the SAMs modified and un-modified Si surface, (b) Wide scan spectrum of PFPE overcoated SAMs such as OTS, APTMS and epoxy SAM and un-modified Si surface.*

The atomic percentages of fluorine (F) obtained from XPS data on, as lubricated PFPE, as lubricated PFPE + rinsed, thermally treated PFPE + rinsed on all SAMs and bare Si are shown in Table 4.3. The atomic percentages of F, as listed in the Table 4.3, are used to estimate the amount of bonded PFPE [Zhu et al 2003].

Table 4.3: *%F obtained from XPS analysis of modified and un-modified Si surface*

Substrate	%F
Si/PFPE-as lubricated	40.00
Si/PFPE-as lubricated+rinsed	12.00
Si/PFPE- thermal treatment+rinsed	26.90
Si/OTS/PFPE- as lubricated	7.81
Si/OTS/PFPE-as lubricated+rinsed	0.23
Si/OTS/PFPE-thermal treatment+rinsed	1.22
Si/APTMS/PFPE-as lubricated	41.23
Si/APTMS/PFPE-as lubricated+rinsed	25.00
Si/APTMS/PFPE-thermal treatment+rinsed	27.00
Si/epoxy SAM/PFPE-as lubricated	47.30
Si/epoxy SAM/PFPE-as lubricated+rinsed	12.18
Si/epoxy SAM/PFPE- thermal treatment+rinsed	37.80

PFPE coating onto OTS SAM has shown the lowest atomic percent of F (7.8%) than other two SAMs and bare Si, which suggests that the amount of PFPE present on OTS SAM is less when compared to the other two SAMs and bare Si. XPS results suggest that approximately 60% of PFPE remains on the APTMS SAM surface and ~30% each on epoxy SAM and bare Si whereas a negligible (~3%) amount of PFPE remains on OTS surfaces after rinsing. The PFPE remaining on the bare Si and APTMS SAM surfaces after rinsing is bonded through hydrogen (H)-bonding whereas in the case of Si/epoxy SAM, the PFPE is bonded covalently [Ellis 1993 and Elender et al 1996]. In the case of OTS SAM, the entire PFPE has been removed during rinsing (as there is no bonding between OTS and PFPE molecules) suggesting that entire PFPE present on OTS SAM is mobile in nature. The strongly adsorbed as well as mobile PFPE have implications on tribological properties, especially on wear durability, which will be discussed in latter

sections. Table 4.3 also suggests that the amount of PFPE remaining after rinsing of thermally treated PFPE was 65% on APTMS SAM, 80% on epoxy SAM, 15% on OTS SAM and 67% on bare Si. It is evident from the XPS results that the thermal treatment improves the extent of bonding between PFPE and reactive SAM molecules and Si. Thermal treatment has greatly increased the amount of PFPE bonding in the case of epoxy SAM (30% to 80%) and bare Si (30% to 67%) whereas there was not much improvement in bonding in the case of APTMS SAM (60.6% to 65.5%). The reduction in the extent of hydrogen bonding in the case of amine groups with the increase in temperature above 50-70^{o}C has been observed and the same phenomenon is attributed for the marginal improvement in the bonding between APTMS SAM and PFPE by heating at high temperature [Tang et al 2002 and Skrovanek et al 1985].

4.5.5 Tribological results

4.5.5.1 Adhesion force results for Si/epoxy SAM/PFPE

In the present section, the adhesion force values (measured using AFM) obtained for PPFE overcoated epoxy SAM are explained. For reliable comparison of adhesion force values of different samples, the measurements on all samples must be carried out with the same tip, but this restriction poses other challenges such as tip wear which may lead to errors in the measurements. To avoid the tip wear problems and obtain the reliable adhesion force values, the present measurements are carried out on only one pair of SAM (epoxy) and PFPE system and results compared. Force vs displacement curves for bare Si, epoxy SAM with and without PFPE overcoat and with post thermal treatment after

PFPE overcoating are shown in Figure 4.4 (a) whereas Figure 4.4 (b) shows the quantitative adhesion force (nN) data.

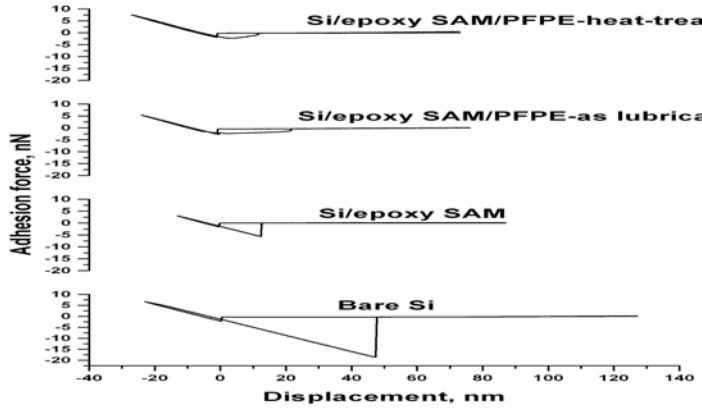

(a)

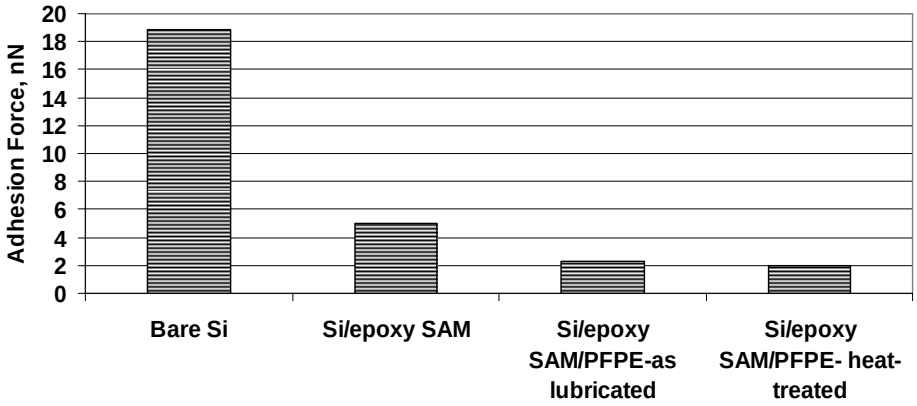

(b)

Figure 4.4: *(a) Adhesion force vs displacement curves for bare Si, Si/epoxy SAM, Si/epoxy SAM/PFPE-as lubricated and Si/epoxy SAM/PFPE-thermally treated and (b) quantitative adhesion force values (nN) for those samples shown in (a).*

Among the four samples tested, bare Si has shown the highest adhesion force and deposition of epoxy SAM has considerably reduced the adhesion force of bare Si. PFPE coating onto epoxy SAM further reduced its adhesion force but the post-thermal treatment did not show any further change in the adhesion force. The trend observed for

the adhesion forces for various samples (bare Si > Si/epoxy SAM > Si/epoxy SAM/PFPE-as lubricated > Si/epoxy SAM/PFPE-thermally treated) is opposite to the trend observed for the water contact angles (bare Si < Si/epoxy SAM < Si/epoxy SAM/PFPE-as lubricated < Si/epoxy SAM/PFPE-thermally treated). The observed relation is consistent with the literature [Bhushan et al 2004 (b), Bhushan and Liu 2001] and can be attributed to the linear relation between adhesion force and surface energy [Israelachvili 1991]. The reduction (6-8 times) in the adhesion force in the case of PFPE coated epoxy SAM is comparable to that observed for PFPE overcoated Si surface [Blackman et al 1990] in which case the PFPE overcoating has reduced the adhesion force of un-modified Si by approximately 5 times.

The adhesion force value of bare Si observed in the present study (~18 nN) is lower than that observed in the literature (~70 nN) for similar cleaning and hydroxylation processes [Ren et al 2004] and the reasons for this behavior are differences in the experimental parameters between the two studies. The relative humidity in our experiments (~17%) is less than that used by Ren et al [2004] (~65%) which will reduce the contribution from capillary forces and moreover, the tip radius is also less (~25 nm) in our study than that used in their study (~50 nm). Therefore, low humidity and smaller tip radius has shown lower adhesion forces for Si in the present study than that reported in the literature [Ruhe et al 2004]. Bhushan and Dandavate [2000] have studied the effect of the relative humidity and tip size on the adhesion force of Z-dol (PFPE) layer on Si surface and have observed that the adhesion force increases as the relative humidity and tip size increases.

The four major forces that contribute to adhesion force are molecular forces (e. g. van der Waals forces), electrostatic forces, capillary forces and forces due to excess charges, among which capillary forces contribute the most [Israelachvili 1991, Scherge and Gorb 2001]. But, the relative contribution from each force can only be measured when forces other than the one to be measured are made ineffective through proper selection of experimental parameters [Weisenhorn et al 1989 and Hayashi et al 2002]. However, under the present conditions of adhesion force measurements individual contribution of each force cannot be quantified, as we have not isolated the effect of remaining forces. But the opposite relation between water contact angles and adhesion forces implies that the capillary forces contribute most to the adhesion force observed in the present study, because the adsorbed water on surfaces with higher surface energy (hydrophilic) leads to meniscus forces (capillary) [Israelachvili 1991, Scherge and Gorb 2001].

4.5.5.2 Coefficient of friction and wear durability results

Table 4.1 shows the coefficient of friction values of unmodified Si and suitably modified Si surfaces measured in sliding tests at a fixed contact pressure of ~330 MPa. Before PFPE overcoating, bare Si and two hydrophilic SAMs have shown coefficients of friction in the range of 0.5-0.6 whereas OTS SAM has shown a value of 0.18. OTS SAM has shown the lowest coefficient of friction among the three SAM surfaces studied showing a remarkable decrease in the friction of bare Si [Satyanarayana et al 2004]. PFPE overcoating onto three SAMs and bare Si has shown coefficients of friction in the range of 0.1-0.2 which is apparently independent of the surface condition before coating.

The ranking of the coefficients of friction of different films in the order from high to low is observed as: bare Si = Si/epoxy SAM > Si/APTMS > Si/APTMS/PFPE > Si/OTS > Si/PFPE > Si/OTS/PFPE > Si/epoxy SAM/PFPE. The thermal treatment after PFPE overcoating has shown a coefficient of friction of 0.13 in the cases of OTS, APTMS and bare Si whereas it has shown a value of 0.17 in the case of epoxy SAM.

Figure 4.5 (a) shows some typical plots of coefficient of friction versus number of cycles in the sliding tests and Figure 4.5 (b) shows the quantitative wear life data (along with error bars) for various samples. Large scatter in the data in some of the tests are due to the sensitivity of the thin-film lubrication to the experimental conditions and are comparable with the findings in the literature [Ruhe et al 1993, 1996 and Zarrad et al 1995]. Also, it is seen that the scatter is wide for cases where the friction coefficients are relatively large. Before PFPE overcoating, bare Si and two hydrophilic SAM surfaces have shown higher initial coefficients of friction and failed within few tens of sliding cycles whereas OTS SAM has shown a wear life of ~1600 cycles [Satyanarayana et al 2004]. The tribological properties of the bare Si and three SAM surfaces are consistent with the literature results obtained with similar kind of sliding tests [Sidorenko et al 2002, Ruhe et al 1993 and Ren et al 2003]. Overall, there is an increase in wear durability when PFPE was coated onto three SAMs and bare Si. There is an appreciable improvement in the wear durability when PFPE is coated onto the bare Si, APTMS and epoxy SAM surfaces, whereas a minor increase is noticed when PFPE is coated onto OTS SAM. The average wear lives of bare Si, OTS, APTMS and epoxy SAMs after PFPE overcoating as observed in our experiments are 5000, 2500, 5200 and 6900 respectively.

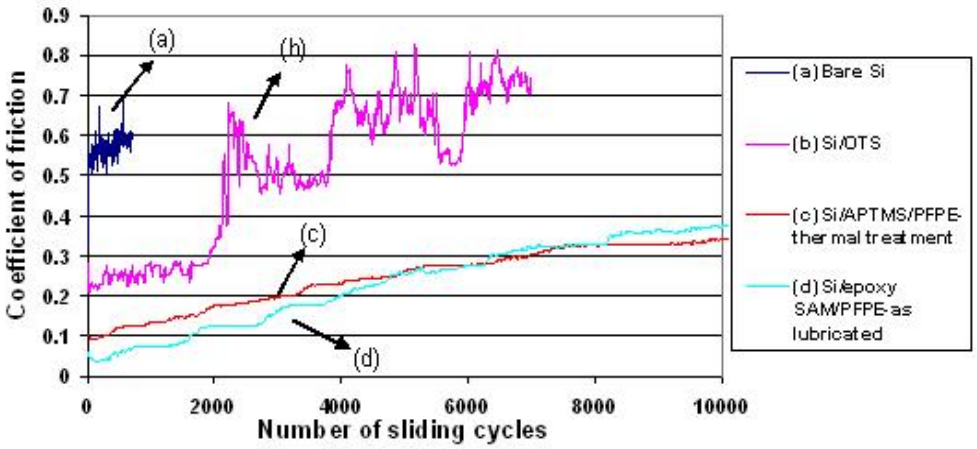

(a)

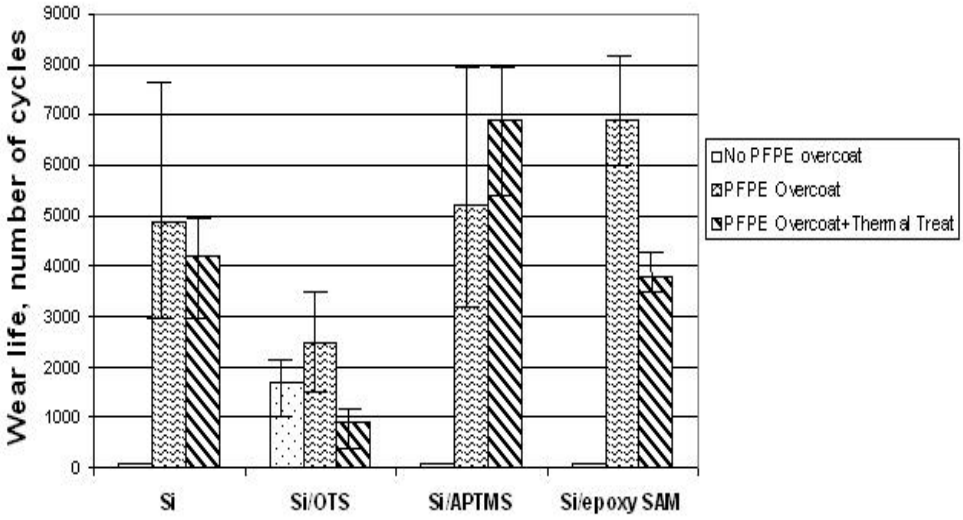

(b)

Figure 4.5: *(a) The variation of coefficient of friction with respect to number of sliding cycles for bare Si, Si/OTS, Si/APTMS/PFPE-thermally treated and Si/epoxy SAM/PFPE-as lubricated, (b) Average wear life data of three SAM surfaces and bare Si, with and without PFPE overcoat and after thermal treatment.*

The observed wear durability data suggests that the extent of improvement in wear resistance is more when PFPE is coated onto hydrophilic SAMs (APTMS and epoxy) than when coated onto hydrophobic SAM (OTS) even though hydrophobic SAM has

shown higher wear durability than that of hydrophilic SAMs without PFPE overcoating. The rankings of the wear lives of all surfaces (from most wear durable to the least) are as follows: Si/epoxy SAM/PFPE > Si/APTMS/PFPE > Si/PFPE > Si/OTS/PFPE > OTS SAM > APTMS SAM or epoxy SAM or bare Si.

Thermal treatment after PFPE overcoating has shown an increase of ~30% in wear life in the case of APTMS SAM whereas it reduced the wear life in the cases of epoxy SAM, OTS SAM and Si surface. The wear life values after thermal treatment of PFPE overcoated Si, OTS, APTMS and epoxy SAMs are 4200, 900, 6900 and 3800 respectively.

4.5.6 Analysis of wear tracks using optical microscopy

Figure 4.6 shows the optical micrographs of wear tracks after an appropriate number of sliding cycles for the bare Si, Si/APTMS/PFPE-thermally treated and Si/epoxy SAM/PFPE-as lubricated samples. After ~700 cycles of sliding, bare Si shows the generation of wear debris along the wear track and severe damage to the Si surface. The wear debris accumulated along the wear track must have been generated by the fracture of the Si surface which has typical brittle fracture behavior.

(a)

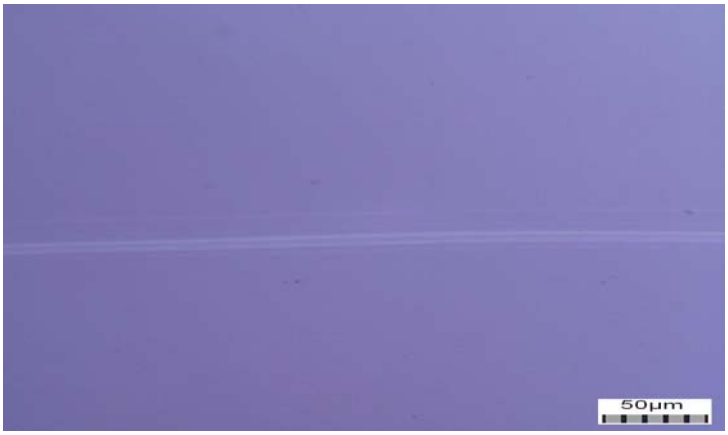

(b)

(c)

Figure 4.6: *Optical micrographs of worn surfaces after appropriate number of cycles. (a) bare Si, run upto 700 cycles, (b) Si/APTMS/PFPE-thermally treated, run upto ~14000 cycles and (c) Si/epoxy SAM/PFPE-as lubricated, run upto 5000 cycles of sliding.*

There is no wear to the Si surface in the case of thermally treated PFPE coated APTMS SAM surface even after ~14,000 sliding cycles as evident in the optical micrograph shown in Figure 4.6 (b). The wear track only shows signs of initiation of mild scratching and supports the potential of thermally treated PFPE coated APTMS SAM in enhancing wear durability. The wear track in the case of Si/epoxy SAM/PFPE-as-lubricated after 5000 cycles (Figure 4.6 (c)) is also very smooth without the presence of any wear debris and shows the beginning of mild scratching.

4.6 Discussion

4.6.1 Effect of PFPE coating onto bare Si

PFPE coating onto Si has reduced the coefficient of friction from 0.6 to 0.16 and increased the wear life from few tens of cycles to ~5000 cycles which are in good agreement with the results observed by Ruhe et al [1996]. The reasons for the improved tribological properties are low surface energy after PFPE coating (which eventually reduces the coefficient of friction [Makkonen 2004]) and little resistance offered by the flexible and mobile polymer molecules of PFPE during sliding [Mate 1992]. PFPE is a linear fluorinated hydrocarbon which acts as an excellent lubricant in bulk liquid or thin film form.

4.6.2 Tribology of SAMs with and without PFPE overcoat

The coefficient of friction has been reduced after PFPE coating onto SAM surfaces (Table 4.1) which is almost identical (0.1-0.2) in all cases and independent of the initial coefficient of friction of SAM surfaces. The coefficient of friction was measured

after initial 6 number of cycles of disk rotation. The reason for this behavior is that the top PFPE layer (which is same in all cases) influences the initial coefficient of friction regardless of underneath SAM.

The sliding wear test results suggest that PFPE overcoating onto SAMs (hydrophilic and hydrophobic) has enhanced the wear durability of SAMs which is attributed to the additional lubrication from the mobile and bonded fractions of PFPE. It is anticipated that in a sliding wear test involving PFPE overcoated SAMs, the mobile PFPE is initially squeezed and removed from the contact. After the removal of mobile PFPE, the strongly bonded (H-bonding or covalent bonding) PFPE provides further lubrication and protects the surface. Finally, after the complete removal of mobile and bonded PFPE, SAM molecules protect the substrate underneath.

We further believe that, when PFPE is coated onto hydrophilic SAM surfaces, a part of PFPE is trapped inside the valleys between SAM molecules, a part is strongly adsorbed (through hydrogen or covalent bonding) and the remaining portion is present as mobile PFPE. In fact, XPS measurements suggest that a portion of PFPE is strongly adsorbed through hydrogen bonding in the case of bare Si and APTMS SAM and covalent bonding in the case of epoxy SAM whereas no portion of PFPE is bonded with OTS SAM because of the non-polar methyl (CH_3) groups of OTS molecules. As APTMS SAM, and to some extent, epoxy SAM, contains defect regions or valleys between various islands of SAM molecules (Figure 4.2), a portion of PFPE will naturally get trap into these valleys and the remaining portion of PFPE stays as a mobile layer. As the surface of Si is very flat and smooth, no trapping of PFPE is expected and all un-bonded PFPE is present as mobile layer. Negligible trapping of PFPE is expected in the case of

OTS SAM also because of its higher molecular packing density* [Lio et al 1997] and absence of any valleys. It is hypothesized that all the three portions of PFPE (the mobile, the bonded and the mechanically trapped PFPE molecules) influence the wear durability in the case of PFPE overcoated SAMs and Si. The interactions between PFPE and SAM molecules are schematically illustrated in a molecular model shown in Figure 4.7, which is adopted based on the model presented by Choi and Kato [2003] with further modifications. The thick lines in the molecular model represent strongly adsorbed PFPE whereas thin lines represent mobile (or un-bonded) PFPE.

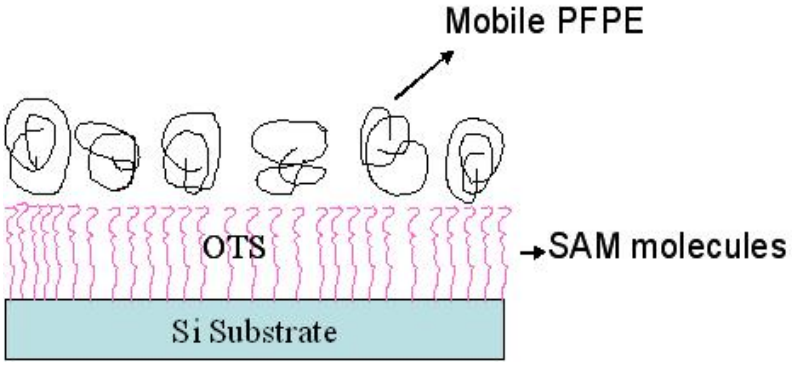

(a)

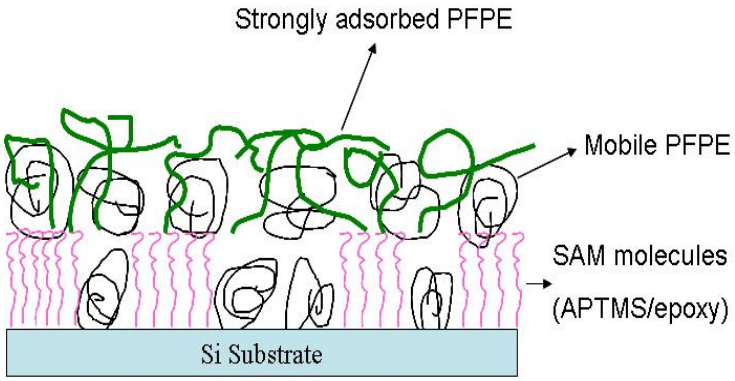

(b)

Figure 4.7*: Molecular model of PFPE on (a) OTS SAM and (b) APTMS/epoxy SAM (refer text for details). Thicker lines in (b) are used for strongly adsorbed and thinner lines for mobile PFPE molecules.*

* *The packing density of SAM is defined as the number of SAM molecules per unit area. The packing density of OTS SAM is 5.42 chains/nm^2 or an average area per molecule of ~0.2 nm^2/molecule [Parikh et al 1994].*

It is evident from the molecular model that an optimum combination of mobility, entrapment and bonding of PFPE led to a greater increase in the wear durability in the case of PFPE overcoating onto hydrophilic APTMS and epoxy SAM surfaces. Moreover, in the case of APTMS and epoxy SAMs, the PFPE fraction that is trapped inside the valleys lubricates the contact through squeezing action during sliding. The beneficial effect of trapped PFPE may appear similar to the effect of boundary lubrication on etched and textured surfaces [Pettersson and Jacobson 2003]. In a study by Pettersson and Jacobson [2003], it has been observed that when a lubricant was applied onto a textured surface, the lubricant filled the depressions or undulations (intentionally made) which acted as a reservoir and finally helped in reducing the friction and increasing the lifetime of the tribological contact. It was further observed that the improvement in tribological properties depended on the size and shape of the depressions and the type of hard coating beneath the lubricant layer. However, the present concept of overcoating PFPE onto SAM surfaces differs in several aspects when compared to the published work (on texture effect under boundary lubrication). The amount of lubricant used in the present work is much smaller (only few nanometers thick) when compared to that used in the published work and also the size of the valleys between the APTMS/epoxy SAM islands (one to few hundreds of nanometers) are smaller than the depressions used in the published work (5-20 μm). Moreover, the chemical interactions between PFPE and SAM molecules in the present case make a major difference. Therefore, the present comparison concludes that the entrapment of PFPE in the case of APTMS/epoxy SAM is very different when compared to a simple texturing effect.

Among APTMS and epoxy SAMs, PFPE coating onto epoxy SAM has shown higher wear life (about ~25% more) than when coated onto APTMS SAM and the specific chemical interactions between PFPE and epoxy molecules must have led to this increase in wear durability. It is evident from XPS results that less amount of PFPE is bonded with epoxy SAM (covalently) whereas more amount of PFPE is bonded with APTMS SAM (through hydrogen bonds). In other words, relatively more amount of mobile PFPE is present on epoxy SAM when compared to that on APTMS SAM. Therefore, an optimum combination of covalent bonding between PFPE and epoxy molecules and higher amount of mobile PFPE could lead to higher durability in the case of Si/epoxy SAM/PFPE when compared to Si/APTMS/PFPE.

There was very minimal increase in wear durability in the case of PFPE coated OTS SAM and the reasons for this behavior could be the lower amount of PFPE present, lack of bonding between the PFPE and SAM molecules and the absence of the trapping of the PFPE molecules inside OTS SAM due to high molecular packing density. The PFPE overcoating onto bare Si also has shown good improvement in wear durability (because of an optimum combination of mobile and hydrogen bonded PFPE) which is approximately similar to that of Si/APTMS/PFPE.

It is not evident whether the replenishment characteristics of PFPE helped for high wear durability observed in the present sliding tests. The replenishment ability of PFPE on a particular SAM can be estimated if the critical reflow time of PFPE on the SAM is known [Tani and Matsumoto 2001], but these values (either theoretical or experimental) are not available. In the present sliding tests, the time for one revolution is 0.6 s and the critical reflow time of PFPE on a particular SAM must be less than 0.6 s for

replenishment of PFPE to take effect. As the critical reflow time of PFPE on the presently studied SAMs is not available, we can not precisely conclude anything about the replenishment characteristics of PFPE on SAMs. It is possible that there is only minor effect of replenishment that takes place near the edges of the wear track.

The reasons for good lubrication property of PFPE molecules is not well explained/understood and it may be attributed to its linear and "smooth molecular profile" as evidenced by the molecular scale friction study by Pooley and Tabor [1972]. They identified that the polymers with linear chain and without having the bulky side groups such as PTFE and HDPE have shown good lubrication properties when compared to LDPE, PVC, PS etc. The PFPE molecules are similar to that of PTFE because both have common CF_2 chemical groups in their backbone and both have linear molecular structure. PFPE is effectively a liquid form of PTFE which shows very low coefficient of friction even in solid state.

As evident from the optical micrographs of wear tracks shown in Figure 4.6, the PFPE overcoating onto SAMs protects the Si surface without the generation of wear particles for many extended cycles of sliding. Generation of wear debris during MEMS (or micro motors) operation is strictly undesirable as they hinder the smooth operation of the sliding components and hence the coatings for MEMS lubrication must not generate any wear debris [Patton et al 2000].

4.6.3 Effect of thermal treatment

Thermal treatment after PFPE overcoating onto epoxy SAM and Si has increased water contact angle values from 81^o to 107^o and from 66^o to 114^o, respectively, whereas,

PFPE on OTS SAM and APTMS SAM did not show any change in the contact angles due to thermal treatment. Thermal treatment of PFPE overcoated surfaces influence its chemical interactions with the underlying surface and may evaporate lower molecular weight fractions and result in an increase of the molecular weight of the polymer [Ruhe et al 1994]. There was an increase in the water contact angle values of PFPE coated epoxy SAM and bare Si after thermal treatment as thermal treatment increases the bonded fraction of PFPE in these two SAMs (which in turn reduces hydroxyl groups of PFPE which usually attracts water molecules) and increases the density of the polymer molecules.

Thermal treatment has increased the wear life of PFPE coated APTMS SAM (~30%) and reduced the same in the cases of OTS and epoxy SAMs and bare Si (Figure 4.5 (b)). It is evident from XPS results (Table 4.3) that there is a very minimal increase in the bonded fraction of PFPE due to the thermal treatment in the case of PFPE coated APTMS SAM and great increase in the case of PFPE coated epoxy SAM and bare Si which in turn suggests that the mobile fraction of PFPE on epoxy SAM and bare Si reduced after thermal treatment. Therefore, the variations in wear life data after thermal treatment are attributed to the changes in the mobile and bonded fractions of PFPE due to thermal treatment. Further studies are needed to quantify the actual effect of bonded and mobile fractions of PFPE on the final wear durability results with and without thermal treatment. In general, the presence of optimum amount of bonded and mobile fractions of PFPE is required for high wear life.

4.7 Conclusions

The conclusions based on the present study are summarized below:

1) PFPE overcoating onto hydrophilic (or chemically reactive due to functional groups) SAMs has made the surface less wettable to water and the extent of increase in water contact angle values is different for different SAMs and depends on the specific interactions between the PFPE and SAM molecules.

2) The chemical interactions between PFPE and SAMs depend on the terminal group chemistry of SAMs and these interactions will influence the amount of bonded PFPE (or the amount present as a mobile layer).

3) PFPE is effective in reducing the adhesion force and coefficient of friction of SAM surfaces. The coefficient of friction has been reduced to 0.1-0.2 when PFPE is coated onto all SAMs studied.

4) The wear durability has been improved (in all cases) when PFPE is coated onto SAM surfaces but the extent of improvement is different for different SAMs and depends on the SAM surface properties such as wettability, chemical interactions between SAM and PFPE molecules, molecular packing density and order in the SAM molecules. There was excellent improvement in wear durability in the case of reactive SAMs (such as APTMS and epoxy) and very minimal improvement in the case of OTS SAM, after PFPE overcoating.

5) Post thermal treatment of PFPE coated SAMs has further influenced the chemical interactions between PFPE and SAM molecules. Thermal treatment has increased the wear durability in the case of Si/APTMS/PFPE whereas it reduced wear durability in all other cases studied.

6) An optimum ratio of chemically bonded and mobile PFPE molecules on SAM surface is necessary for long wear life.

7) Overall, Si/APTMS/PFPE-thermally treated and Si/epoxy SAM/PFPE- as lubricated have shown best performances as far as wear durability is concerned.

Chapter 5

Deposition and tribological properties of novel UHMWPE films coated onto Si surface: Effect of PFPE overcoating

5.1 Deposition and tribological properties of novel UHMWPE films coated onto Si surface

5.1.1 Background

Polymers in the bulk form have numerous tribological applications ranging from tyre material (high friction) to many bearing materials (low friction). In the bulk form, UHMWPE is highly wear resistant compared to many other polymers such as PEEK, LDPE, PS, PMMA etc [Sinha 2002]. UHMWPE has shown low coefficient of friction and high wear resistance because of its extremely long and highly entangled molecular chains [Wang et al 1998]. An UHMWPE molecule consists of large number of repeating units of ethylene monomers where the backbone structure of the molecule is the C-C covalent bond. Therefore, it is expected that if an ultra-thin film of UHMWPE is formed on the Si surface, it will protect the Si surface from wear and tear and reduce the friction. There are no studies in the literature involving the formation of ultra-thin UHMWPE films on Si surface. A recent study by Bao et al [2005] has shown the deposition of UHMWPE coatings on steel substrate using thermal spray deposition for corrosion resistance applications. But such thermal spray processes are very expensive and often not practical to coat on complicated structures. Therefore, we study the feasibility of coating UHMWPE films on Si surface by a simple dip-coating technique [Satyanarayana et al 2006]. Dip-coating technique is routinely used to obtain ultra-thin lubrication

coatings of PFPE on hard-disk surface [Bhushan 1996]. Dip-coating has been used also for the formation of some polymer thin films [Braun and Meyer 1999 and Maas et al 2000], for example polystyrene thin films onto micro-textured Si surface [Braun and Meyer 1999]. Therefore, one of the novelties of the present work is the establishment of a dip-coating method to apply thin UHMWPE films (sub-micron to few tens of microns) onto Si surface. The challenges in the present study are selection of a suitable solvent and optimization of the various parameters such as complete dissolution of the polymer in the solvent, concentration, dipping time and post-thermal treatment in order to obtain uniform and defect free UHMWPE films on Si surface.

Further, one strategy is proposed to enhance the wear durability of pristine UHMWPE films on Si surface and that is by overcoating an ultra-thin film of PFPE layer as top lubricating layer. The results on the effects of PFPE overcoating on UHMWPE film are presented in Section 5.2.

5.1.2 Materials

GUR X143 UHMWPE polymer powder (obtained from Ticona Engineering Polymers, Germany through a local Singapore supplier) was used for the formation of UHMWPE film on Si surface. Table 5.1 shows the physical properties of UHMWPE, as provided by the supplier.

Table 5.1*: Properties of UHMWPE powder*

Property	Units	Value
Bulk Density	g/cm^3	0.33 ± 0.03
Average particle size d_{50}	µm	20 ± 5
Melting temperature	^oC	130-135

After several trials with many solvents, decahydronapthalin (decalin) was selected as a suitable solvent to dissolve UHMWPE.

5.1.3 Preparation of UHMWPE film on Si surface

The procedure of cleaning and piranha treatment of the Si wafer is reported in Section 4.3.1.

Firstly, the polymer solution was prepared by dissolving the UHMWPE powder in decalin through heating at a temperature of 150 ^{o}C for half an hour and at 250 ^{o}C for the next half an hour. Magnetic stirring was used (along with heating) to enhance the rate of dissolution and ensure complete and uniform dissolution of the polymer. A custom built dip-coating machine was used for depositing the polymer thin film and coating was carried out immediately after ensuring the complete dissolution of polymer powder. The withdrawal speed used during dip-coating was 2.1 mm s^{-1} and the dipping time was fixed as 30 s. The polymer coated samples were briefly dried in air and then heat-treated at a temperature of ~100 ^{o}C for about 20 h in a clean air furnace. After the thermal treatment, the samples were slowly cooled to room temperature in the furnace itself and then stored in desciccator until any surface or tribological characterization.

5.1.4 Experimental procedures

Surface characterizations such as water contact angle measurement, AFM topography, SEM morphology, XPS, FTIR are used to measure the properties of the thin films formed. Tribological properties are measured using a micro-tribometer. All these characterization techniques are explained in Section 3.3. Nano-mechanical properties

(Elastic modulus and hardness) are measured using Nano Indenter XP which is explained in Section 3.3.9. The thickness of the polymer was estimated from the cross section observation through SEM [Kuypers et al 2005].

AFM and SEM are used to characterize the wear tracks after sliding tests.

5.1.5 Results and Discussion

5.1.5.1 Physical characteristics of the dual-layer film

The water contact angles of bare Si, Si/UHMWPE and bulk UHMWPE polymer samples are shown in Table 5.2.

***Table 5.2**: Water contact angles of bare Si, Si/UHMWPE and bulk UHMWPE samples used in the present study and literature results.*

Sample	Water contact angle, deg	Reference
Bare Si	12	Present Study
Si/UHMWPE	127	"
Bulk UHMWPE	107	"
Bulk UHMWPE	87	[Heuberger et al 2005]
Bulk UHMWPE	90	[Chen et al 2003]

The coating of UHMWPE film onto Si surface changed the water contact angle from 12^o to 127^o and made Si surface more hydrophobic (water repellant). Table 5.2 also shows the water contact angle values of bulk UHMWPE (obtained in the present study and literature) and the variations (10-20 degrees) in the contact angles of various bulk UHMWPE samples (present study and literature) are due to the differences in their grades and surface conditions [Torrisi 2003]. The water contact angle of the UHMWPE film on Si surface is ~20^o higher than that of bulk UHMWPE solid surface (of present

work) and the reasons are explained based on the differences in the surface roughness values, which are explained later. The high water contact angle of UHMWPE film supports that the chemical state of the film is similar to that of the bulk UHMWPE. This means that neither the solvent nor the thermal treatment changed the polymer in any way.

The surface morphology of the UHMWPE film on Si (obtained with SEM) is shown in Figure 5.1 (a) and depicts uniformly dispersed polymer chains/fibers protruding to the surface and the presence of valleys in between them. Figure 5.1 (b) shows the AFM topography image (along with a typical line profile) of UHMWPE film over a scan area of 40 μm x 40 μm. The AFM image (along with line scan) shows the presence of islands and valleys of few microns size with an overall rms roughness of 0.556 μm (over 40 μm x 40 μm scan area). Figure 5.1 (c) shows the AFM image and line profile of a bulk UHMWPE solid surface. The bulk UHMWPE surface was subjected to fine polishing before imaging.

The features on bulk UHMWPE are very flat and smooth when compared to those on the UHMWPE film. The rms roughness of the bulk UHMWPE is 0.332 μm, which is less than that of the UHMWPE film (0.556 μm). Therefore, the rough and uneven features of UHMWPE film are believed to be the primary reason for higher water contact angle of the film when compared to the bulk polymer in spite of the same chemical structure/nature of the two. It is observed and well explained in the literature that the water contact angle value is higher for surfaces with large roughnesses and those containing needle-like peaks [Miwa et al 2000 and references there in, Osawa et al 2006 and Jung and Bhushan 2006].

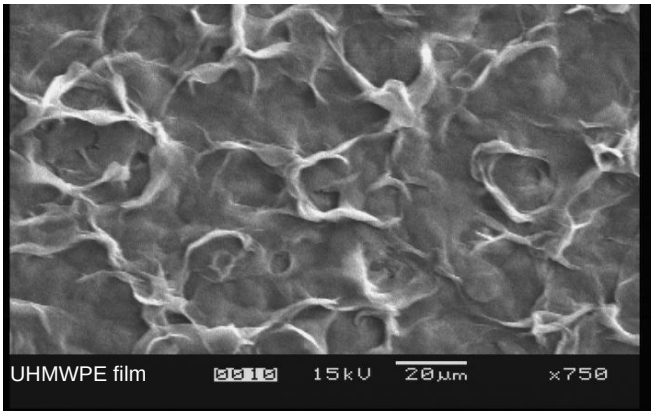

(a)

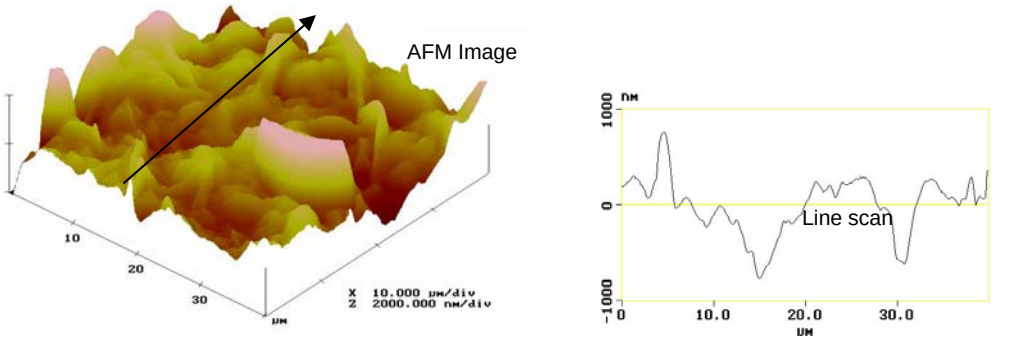

(b)

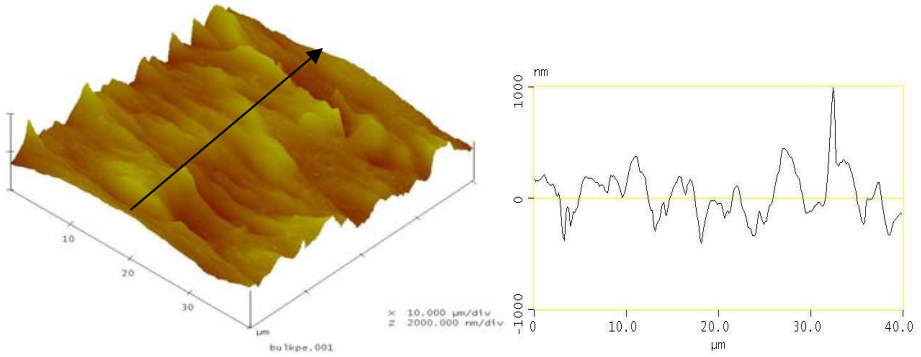

(c)

***Figure 5.1**: (a) SEM morphology of the UHMWPE film on Si surface. It is similar to the structure of bulk UHMWPE. (b) AFM image of the Si/UHMWPE surface with a scan size of 40 µm x 40 µm. The arrow on the 3-dimensional (3D) image shows the location and direction of the line profile shown adjacent to it. (c) AFM image of the bulk UHMWPE with a scan size of 40 µm x 40 µm. A representative line profile on the surface is shown adjacent to it.*

The thickness of the UHMWPE film formed according to the present experimental conditions is 28 μm which is measured by breaking a coated Si wafer and imaging the cross-section inside a SEM.

The mechanical stability of the UHMWPE film on Si surface was studied by subjecting the film coated samples to ultrasonication in decalin (the solvent). The changes in the surface morphology due to ultrasonication for 5, 30 and 100 min were observed using optical microscopy and are shown in Figure 5.2. Care was taken to obtain the images at the same spot of the specimen to see the progress of film removal from the substrate, if any. The optical micrographs did not show any appreciable change in the surface morphology because of ultrasonication for all time durations and this suggests that UHMWPE films are strongly adhered to the Si surface. As there is no covalent bond formation between UHMWPE and Si, the strong adhesion between two must be due to some physical forces and/or mechanical interlocking between the asperities on Si surface and the polymer molecules. It is believed that, the reactive nature of Si with hydroxyl groups on the surface after piranha treatment and post thermal treatment at a temperature of 100 ^{o}C must have helped in good adhesion between the UHMWPE film and the Si surface. But, the exact mechanism responsible for this behavior is not very clear at this moment.

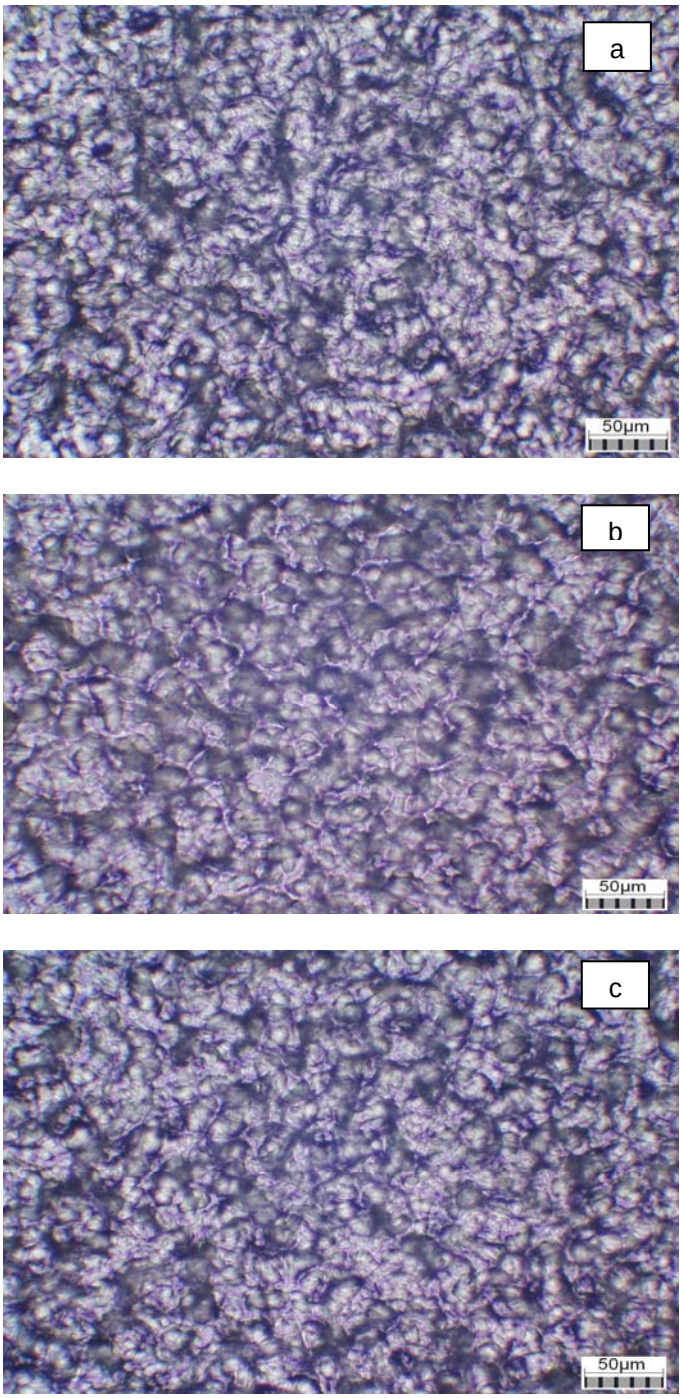

***Figure 5.2**: Optical micrographs of Si/UHMWPE sample after (a) 5, (b) 30 and (c) 100 min of ultrasonication in decalin followed by drying respectively. Note that the scale of the optical images is different from the image shown in Figure 5.1.*

5.1.5.2 Chemical Analysis of the coatings

FTIR and XPS studies are used to investigate the chemical structure of the UHMWPE film.

The transmission spectrum obtained with FTIR is shown in Figure 5.3 and represents four fundamental bands of UHMWPE film. The four characteristic bands include two strong CH stretching modes at 2851 and 2919 cm^{-1}, one band at 1462 cm^{-1} corresponding to polyethylene-methylene (CH_2) bending and one more band, the so-called CH_2 rocking mode at 719 cm^{-1}, which are similar to the characteristic features of the bulk PE or UHMWPE polymers [Elliott 1969, Alves et al 2005 and Kang and Nho 2001]. The similarity between the peaks of UHMWPE film with those of bulk UHMWPE further proves that the chemical structure of the film is the same as that of the bulk polymer.

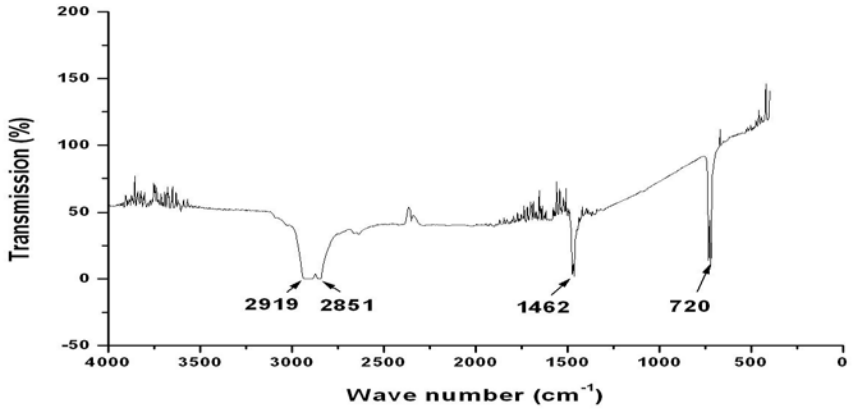

Figure 5.3*: FTIR spectrum of the UHMWPE coated Si surface.*

The wide scan spectra (obtained with XPS) of bare Si and Si/UHMWPE are shown in Figure 5.4. The strong intensity O1s peak on bare Si is due to the presence of oxide layer whereas the presence of C1s (with very less intensity) peak on bare Si might

come from the contaminants which were not removed during piranha treatment or those adsorbed from the atmosphere during handling before XPS tests. The large intensity C1s peak on UHMWPE film is due to its ethylene groups of backbone polymer chain and the absence of O1s, Si2s and Si2p peaks suggests that the polymer film completely shielded the Si surface and its hydroxyl groups.

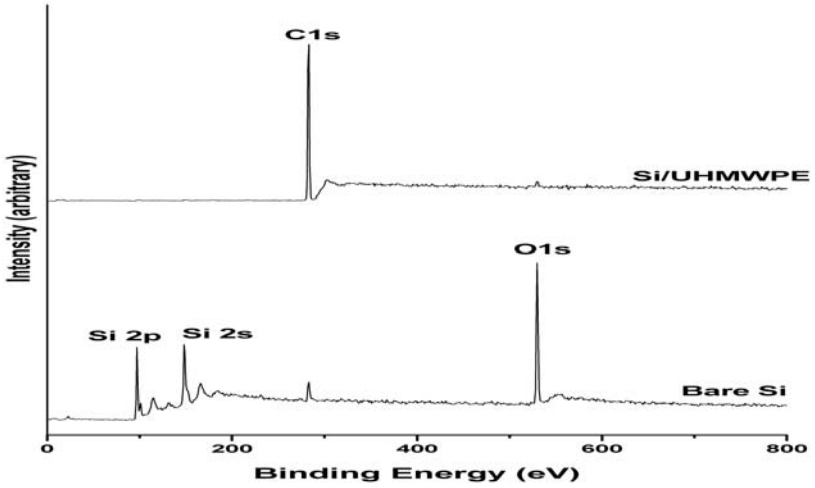

Figure 5.4*: XPS wide scan spectrum for bare Si and Si/UHMWPE samples.*

The surface characterization techniques (physical and chemical) and mechanical stability tests have shown that a well-adhered UHMWPE film (of sub-micron to few microns thickness) onto Si surface can be achieved through the presently demonstrated dip-coating technique. The film is strongly adhered even after a prolonged (100 min) ultrasonication in the solvent (decalin). The absence of Si peak (in the XPS spectrum) on the coated surface suggests that the film is free from defects such as pin-holes or un-wetted substrate.

5.1.5.3 Nano-indentation results

The Young's modulus and hardness values of the UHMWPE film formed in the present work obtained from nano-indentation are 3.7 GPa and 0.12 GPa respectively. The slope of the unloading curve is different to that of loading curve which must be because of the creep phenomenon during unloading [Hur et al 2004]. The creep phenomenon may have some effect on the absolute elastic modulus values. The creep phenomenon during unloading is not further studied because the investigation and the understanding of the tribological properties of the organic films is the primary objective of the present thesis. Moreover the nanoindentation results are primarily used to compare the UHMWPE films prepared at two different post-heating temperatures (Appendix A). The effect of creep can be minimized as the comparison is between the same materials in both cases. The typical penetration depth at the indentation load of 250 μN is ~300 nm which is very much less than 10 percent of the thickness of the film and suggests that the nano-mechanical properties obtained are purely those of the film without any substrate effect. Figure 5.5 shows a typical load versus displacement curve obtained for UHMWPE film on Si surface.

Bulk UHMWPE has shown elastic modulus and hardness values as 1-2 GPa and 0.04-0.06 GPa, respectively, measured using nano-indentation technique [Briscoe et al 1998 and Dong et al 2000]. Therefore, the presently formed UHMWPE film shows higher elastic modulus and hardness (almost double) when compared to bulk UHMWPE.

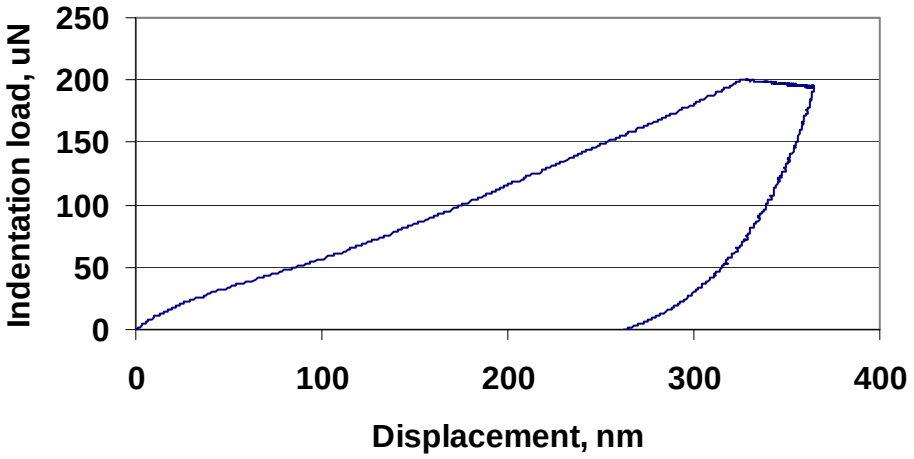

***Figure 5.5**: Load versus displacement curve for Si/UHMWPE film obtained during nano-indentation at a load of 250 μN.*

5.1.5.4 Tribological properties

The coefficients of friction of bare Si and Si/UHMWPE are shown in Table 5.3. The UHMWPE film has drastically reduced the coefficient of friction of bare Si from 0.6 to 0.09. The low coefficient of friction of UHMWPE film is comparable with that obtained for bulk UHMWPE (~0.12) sliding against Si_3N_4 ball under the same loading conditions. The low coefficient of friction of UHMWPE film is due to its lower shear strength and inherent lubrication property of its molecules because of "smooth molecular profile" [Pooley and Tabor 1972]. Smooth molecular profile is a name given to polymers such as HDPE, PTFE and UHMWPE [Pooley and Tabor 1972, Wang and Li 1999 and Unal and Mimaroglu 2003] where the polymers contain the linear molecules without any side groups, branching or cross-linking. These polymers have shown very low friction which is attributed to the easiness with which the long chain molecules shear across each other.

Table 5.3: *Coefficient of friction and wear life of bare Si and UHMWPE film modified Si. For comparison, the data for OTS SAM is also included.*

Sample	Coefficient of friction	Wear life, number of cycles
Si	0.6	100
Si/UHMWPE	0.09	12000*
Si/OTS#	0.18	1600*

*the lowest and highest wear life data among three tests for UHMWPE film are 8000 and 15000 cycles, respectively, and for OTS SAM are 1000 and 2100 cycles, respectively.
#Data taken from Chapter 4 for comparison purpose

The variations of the coefficient of friction with respect to the number of sliding cycles for bare Si, Si/OTS and Si/UHMWPE are shown in Figure 5.6 and the summary of the wear life data is presented in Table 5.3 above.

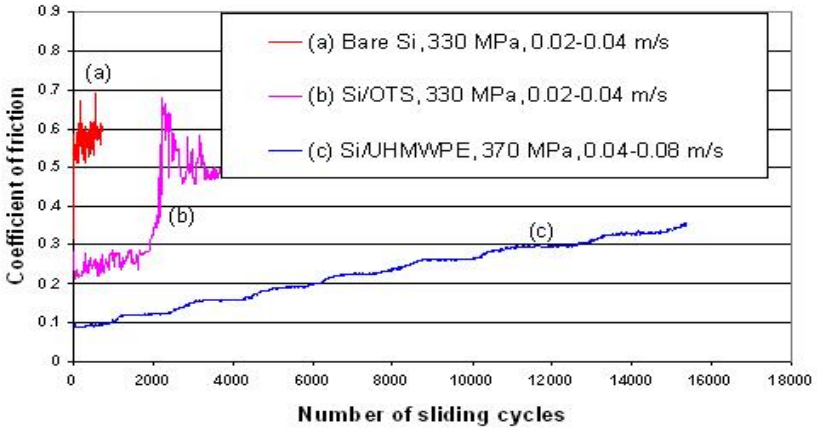

Figure 5.6*: Coefficient of friction versus number of sliding cycles curves for bare Si and Si/OTS SAM surfaces tested at 330 MPa and 0.02-0.04 ms^{-1} sliding velocities and Si/UHMWPE surface tested at 370 MPa and 0.04-0.08 ms^{-1} sliding velocities.*

The wear durability data strongly suggests that the UHMWPE film is superior in reducing the friction and wear of the Si surface when compared to the conventional OTS SAM. As explained in Chapter 4, bare Si failed within few tens of sliding cycles whereas

the UHMWPE film has shown a wear life of ~12,000 cycles*, which is much larger when compared to that of conventional OTS SAM (~1600 cycles) [Satyanarayana and Sinha 2005 and Chapter 4].

The SEM micrograph of the wear track of Si/UHMWPE after ~21,000 cycles of sliding is shown in Figure 5.7. The wear track does not contain any wear debris and shows the compressed state of the film with localized plastic deformation. The rough asperities and protrusions get ironed or flattened by the ball sliding process. EDS analysis was used to assess the extent of the wear of the film and Si surface and the results are shown in the same figure. The wear track (point A) does not contain Si peak and shows only strong C peak. The EDS spectrum inside the wear track (point A) is identical to that outside the wear track (point B). The strong Si peak obtained (with EDS) on piranha treated Si wafer is shown in Figure 5.7 (d) for comparison.

The extent of wear of the polymer film cannot be accurately estimated from the intensities of the C peak (inside and outside the wear track) because of the limited accuracy of the EDS as far as quantification of C is concerned. Therefore, EDS results only suggest that the wear of the Si surface has not started even after ~21,000 cycles in the case of Si/UHMWPE, which is also evident from the SEM morphology inside and outside the wear track (Figure 5.7 (a)).

* *using the definition that the film is considered failed when the coefficient of friction exceeds a value of 0.3*

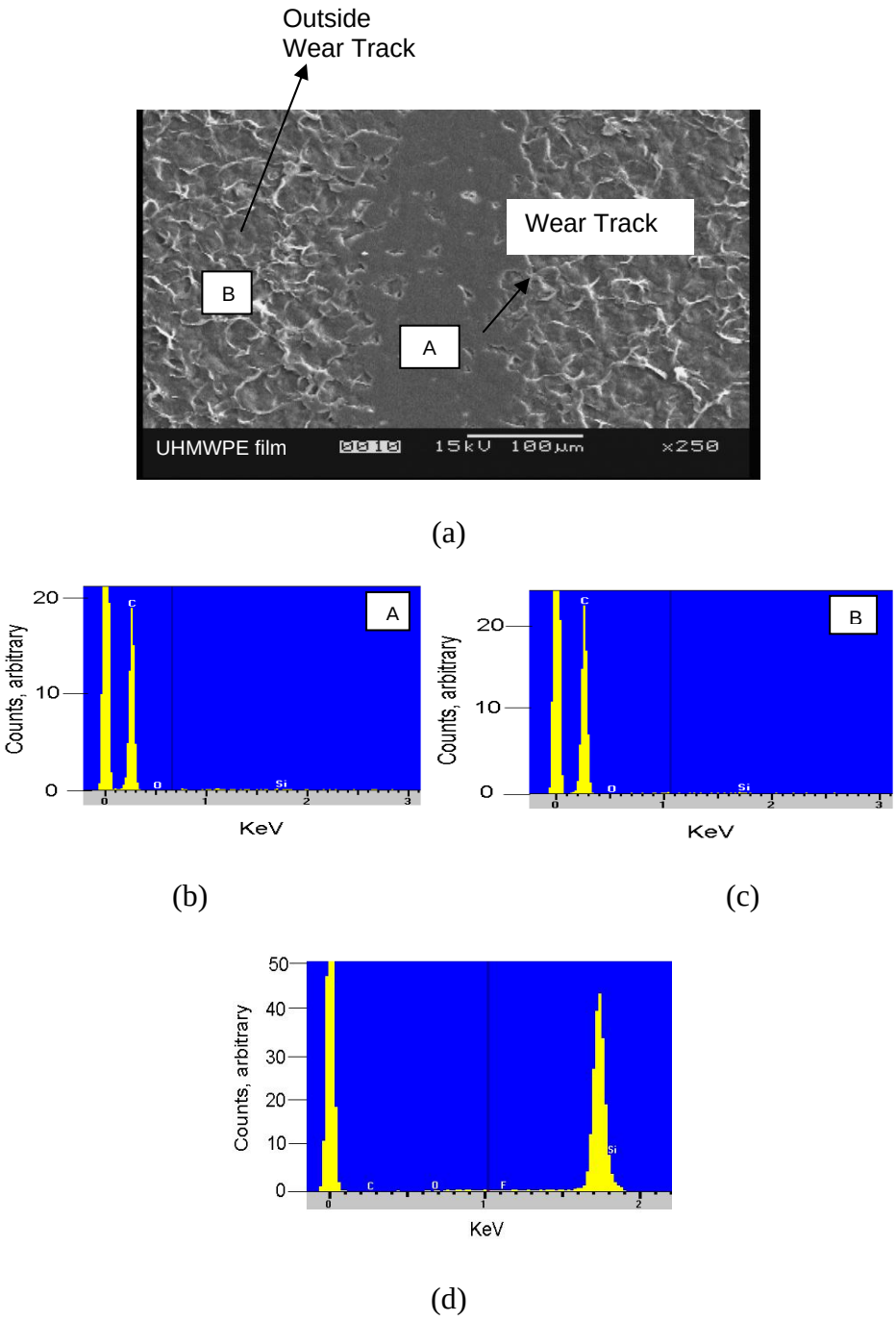

***Figure 5.7**: (a) SEM image of the wear track of Si/UHMWPE, run upto 21,570 sliding cycles at a contact pressure of 370 MPa. EDS spectrum (b) inside the wear track and (c) outside the wear track for the sample shown in (a). (d) EDS spectrum on piranha treated Si.*

SEM/AFM analysis of the wear tracks after ~2,000 and ~10,000 cycles of sliding is carried out to understand the reasons for the increase in the coefficient of friction of the UHMWPE film as the sliding progresses with no detectable wear to the polymer film or the Si substrate (Figure 5.8).

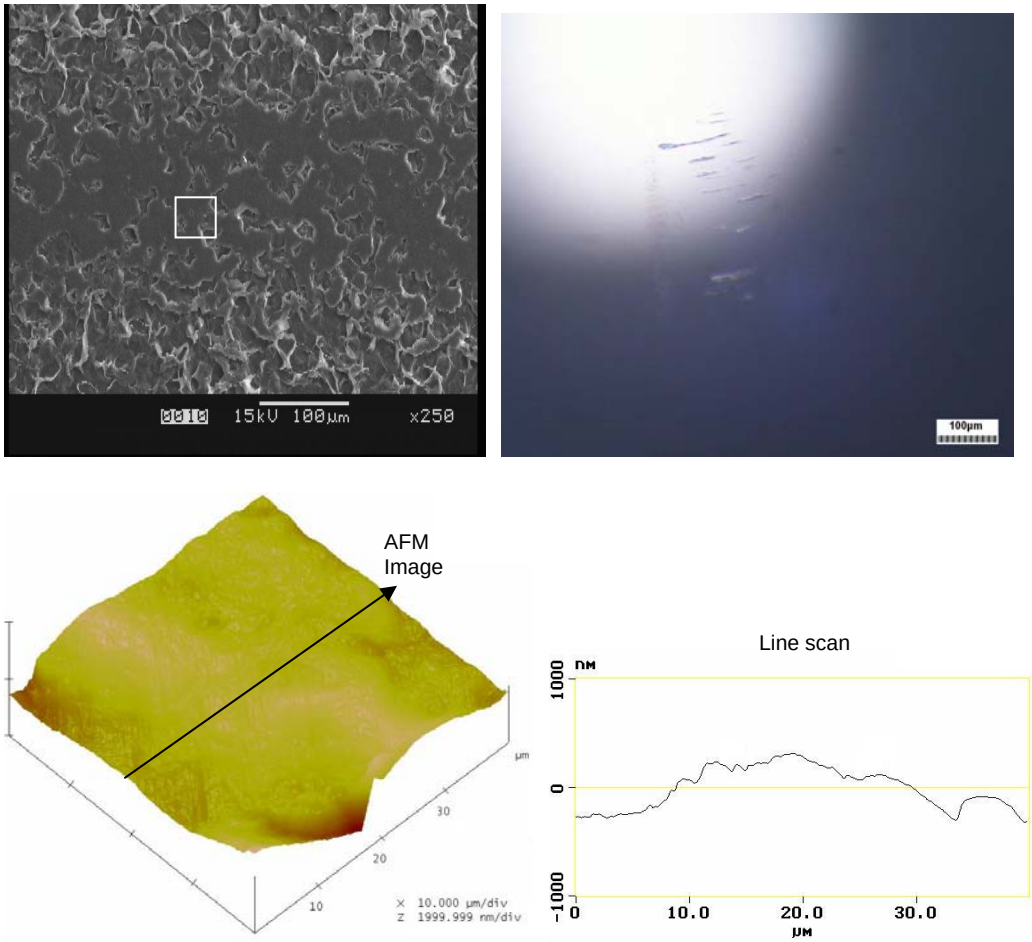

(a)

(Continue to the next page)

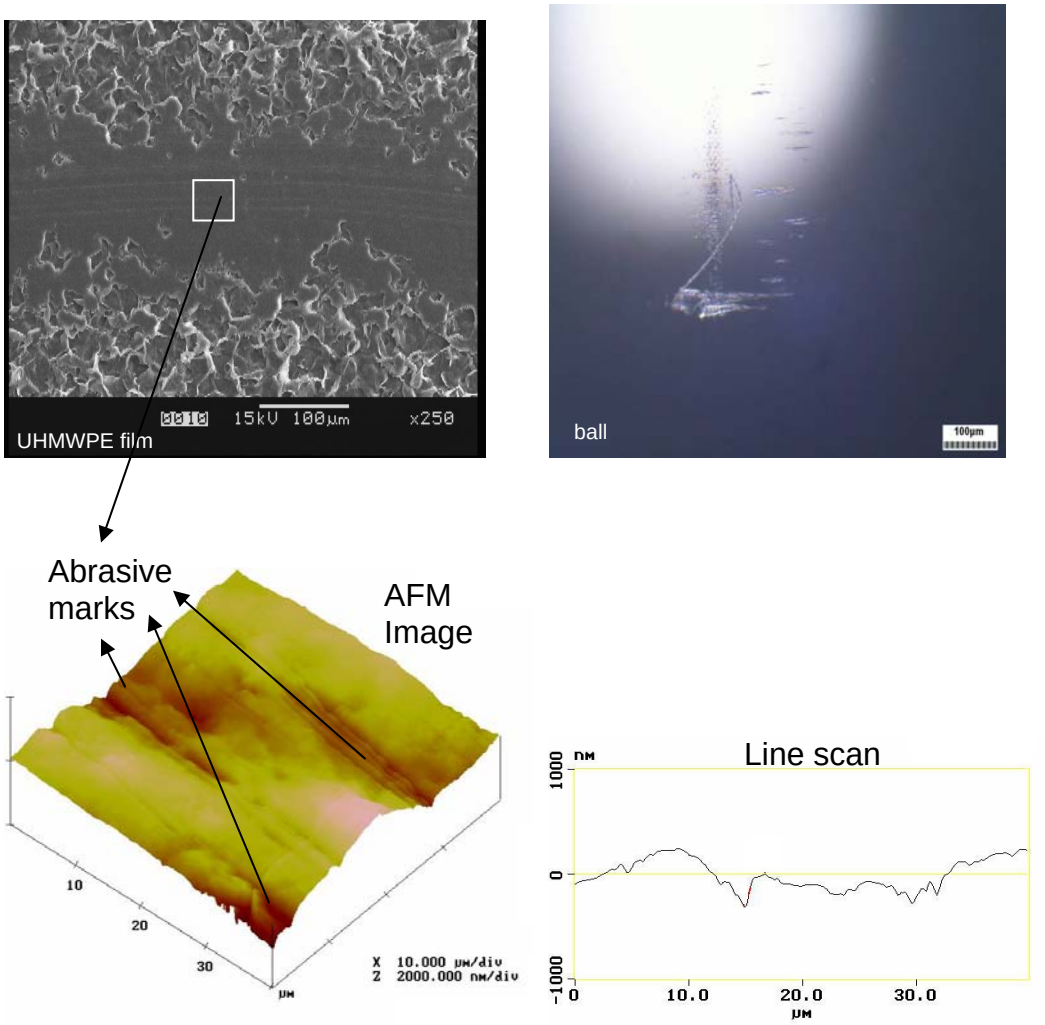

(b)

Figure 5.8*: (a) Si/UHMWPE sample run upto 2,033 cycles. (b) Si/UHMWPE sample tested upto 10,103 cycles. AFM image of the respective worn surface (the area used for the AFM study is shown with square box on SEM micrograph) together with a line scan is also shown. The magnification of the ball image is 100x.*

The wear track after ~2,000 cycles is very smooth (roughness is 0.219 µm) when compared to the un-worn polymer film (roughness is 0.556 µm) showing the compressed state of surface asperities and the corresponding ball surface (after the test) shows negligible material transfer. The AFM image also shows the flattening of the surface features of the polymer film supporting the SEM observation. The AFM image inside the

wear track shows higher extent of the compression of the polymer chains when compared to the SEM image of wear track and the difference is attributed to the variation in the scan area used for AFM and SEM morphological studies. The AFM imaging is much localized (when compared to SEM) and hence the surface profile in AFM depends on the image location selected.

As the sliding progresses, further compression of the polymer film and an increase in the material transfer to the ball surface is expected, which is supported on the wear track after ~10,000 cycles (by the evidence of few signs of abrasive marks (Figure 5.8 (b)) and adhesive plastic flow). The wear track after ~10,000 cycles is even smoother (roughness is 0.196 μm) when compared to that after ~2,000 cycles and un-worn polymer surface. Interestingly, there is no wear debris formation due to the abrasive and adhesive interactions which slightly increased the material transfer to the counterface (ball). It is anticipated that the plastic deformation of the asperities on the UHMWPE film increases the real contact area between the ball and UHMWPE film which finally results in an increase in the coefficient of friction as the sliding progresses (Figure 5.6). Finally, because of this process, the coefficient of friction exceeds a value of 0.3 after ~12,000 cycles which is considered as the film failure in the present study even though the film is still intact to the Si surface and no wear particle is observed on the wear track. The anticipated wear mechanism for UHMWPE films on Si is similar to that observed for bulk UHMWPE sliding against several ceramic counterparts [Abdallah 1991]. As the coefficient of friction of UHMWPE film exceeds 0.3 after ~12,000 cycles, further possibilities are explored to reduce the coefficient of friction beyond ~12,000 cycles. One such strategy (PFPE overcoating) is explained in Section 5.2.

5.2 Effect of PFPE overcoating onto UHMWPE film modified Si surface on tribological properties

5.2.1 Background

Eventhough UHMWPE film did not show any wear debris until ~20,000 cycles, the coefficient of friction exceeded 0.3 after ~12,000 cycles. Many applications require verry low coefficient of friction until the end of the service. Therefore, we looked into the possibilities of improving the wear durability of UHMWPE film even further. Motivated by the improvement in wear durability due to PFPE overcoating onto SAMs (Chapter 4), we overcoated UHMWPE film with an ultra-thin layer of PFPE to enhance the wear durability of UHMWPE film. The results based on the effect of PFPE overcoating onto UHMWPE film are discussed in this section.

Zdol 4000 PFPE (which was explained in Section 4.2) was used to coat the UHMWPE films.

The PFPE is coated onto UHMWPE film according to the procedure explained in Section 4.3.3.

5.2.2 Results and Discussion

5.2.2.1 Physical characteristics of the dual-layer film (UHMWPE/PFPE)

The PFPE overcoating onto UHMWPE film has further increased the water contact angle from 127^{o} to 134^{o} and made the surface even more hydrophobic.

SEM observation did not show any further change in the morphology after PFPE overcoating onto UHMWPE film. Also, the SEM measurements did not detect any

change in the thickness after PFPE overcoating onto UHMWPE film and suggest that PFPE formed as an ultra-thin film (probably only a few nanometers in thickness). The PFPE film formed on the DLC coated magnetic hard-disk surface under the same depositional conditions used in the present research has shown a thickness of ~2 nm [Sinha et al 2003].

5.2.2.2 Chemical analysis of the coatings

Figure 5.9 shows the XPS wide scan spectra for UHMWPE film and PFPE overcoated UHMWPE film. The appearance of F1s peak after PFPE overcoating onto UHMWPE film confirms its presence.

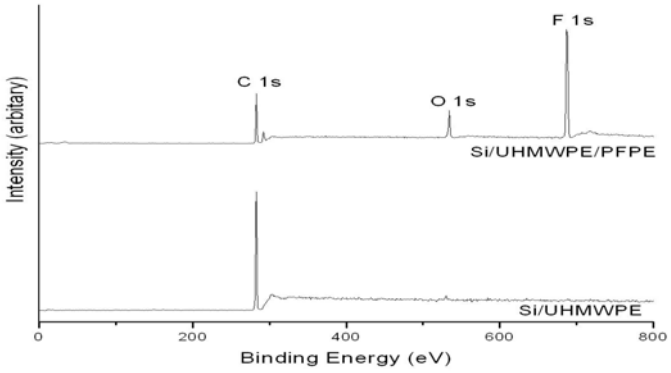

Figure 5.9*: XPS wide scan spectrum for Si/UHMWPE and Si/UHMWPE/PFPE samples.*

5.2.2.3 Tribological properties

The PFPE overcoating onto UHMWPE film has slightly reduced coefficient of friction from 0.09 to 0.08, which is attributed to the low surface energy and lower resistance offered to the sliding by the flexible PFPE molecules. Figure 5.10 shows the coefficient of friction variation in the sliding test and suggests that PFPE effectively

reduced and maintained the coefficient of friction value below 0.2 until 100,000 cycles of sliding. PFPE overcoating onto UHMWPE film has increased the wear durability from 12,000 to > 100,000 cycles (the tests were stopped after 100,000 cycles due to long test duration).

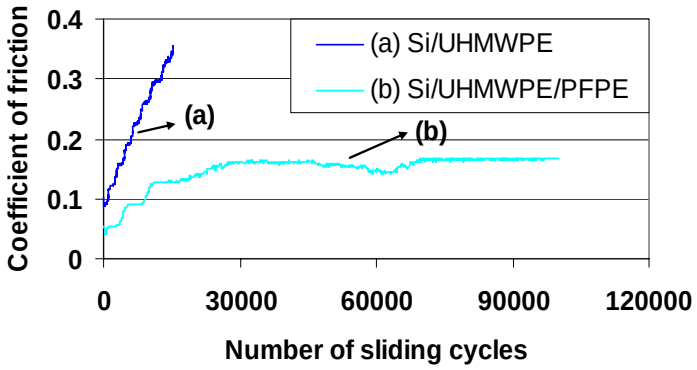

Figure 5.10: *Coefficient of friction versus number of cycles for UHMWPE film with and without PFPE overcoating at a contact pressure of 370 MPa and a sliding velocity of 0.04-0.08 m* s^{-1}.

Figure 5.11 shows the SEM micrograph of the wear track of Si/UHMWPE/PFPE after 100,000 cycles of sliding.

The wear track shows no signs of abrasive marks (which is also evident from AFM image inside the wear track) and is very smooth (roughness is 0.095 µm) with much less plastic deformation when compared to the wear track for Si/UHMWPE after ~10,000 cycles [Figure 5.8 (b)]. The improved tribological properties suggest that the PFPE overcoating greatly influenced the wear mechanism of the UHMWPE film. The role of PFPE has to be understood to explain the reasons for a greater increase in the wear durability. There is no possibility of chemical bonding/interactions between the

UHMWPE and PFPE molecules as UHMWPE film surface does not contain any reactive chemical groups.

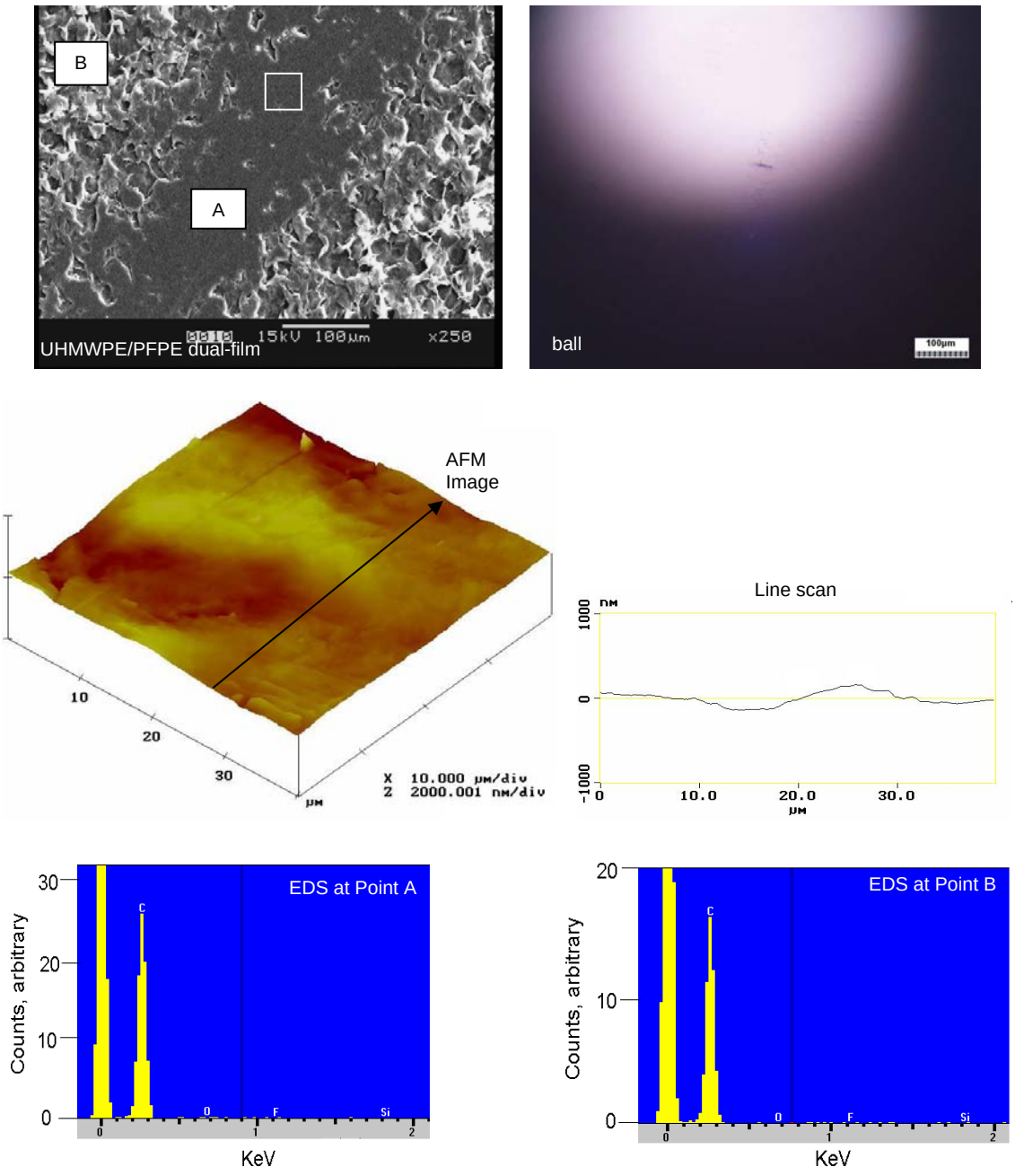

Figure 5.11*: Wear track of Si/UHMWPE/PFPE, run upto 100,000 cycles. EDS spectrum inside the wear track (Point A) and outside the wear track (Point B) are also shown. AFM image of the respective worn surface together with a line scan is also shown.*

We speculate that the PFPE molecules are trapped into the valleys/gaps between the polymer chains/fibers (similar to that anticipated on reactive SAMs in Chapter 4) present on the UHMWPE film surface (Figure 5.1 (a)). We further speculate that the trapping is only of mechanical type due to plastic deformation of the asperities in the initial few runs of sliding. The trapped PFPE molecules further lubricate the contact (additional to that obtained from UHMWPE film itself) and extend the low friction nature of the film for many thousands of cycles. Therefore, Si/UHMWPE/PFPE has shown very low (~0.15) and stable coefficient of friction upto 100,000 cycles of sliding instead of linearly increasing coefficient of friction with respect to the number of cycles as in the case of UHMWPE film on Si. Moreover, there is no (or little) material transfer to the ball after 100,000 cycles in the case of Si/UHMWPE/PFPE (Figure 5.11) whereas some amount of material transfer has been observed in the case of Si/UHMWPE even after only 2000 cycles of sliding (Figure 5.8 (a)). Further, there is no wear to the Si surface (evident from the absence of Si peak in EDS spectrum inside the wear track) even after 100,000 cycles of sliding in the case of Si/UHMWPE/PFPE at a contact pressure of 370 MPa.

Finally, the composite film Si/UHMWPE/PFPE can find applications in reducing the wear of components made from Si because of its improved properties such as low coefficient of friction, high wear durability and hydrophobicity.

5.2.2.4 Effect of surface features of underneath UHMWPE film on tribological properties of Si/UHMWPE/PFPE- possible explanation of the role of PFPE

In the previous section, it was anticipated that the trapped PFPE contributes greatly to the improvement in the wear durability when it was overcoated onto

UHMWPE. To prove this concept, we overcoated PFPE onto two different UHMWPE films with different morphologies (different valley sizes). The UHMWPE coating which is heated at a temperature of 130^{o}C has shown very flat features without the presence of any valleys (Appendix A). The film is very smooth (roughness is 0.081 µm) when compared to that heated at 100^{o}C (roughness is 0.552 µm). Therefore, the PFPE is overcoated onto these two different surfaces and their tribological properties are carried out. The PFPE overcoating onto UHMWPE film which is heated at 130^{o}C has shown a coefficient of friction of 0.16 and a wear life of ~3,000 cycles. The coefficient of friction versus number of cycles curves for both UHMWPE films heated at two different temperatures after PFPE overcoating are shown in Figure 5.12. Figure 5.12 clearly suggests that the improvement in wear durability is huge when PFPE overcoated onto UHMWPE film heated at 100^{o}C whereas the improvement is marginal when PFPE coated onto UHMWPE film heated at 130^{o}C (compare with Figure A.3 on page 188).

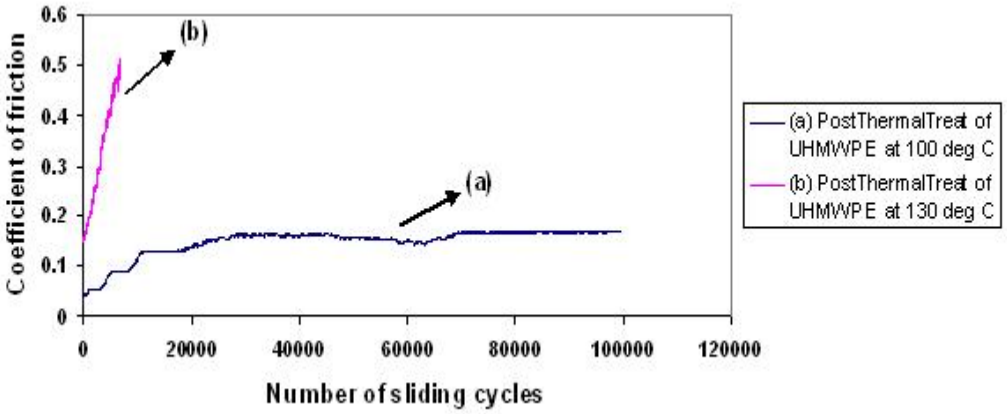

Figure 5.12: *Coefficient of friction versus number of cycles of PFPE overcoated UHMWPE films where the two UHMWPE films were heated at two different temperatures (100^{o}C and 130^{o}C respectively) after the dip-coating.*

AFM topography images have shown that the UHMWPE film heated at 100^{o}C have deep valleys and the surface is very uneven whereas the film heated at 130^{o}C has very flat surface without the presence of deep valleys. Therefore, it is assumed that less amount of PFPE is present on the surface of the film heated at 130^{o}C than that heated at 100^{o}C.

XPS characterization is carried out to estimate the amount of PFPE present on the two UHMWPE films heated at different temperatures. Figure 5.13 shows F1s spectrum after PFPE overcoating onto two UHMWPE films.

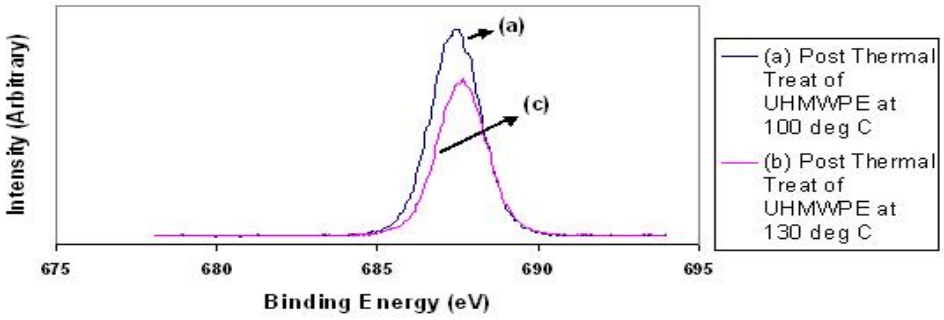

Figure 5.13: *XPS F 1s spectrum of PFPE overcoated UHMWPE films where the two UHMWPE films were heated at two different temperatures (100 and 130^{o}C respectively) after dip-coating.*

Figure 5.13 suggests that the amount of PFPE on UHMWPE heated at 100^{o}C is higher than that heated at 130^{o}C. The UHMWPE film heated at 130^{o}C is flatter than that heated at 100^{o}C with negligible valleys. Therefore, the absence of deep valleys results in less amount of PFPE in the case of heat treatment at 130^{o}C. Certainly, less amount of PFPE leads to minor increase in the wear life in the case of 130^{o}C treated sample. In addition to the less amount of PFPE, there is no additional contribution from the squeezing action of PFPE because of the absence of PFPE entrapment in valleys in the

case of 130^{o}C heat-treated UHMWPE film. These two reasons are responsible for greatly reduced wear durability of PFPE overcoating onto UHMWPE film heated at 130^{o}C. This result suggests that the morphology of the UHMWPE film greatly influences the wear durability after PFPE overcoating onto it. Moreover, this also supports the hypothesis that the entrapment of PFPE (which helps in lubrication due to squeezing action) largely contribute to the high wear durability observed.

5.3 Conclusions

5.3.1 Deposition and tribological properties of novel UHMWPE films coated onto Si surface

Following conclusions are drawn from the present study:

1. A uniformly coated UHMWPE film is obtained on Si surface using a simple dip-coating technique. The thickness of the film obtained depends upon the concentration of the polymer in the solution and it ranges between sub-microns to 28 μm.

2. The UHMWPE film on Si has shown a water contact angle of 127^{o}.

3. FTIR and water contact angle measurements have shown that the chemical structure of UHMWPE film is identical to that of the bulk UHMWPE. The solvent does not alter the chemistry of the polymer in any way.

4. The presently developed UHMWPE film has shown a very low coefficient of friction (0.09) and high wear life (~12,000 cycles). The wear life of UHMWPE film is very much higher when compared to that of OTS SAM. The worn surface did not show the presence of wear debris even after ~20,000 cycles of sliding.

Good adherence between the UHMWPE film and Si surface and self-lubricating properties of UHMWPE are responsible for good tribological properties of the UHMWPE film.

5.3.2 Effect of PFPE overcoating onto UHMWPE film modified Si surface on tribological properties

Following conclusions are drawn from the present study:

1. PFPE overcoating further increased the hydrophobicity of UHMWPE film by increasing the water contact angle from 127^{o} to 134^{o}.

2. The PFPE overcoating has reduced the coefficient of friction of UHMWPE film from 0.09 to 0.08 and increased the wear life from 12,000 cycles to 100,000 cycles (experiment stopped). The wear track is very smooth even after 100,000 cycles without any wear debris and wear to the Si surface.

3. It has been observed that the large amount of PFPE entrapped into the valleys present on the UHMWPE films lubricates the contact in-situ due to the squeezing action and hence shows greater improvement in the wear durability. This concept has been supported by the less improvement in wear durability when PFPE overcoated onto UHMWPE film with flatter features with the absence of valleys.

4. Finally, an optimum combination of good mechanical and tribological properties of UHMWPE and lubrication characteristics of PFPE is greatly beneficial to the wear durability of Si substrate.

Chapter 6

Influence of the addition of SWCNTs to Polyimide film on Tribological properties

6.1 Background

In the area of polymer films tribology, we have investigated the enhancement of the wear durability of a particular polymer thin film by adding a filler material. Current literature indicates that the wear of many bulk polymers (both thermoplastic and thermoset) can be effectively reduced by the addition of filler materials such as short carbon fiber, graphite, PTFE, MoS_2, CNTs, nano-particles etc [Friedrich et al 2002, Zoo et al 2004 and Cai et al 2004]. However, there are no studies (except one recent study by Pavoor et al [2004]) involving the addition of filler materials to polymer films to enhance its wear durability. Pavoor et al [2004] have observed that the addition of MWCNTs to PEMs on Si enhanced the wear durability of unmodified PEMs. Therefore, in this thesis we have studied the effect of the addition of SWCNTs to PI film on its tribological properties. PI film is selected for the present study, because it possess superior physicochemical properties such as high thermal stability, chemical resistance, mechanical strength, low dielectric constant and reasonable tribological properties [Deligoz et al 2005, Kinbara et al 2003, Fukushima et al 2001, Yamada et al 1990 and Kitoh and Honda 1995]. It is very interesting to enhance the wear durability of PI film in view of its many industrial applications [Gorlach and Holweger 2005, Fusaro 1987, Sidorov et al 1999 and Sun et al 2006]. In recent years, there has been a great effort on improving the tribological properties of PI thin films, for example, the surface

modification of PI films by ion implantation has shown good improvement in reducing the friction and wear of unmodified PI films on Si substrate [Kim et al 2002]. Further developments in this respect are needed to enhance the tribological properties of the PI thin film.

Since their discovery in 1991, CNTs continue to be a subject of unabated scientific research and development [Iijima 1991]. CNTs are considered as a possible reinforcement material because of their exceptional mechanical properties, chemical stability and tribological properties [Yang et al 2004 and Falvo et al 1999]. Moreover, the addition of CNTs to bulk polymer composites have shown good improvement in tribological properties [Zoo et al 2004 and Cai et al 2004] as well as mechanical [Cadek et al 2002 and Li et al 2004] and electrical properties [Sandler et al 1999]. Zoo et al [2004] have reported that the addition of MWCNTs of 0.5 wt% to UHMWPE have reduced the wear volume from 0.35 g to 0.05 g (86% reduction) and Cai et al [2004] have observed that the addition of 30 wt% CNT to PI has reduced the wear volume from 4.5 mm^3 to 2.5 mm^3 (44% reduction).

Therefore, the primary objective of the current study is to investigate the effect of the addition of SWCNTs to thin PI film on Si on its tribological properties especially wear durability. Until now there is no reported literature on the friction and wear behavior of PI film containing SWCNT. The current study is also important in view of many advanced technological applications (in the areas such as electrical and electronic, biological, nanotechnology etc) of carbon nanotube/polymer composites [Dresselhaus et al 2001].

6.2 Materials

PAA (polyamic acid) obtained from Hitachi Chemicals Asia Pvt Ltd, Singapore was used for the preparation of the PI film on Si surface. The chemical structure of the PI is shown below:

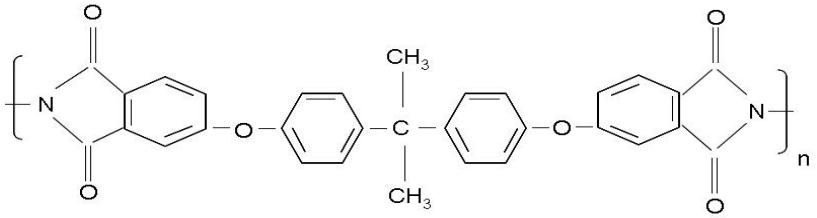

SWCNTs (obtained from Iljin Nanotech Co., Ltd, Korea) were used as the filler material for PI. These SWCNTs were produced using arc-discharge process and used without any further treatment (as processed grade) in the preparation of composite polymer solution. The FE-SEM image of the SWCNTs (diameter of ~10 nm) used in the present study is shown in Figure 6.1. N-methyl 1, 2- pyrrolidone (NMP) was used as the solvent for the preparation of the polymer solution (with and without the addition of SWCNTs).

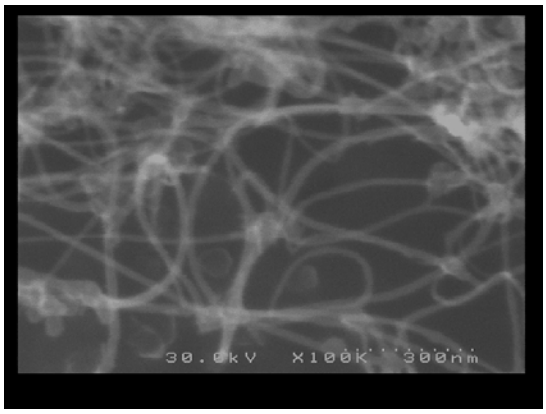

Figure 6.1*: FE-SEM image of the SWCNTs used in the present study, which were physically spread on the carbon tape to facilitate the SEM imaging. The diameter of the CNTs is ~10nm.*

6.3 Preparation of Si/PI and Si/PI+CNTs films

The details of the cleaning and piranha treatment of Si surface are explained in Section 4.3.1.

PAA was added to NMP in a ratio of 3:1 (by weight) and then the solution was subjected to homogenization using a motorized homogenizer for ~2.5 h at a speed of 10000 rpm, with an attached facility of continuous cooling. The homogenized solution was then used to coat the polymer film onto the Si surface by spin coating technique at a speed of 600 rpm for a period of 60 s. The spin coated samples were then heated in an oven under vacuum successively for 12 h at 50^{o}C, 1 h at 100^{o}C, 1h at 200^{o}C and finally 1 h at 300^{o}C, and slowly cooled to room temperature to complete the imidization of PAA [Pronjoto and Denton 1991].

For the preparation of the composite film, the mixture of SWCNTs (0.05 wt%) and NMP was subjected to ultra-sonication for 15 min to ensure uniform dispersion of SWCNTs without any agglomeration. The PAA was then added to SWCNTs-NMP mixture and subjected to the homogenization followed by spin coating and imidization as explained previously. The modified samples were then stored in a desiccator until further characterization or testing.

6.4 Experimental procedures

Surface characterizations such as water contact angle measurement, AFM topography, SEM morphology, FTIR are used to measure the properties of the thin films formed. Tribological properties are measured using a micro-tribometer. All these characterization techniques are explained in Section 3.3. The thickness of the polymer

film is measured using laser profilometer according to the procedure explained in section 3.3. Elastic modulus and hardness of PI film with and without SWCNTs are measured using CSM nano-indentation according to the procedure reported in Chapter 3 (Section 3.3.9).

AFM and SEM are used to characterize the wear tracks after sliding tests.

6.5 Results and Discussion

6.5.1 Contact angle results

Table 6.1 shows the water contact angles of bare Si, PI and PI+SWCNTs films coated Si.

Table 6.1*: Mean water contact angle values, hardness, elastic modulus, coefficient of friction and wear life data of bare Si, Si/PI and Si/PI+SWCNTs.*

Material	Water contact angle, degrees	Hardness, GPa	Elastic Modulus, GPa	Coefficient of friction	Wear life, number of cycles
Si	12	-	-	0.6	100
Si/PI	72	0.43	5.23	0.1	3000*
Si/PI+SWCNTs	82	0.72	8.41	0.12	7200*

*the lowest and highest wear life data among three tests for PI film are 1200 and 4600 cycles, respectively, and for PI+SWCNTs film are 6500 and 8200 cycles, respectively

PI film has shown a water contact angle of 72° which is much higher than that of bare Si (12°) and implies the differences in their surface energies/wetting characteristics. The water contact angle of PI is consistent with that reported in the literature [Kinbara et al 2003, Gotoh et al 2001 and Egitto 1990] and supports its successful deposition. The water contact angle has increased from 72° to 82° after the addition of SWCNTs to PI film

which is attributed to the surface property of CNT, which is essentially a graphite material (water contact angle of 84-86^{o}) [Fowkes and Harkins 1940 and Morcos 1972].

6.5.2 Thickness measurement using laser profilometer

The PI film coated according to the procedure mentioned in the present study has shown an average thickness of 6-7 µm. There is no change in the thickness value after the addition of SWCNTs which is attributed to the nanometer dimensions of the CNT.

6.5.3 FTIR Characterization

The FTIR spectrum of PI film is shown in Figure 6.2. The transmission spectroscopy of the PI film has shown three characteristic peaks at 1780 cm^{-1}, 1733 cm^{-1} (stretching of C=O) and 1382 cm^{-1} which are usually observed in an aromatic PI film [Jia et al 2005 and Karamancheva et al 1999]. Addition of CNTs did not show any change in the characteristic peaks of the PI film.

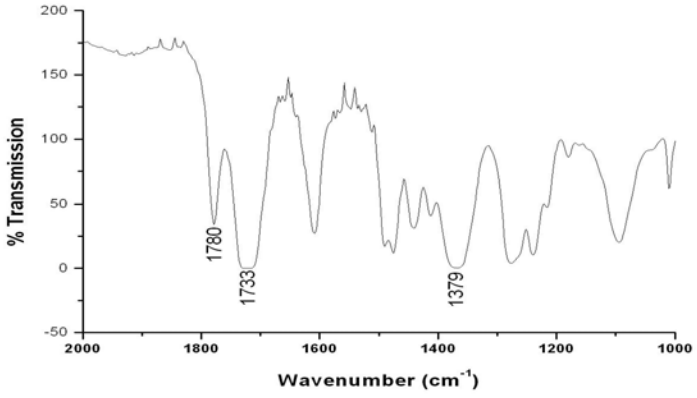

***Figure 6.2**: FTIR spectrum for PI film on Si surface.*

6.5.4 AFM topography results

Figure 6.3 shows AFM images of Si/PI and Si/PI+SWCNTs. PI film on Si has shown island structure with uniform distribution of islands and valleys (average depth is ~8 nm) and has shown a surface roughness of 2.4 nm (over 1 µm x 1 µm scan area). The topography of the present PI film is comparable to that reported in the literature for PI films formed by solution casting [Xu and Coleman 1997] and spin-coating [Narayanan et al 2005]. The SWCNTs addition to the PI film has still shown the island structure but the islands are non-uniform and very irregular. The addition of SWCNTs increased the surface roughness from 2.4 nm to 9 nm and the average size of the valleys from ~8 nm to ~15 nm. The reason for the non-uniformity and increased roughness after the addition of SWCNTs could be because of the agglomeration of nanotubes to some extent which could not be avoided even after extensive shear mixing.

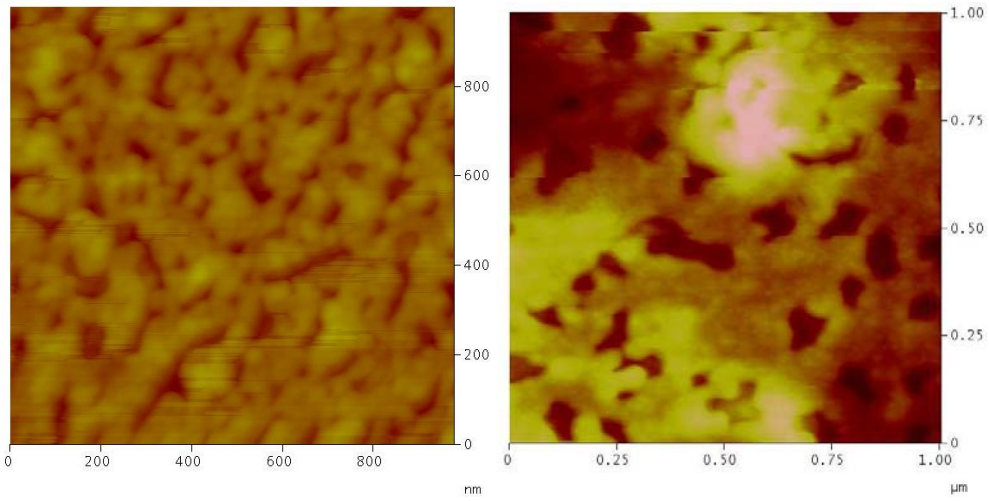

(a) (b)

***Figure 6.3**: AFM images of (a) Si/PI and (b) Si/PI+SWCNTs. The scan area is 1 µm x 1 µm and the vertical scale is 50 nm in both cases.*

6.5.5 Nanoindentation results

Figure 6.4 shows the hardness and elastic modulus data for Si/PI and Si/PI+SWCNTs obtained using the CSM nanoindentation test.

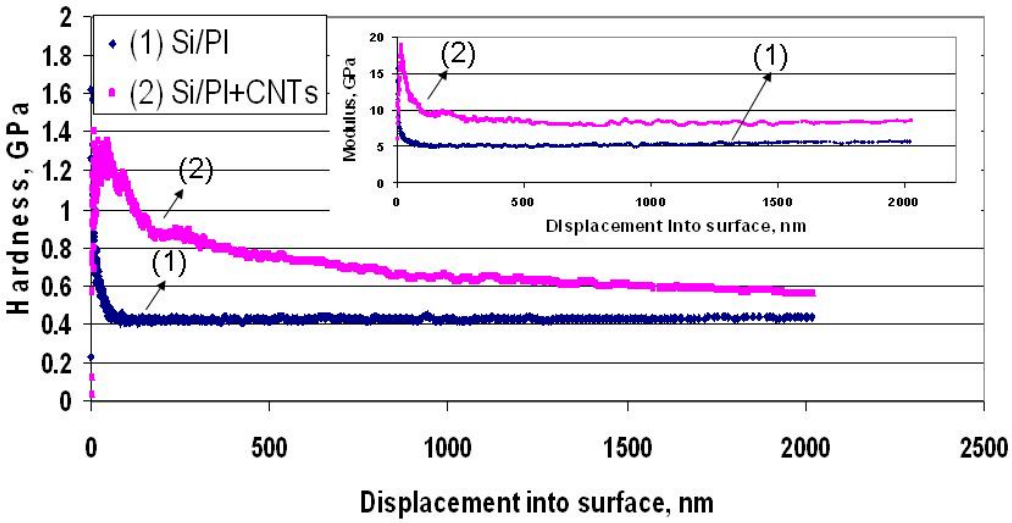

***Figure 6.4**: Hardness with respect to the nanoindentation depth for Si/PI and Si/PI+SWCNTs during CSM nanoindentation test. Inset shows the elastic modulus versus indentation depth curve.*

The hardness and elastic modulus versus the indentation depth curves (for both samples) are approximately horizontal except at the initial stage (on the film surface) of contact which is attributed to the difficulty in determining the point of contact and the inaccuracy of the indenter tip function at the shallow depths of the indentation [Shen and Zeng 2004]. Similar effect has been observed by many researchers in the literature in CSM nanoindentation tests [Ma and Clarke 1995, De Guzman et al 1993 and Volinsky and Gerberich 2003]. Table 6.1 shows the average hardness and elastic modulus values of PI and PI+SWCNTs films. The data for indentation depths only between 500-2000 nm is used for the determination of the average values of hardness and elastic modulus because Oliver and Pharr [2004] have shown that the data below 500 nm indentation depth is not

very reliable due to the difficulty in accurate estimation of the area function at very small indentation depths. The addition of SWCNTs to the PI film has increased the hardness of PI from 0.43 GPa to 0.72 GPa and elastic modulus from 5.23 GPa to 8.41 GPa (~1.6-1.7 times improvement to that of pristine film). The improvement in hardness and elastic modulus observed in the present study by the addition of SWCNTs to the PI film is comparable to the improvement in the mechanical properties of bulk polymers through the addition of CNTs [Cadek et al 2002 and Li et al 2004]. For example, in a study by Cadek et al [2002], the addition of MWCNTs have increased the Young's modulus and hardness by factors of 1.8 and 1.6 at 1 wt% CNT in polyvinyl alcohol (PVA) and 2.8 and 2 at 8 wt% CNT in poly (9-vinyl carbazole) (PVK) respectively. The improvement in the hardness and elastic modulus after the addition of SWCNTs to PI film is attributed to the good interfacial bonding between SWCNTs and the polymer as well as exceptional mechanical properties of SWCNTs. Good interfacial bonding between the polymer and SWCNT is possible because of high reactivity of the carbon nanotube surface [Lourie and Wagner 1998 and Wei et al 2001]. The improved mechanical properties after the addition of SWCNTs have led to an improvement in wear resistance of the composite film, which is explained in the next section.

6.5.6 Tribological results

The coefficients of friction for bare Si, Si/PI and Si/PI+SWCNTs are shown in Table 6.1. The coating of PI film has reduced the coefficient of friction of Si from 0.6 to 0.1 whereas the addition of CNTs to the PI film has slightly increased the coefficient of friction from 0.1 to 0.12. Similar increase in the coefficient of friction after the addition

of SWCNTs (0.5 wt%) has been observed by Zoo et al [2004] where the coefficient of friction of UHMWPE increased from 0.05 to 0.11 and they attribute this behavior to the increase in shear strength and surface roughness by the addition of SWCNTs. The same mechanism might be responsible for a slight increase in the coefficient of friction after the addition of SWCNTs to PI film. Considering the fact of very low coefficient of friction of graphite the addition of SWCNTs to PI film was expected to reduce the coefficient of friction, but experimental results have shown an increase in the coefficient of friction. The inherent lamellae structure of the graphite leads to an easy shearing in the direction of the sliding and shows very low coefficient of friction [Bowden and Tabor 1950] but this is not the case with SWCNTs. Pristine PI film (without SWCNTs) has shown very low coefficient of friction (0.1) which is attributed to its low surface energy and flexible polymer chains (and low shear strength). Several thermoplastic polymer films have shown low friction because of their low shear strengths which offer little resistance [Sidorenko et al 2002 and Satyanarayana et al 2005].

Table 6.1 shows the quantitative wear life data for bare Si, Si/PI and Si/PI+ SWCNTs. The scatter in the wear durability data is comparable to that observed in the case of PFPE overcoating onto SAMs (Chapter 4) and that observed in the literature for thin-film lubrication [Ruhe et al 1993]. The PI film on Si has shown a wear life of ~3000 cycles which is much greater than that of Si (only few tens of cycles) and approximately double of that observed for conventional OTS SAM (~1600 cycles, Chapter 4). The wear durability of the current PI film is comparable with that observed in the literature despite some differences in testing procedure and loading conditions [Kitoh and Honda 1995 and Fukushima et al 2001]. PI film has shown good wear durability which can be attributed to

its good mechanical strength, flexible molecular chains, low surface energy and shear strength [Yamada et al 1990 and Chitsaz-Zadeh and Eiss Jr 1986]. The addition of SWCNTs to the PI film has increased the wear life from ~3000 to ~7200 cycles (approximately more than double). It is to be noted that the quantitative wear life data (Table 6.1) are from the criteria of the coefficient of friction only (i.e. the film is deemed failed when the coefficient of friction exceeded 0.3). But the SEM/EDS analysis of the worn surfaces have shown that there was no visible wear after the above said number of cycles to both PI and PI+SWCNTs film and hence, if a coefficient of friction greater than 0.3 could be tolerated then the wear life would be much higher. Actually, PI and PI+SWCNTs films did not show wear until 15,000 and 100,000 cycles of sliding, respectively, in continuous wear tests (explained later on P. No. 125).

SEM/EDS analysis of the wear tracks (after appropriate number of sliding cycles) was carried out to investigate the extent of wear of the film and/or Si surface. The SEM observation of the wear track of PI film has revealed that there was no appreciable wear until 15,000 cycles even though it was considered failed after ~3,000 cycles based on the dynamic coefficient of friction criterion. The SEM image of the wear track of PI film after ~20,000 cycles is shown in Figure 6.5.

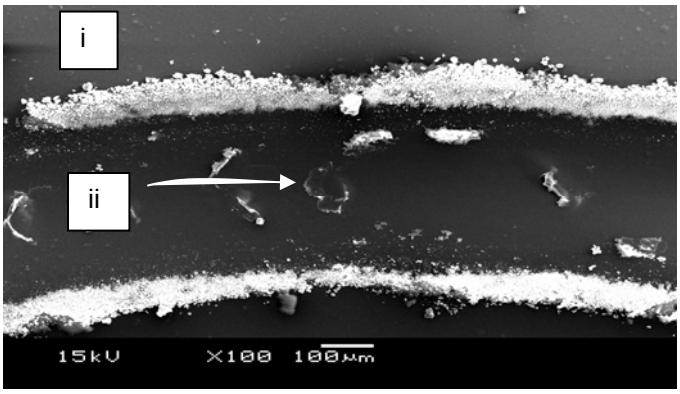

(a)

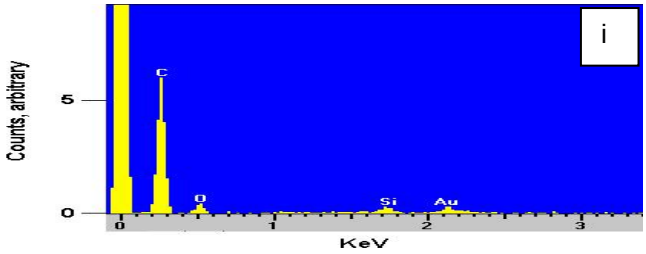

(b)

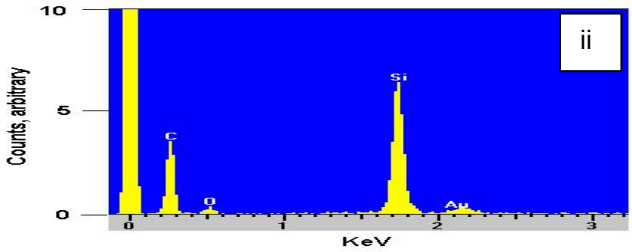

(c)

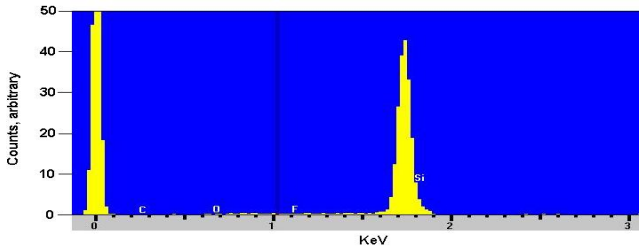

(d)

Figure 6.5*: (a) SEM image of the wear track of Si/PI, run upto 20,000 sliding cycles at a contact pressure of ~370 MPa (Arrow indicates the sliding direction).(b) and (c) show the EDS spectrum outside and inside the wear track respectively for the image shown in (a). (d) EDS spectrum on bare Si after piranha treatment.*

The worn surface of the pristine PI film shows signs of ploughing and delamination and shows the accumulation of wear debris along the sides of the wear track. Comparison of EDS spectrum outside (Figure 6.5 (b)) and inside (Figure 6.5 (c)) the wear track of PI film and on original Si surface (Figure 6.5 (d)) suggest the following observations: (i) higher intensity of Si peak and lower intensity of C peak inside the wear track indicate the wearing of PI film and appearance of the Si surface, (ii) lower intensity of Si peak in Figure 6.5 (c) than in Figure 6.5 (d) suggests that some PI film is still left on the wear track covering the substrate and (iii) the presence of C peak in Figure 6.5 (c) and not in Figure 6.5 (d) also suggests that some PI film is still present on the wear track. Therefore, SEM/EDS results suggest that the PI film protects the Si surface upto less than ~20,000 cycles.

Figure 6.6 (a) shows the SEM image of the wear track of Si/PI+SWCNTs after 100,000 cycles of sliding. The wear track is barely identifiable in the case of Si/PI+SWCNTs after 100,000 cycles and shows slightly compressed state of the surface protrusions. Figures 6.6 (b) and (c) show the FE-SEM images of Si/PI+SWCNTs, outside and inside the wear track, respectively. The SEM image shown in Figure 6.6 (b) suggests that the PI+SWCNTs film has shown island structure and valleys confirming the AFM observation as shown in Figure 6.3 (b). EDS spectrum inside the valleys has shown a strong C peak with negligible Si peak suggesting that the valleys were covered with PI and this was not a case of dewetting of the polymer on Si surface. The SEM image inside the wear track (Figure 6.6 (b)) is very similar to that outside the wear track (Figure 6.6 (c)) except that the width of the valleys has been reduced and the islands have became flatter spreading over large area.

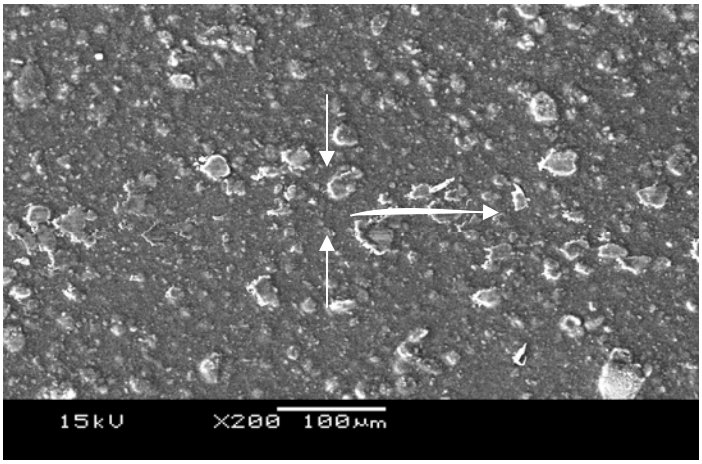

(a)

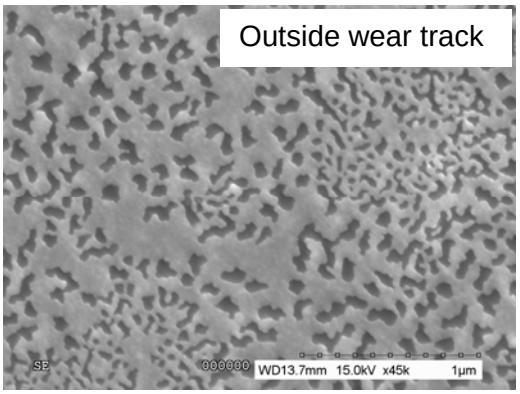

(b)

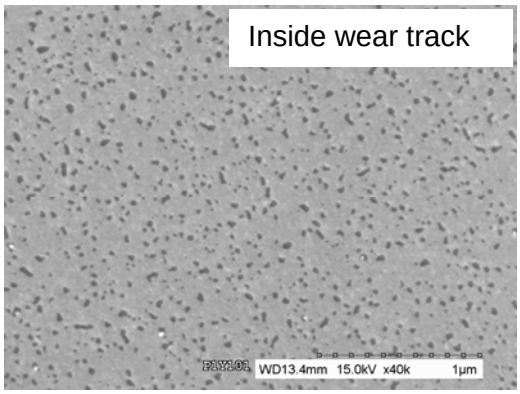

(c)

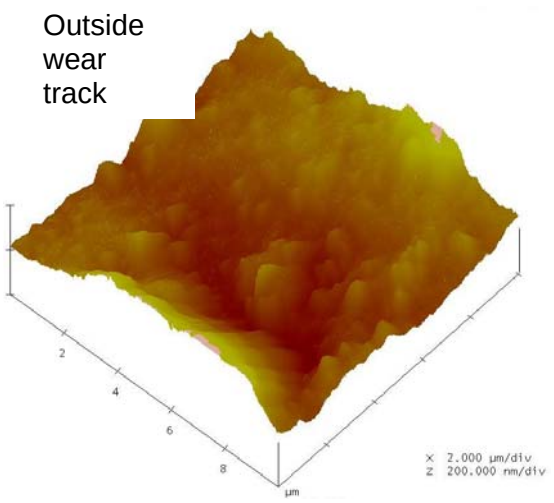

(d)

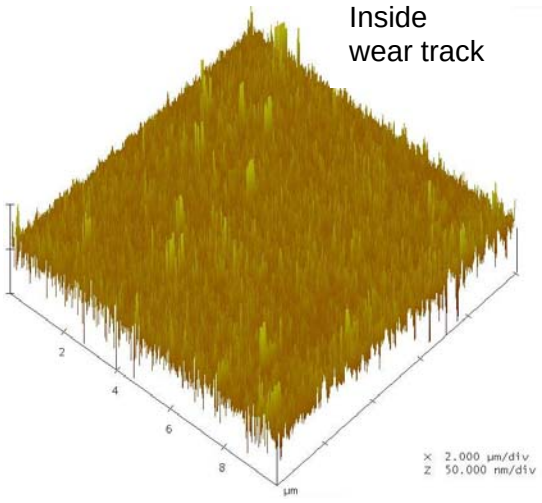

(e)

Figure 6.6 (Continue to the next page)

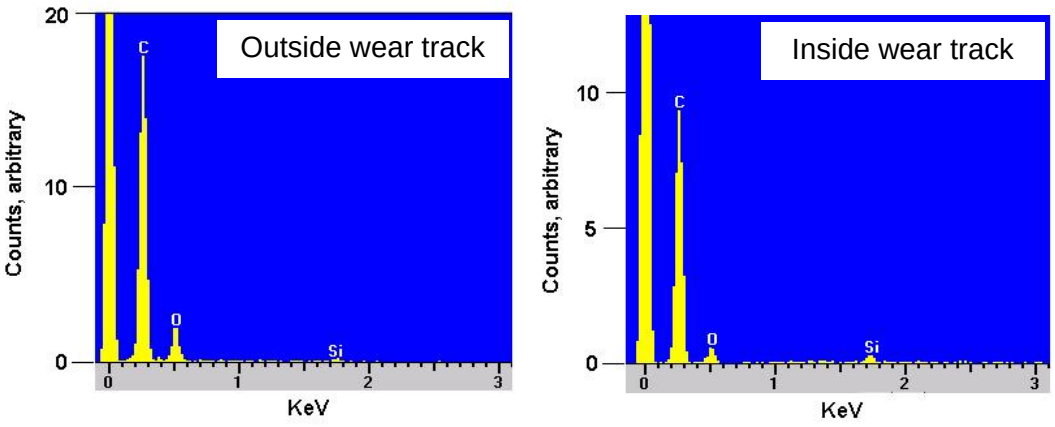

(f) (g)

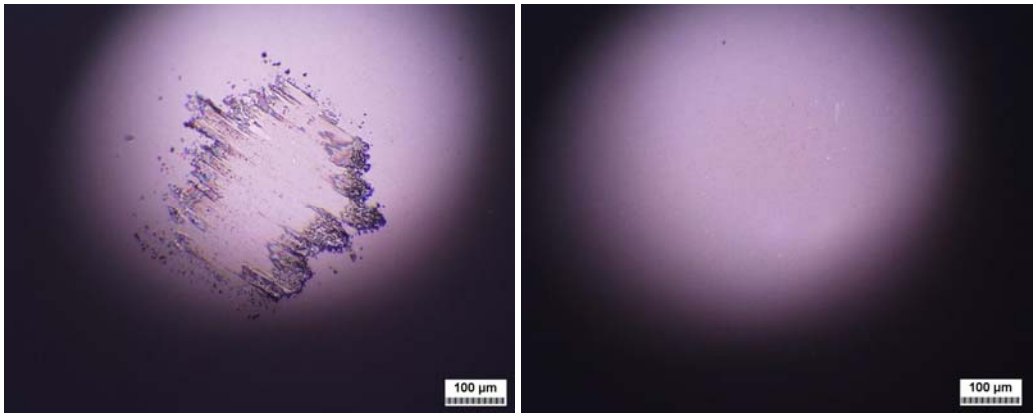

(h) (i)

***Figure 6.6**: (a) Wear track of Si/PI+SWCNTs, run upto 100,000 cycles (arrows indicate the location of ball sliding and the sliding direction). FE-SEM images of Si/PI+SWCNTs, (b) outside the wear track and (c) inside the wear track. AFM images (10 µm x 10 µm scan area) of Si/Pi+SWCNTs, (d) outside the wear track and (e) inside the wear track. The vertical scale for the image in (d) is 200 nm whereas for (e) is 50 nm. (f)EDS spectrum outside the wear track and (g) EDS spectrum inside the wear track for the image shown in (a). Optical images of the Si_3N_4 ball slid against to the sample in (a): (h) immediately after the sliding test and (i) after cleaning the transferred material on the ball surface with acetone.*

The AFM images of the film inside and outside the wear track are shown in Figure 6.6 (c) and (d) respectively. The surface roughness values measured using AFM have shown that the worn surface (RMS of 10 nm) is smoother when compared to the un-worn film surface (RMS of 66 nm) and in turn support the absence of the wear to the film. The EDS

spectrum has shown strong C peak both inside and outside the wear track (where the intensity was less inside the wear track than that outside the track) and absence of Si peak either outside or inside the wear track (Figure 6.6 (f) and (g)). There is no appearance of wear debris along the wear track as evident from the SEM image shown in Figure 6.6 (a). The low intensity (~50%) of the C peak inside the wear track than that outside the wear track suggests the beginning of the wear of the film, but this is not evident from SEM image (Figure 6.6 (f) and (g)). Figures 6.6 (h) and 6.6 (i) show the optical micrographs (100x magnification) of the ball surface, after the sliding test and after cleaning with acetone respectively, and suggest that there is no wear or scratching to the ball surface even after sliding for 100,000 cycles except a small amount of material transfer (Figure 6.6 (h)).

From the quantitative wear durability data and qualitative SEM/EDS analysis of worn surfaces, it can be concluded that the addition of SWCNTs to the PI film contributed to restrain the wear of the PI film sliding against Si_3N_4 counterface. Two main reasons are proposed to explain the mechanism responsible for the improvement in wear durability. Firstly, the addition of SWCNTs increases the load-bearing capacity of the PI film by improving the hardness and elastic modulus. The addition of CNTs has shown similar improvement in load-bearing capacity in bulk polymers such as polystyrene [Yang et al 2005], UHMWPE [Zoo et al 2004] and PI [Cai 2004]. Therefore, the addition of SWCNTs to PI have restricted the wear particle generation/material removal phenomena during sliding and improved wear resistance because of the improvement in load-bearing capacity and smaller real contact area due to the textured microstructure. Secondly, the vertical alignment/exposure of SWCNTs (see Figure 6.6

(e)) due to topographical changes during sliding could have further contributed to enhancement in the wear durability because of difficulty in breaking these nanotubes (and pulling out of polymer matrix) due to their exceptional elongation tensile strength properties and excellent bonding between the SWCNTs and the PI matrix [Lourie and Wagner 1998]. For example, an average bending strength of 14.2 GPa was reported for MWCNT of 4.4 nm diameter by Wong et al [1997]. Moreover, the gradual increase in the coefficient of friction despite no wear to the film can be explained through the continuous increase in the contact area and the vertical alignment of CNTs (induced during sliding) which offer greater resistance to the sliding because of their higher stiffness.

Such CNT strengthened polymer (whether in bulk or film form) can be used for machines requiring wear resistant coating. Micromachine gears and parts are some possible application areas.

6.6 Conclusions

From the present study, following conclusions can be drawn:

1. The addition of SWCNTs has made the PI film more hydrophobic (the water contact angle increased from 72° to 82°).

2. The addition of SWCNTs to PI film did not influence its chemical structure, as evident from FTIR.

3. The nanoindentation results have shown that the addition of SWCNTs to PI film has increased the hardness from 0.43 GPa to 0.72 GPa and elastic modulus from 5.23 GPa to 8.41 GPa.

4. The coefficient of friction of PI film has been slightly increased from 0.1 to 0.12 by the addition of SWCNTs.

5. The quantitative wear life data has shown that the polyimide composite film containing SWCNTs has shown wear durability upto ~7200 cycles with coefficient of friction values less than 0.3. The SEM/EDS analysis of worn surface has shown that the composite film did not show any wear even after 100,000 cycles (with coefficient of friction reaching upto 0.5).

6. Finally, the addition of SWCNTs to PI film has helped to increase the wear durability which is attributed to the improved mechanical properties and the microstructural changes induced during sliding.

7. The present results have shown that CNTs can be considered as a promising filler material for polymer based thin films on Si surface for excellent wear resistance applications.

Chapter 7

Effect of molecular structure on friction and wear of polymer thin films covalently bonded to Si surface

7.1 Background

As explained in the Chapter 2, despite few studies involving the investigation of tribological properties of polymer thin films [Sun et al 2006, Liu et al 2002 and Tsukruk et al 2002 (a)], there is no systematic study (as per our literature survey to date) involving the investigation of the effect of molecular structure of the polymer film on the tribological properties. Such studies will be helpful in the development of new molecular ultra-thin films with improved tribological properties, as molecular chemical, physical and mechanical properties of polymers are ultimately responsible for the tribological responses. Further, research is needed to identify the mechanisms responsible for high wear durability in some polymers in bulk or film forms. Many of the other polymers provide good tribological performance of low friction and low wear only when they are used in highly modified composite forms and not in pristine form. In their pioneer work, Pooley and Tabor [1972] have shown that the molecular structure of the bulk polymers greatly affects their tribological properties (such as coefficient of friction and wear resistance). They reported that the polymers with "smooth molecular profile" greatly reduce the coefficient of friction and wear, however, the precise meaning of "smooth molecular profile" is not understood. The motivation for the present investigation is to elucidate the effect of molecular structure of ultra-thin polymer films on their tribological properties. Therefore, two thermoplastic films coated onto Si (PE and PS, which have

different molecular structure) are selected and investigated their tribological properties using sliding tests [Satyanarayana and Sinha 2007 (c)]. The PS contains bulky benzene groups sequentially located at the side of the backbone carbon chain whereas PE contains hydrogen atoms at the side of the backbone chain. The glass transition temperatures of PE and PS are -110^{o}C and 100^{o}C respectively [Callister 2006]. Thermoplastic polymers have, in general, high wear resistance and low coefficient of friction than those of thermosets or elastomers in their pristine forms.

The coefficient of friction data of bulk PE and PS are 0.08 and 0.3 respectively whereas wear rates are 6 x 10^{-4} and 5 x 10^{-2} mm^3 N^{-1} m^{-1}, respectively, measured in sliding wear tests against stainless steel counterface [Pooley and Tabor 1972 and Sinha 2002]. The above data show that the PE has lower coefficient of friction and wear rate than those of PS. The above data clearly explain the effect of molecular structure (in addition to other properties such as crystallinity, thermal and mechanical properties) on tribological properties and hence support the idea in selecting PE and PS films in the present study.

The two polymer molecules selected contain maleic anhydride chemical groups so that they can be chemisorbed onto reactive SAM surfaces such as APTMS, which contains amine groups [Satyanarayana et al 2004]. The covalent bond formation between the maleic anhydride groups and amine groups have been previously utilized in the formation of polymer thin films [Jiang and Hammond 2000] and bulk polymer composites [Horiuchi et al 1997]. Therefore, maleic anhydride groups of the polymer films are reacted with amine groups of the APTMS SAM, which in turn is covalently adsorbed onto Si.

7.2 Materials

The details of the Si wafer and APTMS SAM molecules are explained in Section 4.2.

PE (polyethylene-graft-maleic anhydride) and PS (poly (styrene-co-maleic anhydride)), with maleic anhydride functional groups, were obtained from Aldrich, and used for the preparation of polymer solution. The molecular structures of the polymers are shown in Figure 7.1.

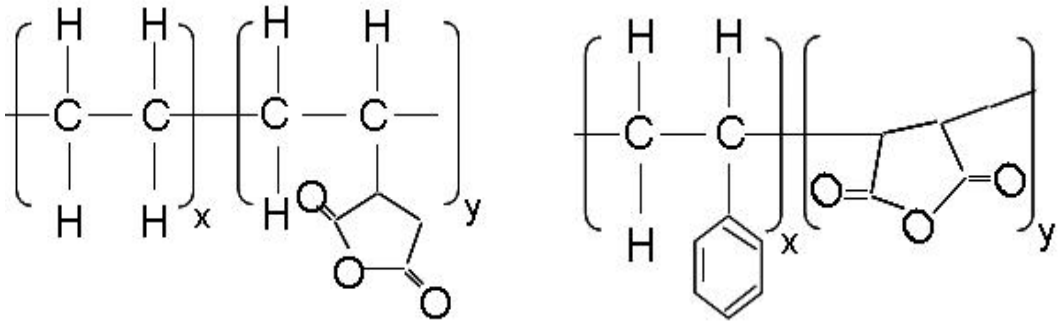

(a) (b)

Figure 7.1*: Chemical structure of (a) Polyethylene-graft-maleic anhydride (PE) and (b) Poly (styrene-co-maleic anhydride) (PS).*

7.3 Preparation of Si/APTMS/PE and Si/APTMS/PS films

The details of the cleaning and piranha treatment of Si surface are explained in Section 4.3.1 and APTMS SAM preparation was explained in Section 4.3.2.

Si/APTMS sample was used as the substrate for PE and PS films coating. The APTMS SAM modified samples were dipped in the respective polymer solutions in toluene (1 vol%) for a period of 24 h in ambient atmosphere (temperature of 22 ± 1 ^{o}C and humidity of 55 ± 5 % RH). After the deposition of the polymer films, the physisorbed

molecules were removed by successive sonication in toluene and methanol respectively for 7-8 min. Finally, the modified samples were dried with N_2 gas and stored in a desiccator, until any characterization.

7.4 Experimental procedures

Surface characterizations such as water contact angle measurement, AFM topography, SEM morphology, ellipsometry, XPS and ToF-SIMS are used to measure the properties of the thin films formed. Tribological properties are measured using a micro-tribometer. All these characterization techniques are explained in Section 3.3. For the measurement of thickness of polymer films using ellipsometry, refractive index values of 1.54 [Aldrich®] and 1.59 [Aldrich® and Julthongpiput et al 2003 (b)] are used for PE and PS respectively.

SEM is used to characterize the wear tracks after sliding tests.

7.5 Results

7.5.1 Contact angle results

Table 7.1 shows the water contact angles of the modified and unmodified Si surface. Si/APTMS/PE and Si/APTMS/PS films have shown water contact angles of 97^o and 80^o, respectively, whereas bare Si and APTMS SAM surfaces have shown water contact angle values of 12^o and 52^o respectively. The water contact angle values of the polymer films suggests that the PE modified Si is more hydrophobic than PS film. Table 1 further suggests that the water contact angles of the present polymer films are consistent with the water contact angles of the corresponding bulk polymers. The

corresponding change in the water contact angles after deposition of the polymer films, when compared to that of APTMS SAM, supports the successful formation of the polymer films.

***Table 7.1**: Water contact angle values of bare Si, Si/APTMS and polymers films. Water contact angle values of bulk polyethylene and polystyrene are also included in the table.*

Sample	Water contact angle, degrees	Reference
Bare Si	12	Present study
Si/APTMS	52	"
Si/APTMS/PE	97	"
Si/APTMS/PS	80	"
Bulk PE	91	[Sira et al 2005]
Bulk PS	79	[Lee et al 1998]

7.5.2 AFM topography

Figure 7.2 shows the three dimensional surface topography images (obtained using AFM) of bare Si, Si/APTMS, Si/APTMS/PE and Si/APTMS/PS samples. Both polymer films have shown island structure, but the islands are very irregular and non-uniform in the case of Si/APTMS/PE whereas regular and uniform in the case of Si/APTMS/PS. Hence, Si/APTMS/PS has shown lower roughness value (1.6 nm) than that of Si/APTMS/PE (1.9 nm). Moreover, both polymer films have shown higher roughness values than bare Si (0.16 nm) and Si/APTMS (0.37 nm).

Finally, the AFM topography also confirms the full coverage of polymer layers on APTMS SAM, supporting the corresponding changes in water contact angles, as reported above.

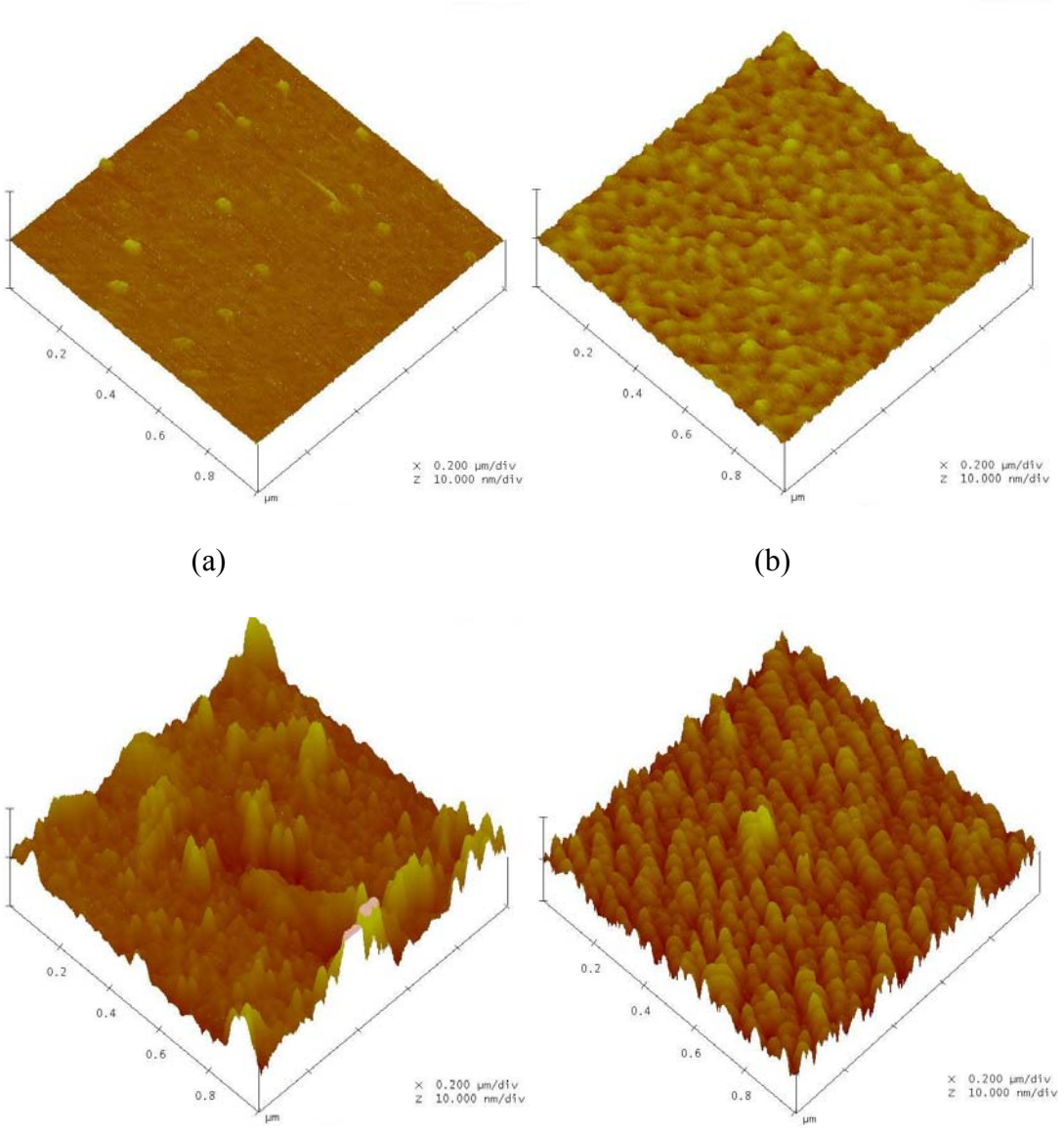

***Figure 7.2**: AFM topography of (a) bare Si, (b) Si/APTMS, (c) Si/APTMS/PE and (d) Si/APTMS/PS samples. The scan size is 1µm x 1µm and the vertical scale is 10 nm for all the images.*

7.5.3 Thickness results

APTMS SAM has shown a thickness of 4.1 nm where as the silicon oxide (after piranha treatment) has shown a value of ~2 nm [Chapter 4]. The PE and PS films have shown thickness values of 15 nm and 12.1 nm respectively. All measurements were carried out using ellipsometer.

7.5.4 ToF-SIMS results

Figure 7.3 shows the positive SIMS spectra of PE and PS films modified APTMS SAM. The positive spectrum of PE shows several hydrocarbon peaks at mass values of 27 ($C_2H_3^+$), 29 ($C_2H_5^+$), 41 ($C_3H_5^+$), 43 ($C_3H_7^+$), 55 ($C_4H_7^+$), 57 ($C_4H_9^+$) etc which are consistent with the standard peaks of polyethylene [Oiseth et al 2002]. The positive spectrum of PS contains two distinct aromatic ions at mass values of 77 ($C_6H_5^+$) and 91 ($C_7H_7^+$) in addition to the few other hydro carbon peaks which are identical with those reported for bulk polystyrene [Zeng et al 2001]. The ToF-SIMS data clearly support the successful formation of the respective polymer films on APTMS SAM.

7.5.5 XPS results

Figure 7.4 shows the XPS wide scan spectra of bare Si, Si/APTMS, Si/APTMS/PE and Si/APTMS/PS. The explanation of XPS spectra for bare Si and APTMS SAM can be found in Chapter 4. The increase in the intensity of C 1s peak after polymer film deposition, when compared to that of APTMS SAM, supports their successful formation. The chemical bonding between the maleic anhydride groups and amine groups is difficult to identify from XPS results, as both amides and amines have

binding energies in the range of ~399.5-400.5 eV [Baker et al 2002 and Moulder et al 1992].

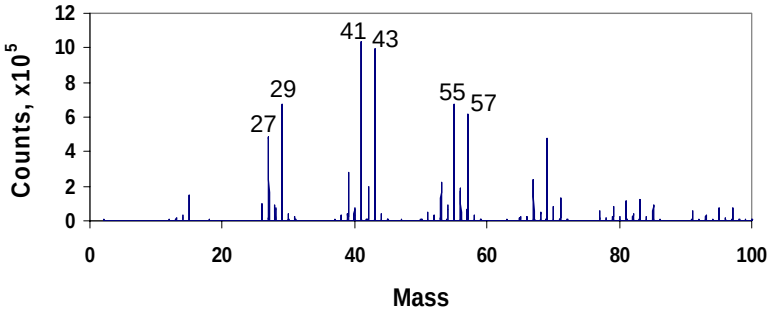

(a)

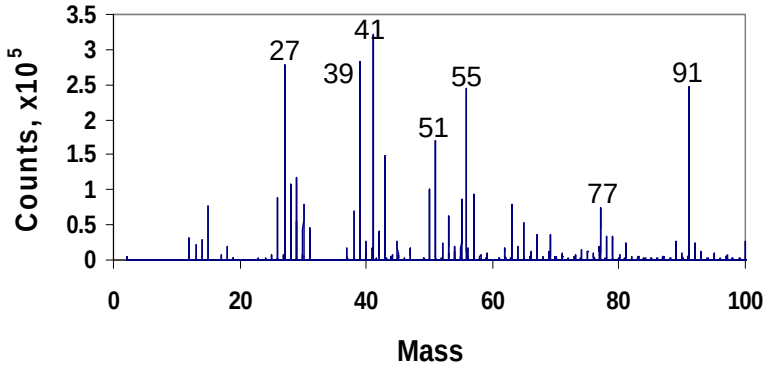

(b)

Figure 7.3: *The positive ion SIMS spectra of (a) Si/APTMS/PE and (b) Si/APTMS/PS samples. Please refer to the text for the explanation of the marked peaks*

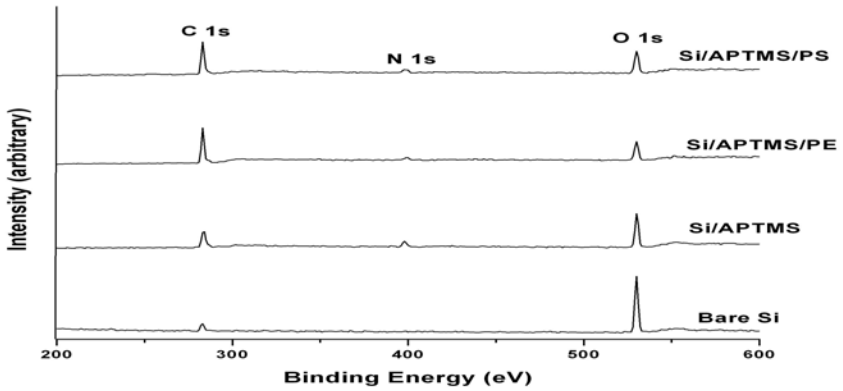

.

Figure 7.4*: XPS wide scan spectrum of bare Si, Si/APTMS, Si/APTMS/PE and Si/APTMS/PS samples.*

7.5.6 Tribological properties

Figure 7.5 shows the coefficient of friction values of polymer films modified and unmodified samples. Bare Si and APTMS SAM have shown coefficient of friction values of 0.4 and 0.8 respectively. PE film has shown a coefficient of friction of 0.08 whereas PS film has shown a coefficient of friction value which is close to that of un-modified Si (i.e. 0.4). Therefore, the data showed in Figure 7.5 demonstrates that PE film is very effective in reducing the coefficient of friction while PS film has shown similar coefficient of friction values as that of bare Si.

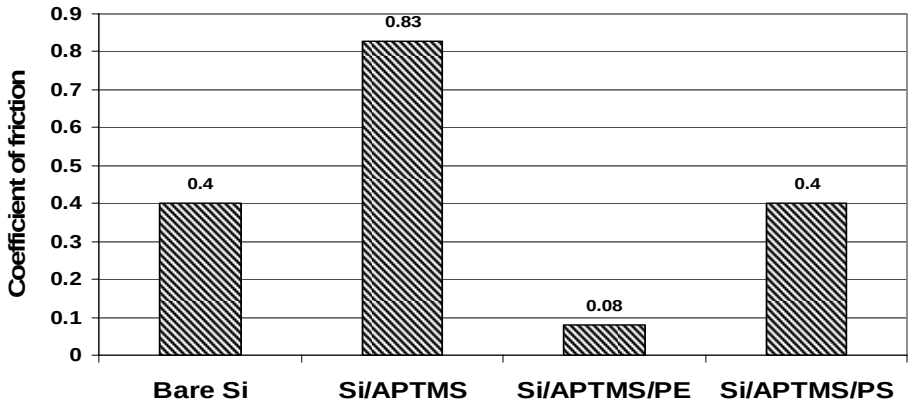

***Figure 7.5**: Coefficient of friction values of bare Si, Si/APTMS, Si/APTMS/PE and Si/APTMS/PS, tested against 4mm diameter Si_3N_4 ball, at a normal load of 5g and a sliding velocity of 1mm sec^{-1} using ball-on-plate configuration.*

Figure 7.6 shows the variation of frictional force with respect to the change in normal load applied. The variation is nearly linear for all the samples.

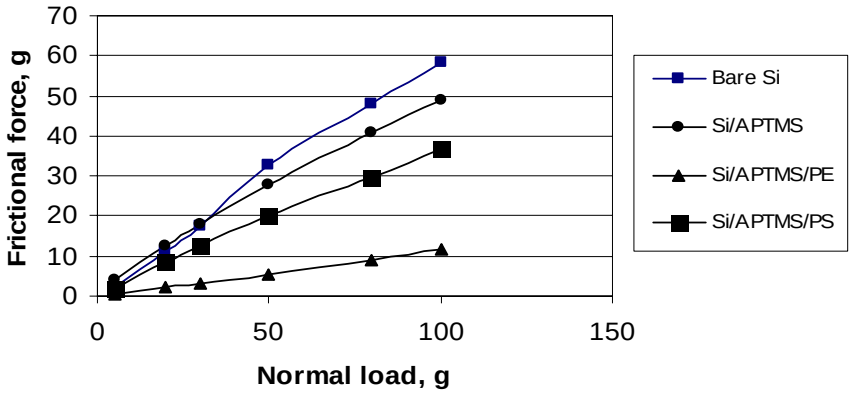

***Figure 7.6**: Variation of frictional force with respect to the normal load applied for bare Si, Si/APTMS, Si/APTMS/PE and Si/APTMS/PS, tested against 4 mm diameter Si_3N_4 ball, at a sliding velocity of 1 mm sec^{-1} using ball-on-plate configuration.*

Figure 7.6 also shows that the Si/APTMS/PE sample demonstrates very low coefficient of friction when compared to Si/APTMS/PS. The linear relation between the frictional force and normal load can be understood from Bowden and Tabor adhesive friction model [Bowden and Tabor 1950]. According to this model, the frictional force is directly proportional to the real area of contact which is expressed as:

$$F_f = \tau A_r$$

where, τ is the shear strength, an interfacial property and A_r is the real area of contact. Moreover, the contact area depends on the applied normal load and the size of the sphere (ball in the present case), according to the JKR (Johnson-Kendall-Roberts) model [Johnson et al 1971], which is given as:

$$A_r = \pi [R/K (F_n+6\pi\gamma R+[12\pi\gamma R F_n+(6\pi\gamma R)^2]^{1/2})]^{2/3}$$

where, R is the size of the sphere, K the effective elastic modulus, F_n the applied normal load and γ, the interfacial energy of the material. Therefore, the real area of contact increases with increase in the applied normal load for a fixed size of the sphere (ball)

(from JKR theory). Hence, the frictional force increases with respect to the applied normal load (as the contact area increases with respect to the applied normal load). Singh et al [2007] have observed the similar behavior for several SAM surfaces. The exact linear relationship between the frictional force and normal load suggests that there is either no contact temperature rise with the increase in the normal load at the prevailing contact conditions or there is well dissipation of the frictional heat generated even at higher loads. The friction variation with respect to the normal load has shown decreasing slope at higher normal loads because of the higher amount of heat generated in the case of bulk polymers [Williams 1994], which is not observed in the present polymer films case.

The variation of the coefficient of friction with respect to the sliding velocity tested at a constant normal load of 5 g for all the samples is shown in Figure 7.7. Different samples have shown slightly different behavior. A close observation of all the curves shows that the coefficient of friction is almost invariant with respect to the sliding velocity for Si/APTMS/PE and Si/APTMS/PS. Some variation is within the data scatter due to experimental errors. This might be because of their hydrophobic behavior. It has been reported in the literature that the frictional force of hydrophobic SAMs is invariant with respect to the sliding velocity [Liu et al 2001 (b) and Liu and Bhushan 2003 (b)]. The coefficient of friction reduces with respect to the sliding velocity in the case of bare Si and reaches a minimum value beyond certain sliding velocity. Bare Si always contains thin water film on its surface which forms capillary and leads to high friction (especially static friction) during sliding.

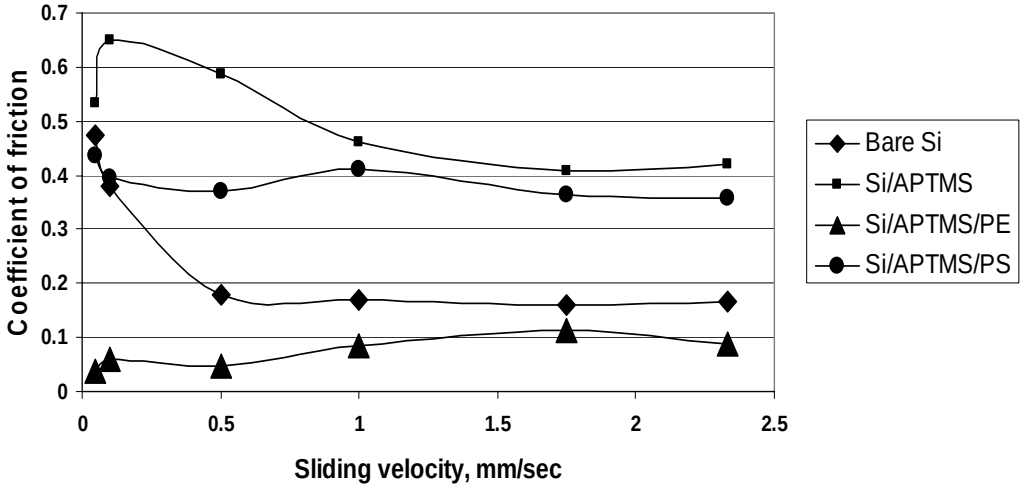

***Figure 7.7**: Variation of coefficient of friction with respect to the sliding velocity for bare Si, Si/APTMS, Si/APTMS/PE and Si/APTMS/PS, tested against 4mm diameter Si_3N_4 ball, at a normal load of 5 g using ball-on-plate configuration.*

But there is no sufficient time for the formation of the capillary at higher sliding velocities due to fast dynamic situation and hence bare Si shows low friction as the sliding velocity increases [Liu et al 2001 (b)]. Moreover at higher sliding velocities, tribo-chemical reactions between water and Si leads to the formation of lower shear strength Si $(OH)_4$ which contribute to the reduction of the coefficient of friction [Liu and Bhushan 2003 (b)]. In the case of Si/APTMS, the coefficient of friction increases initially with the sliding velocity and then reduces beyond certain sliding velocity. The reason for the observation of maxima is attributed to the local phase transition in the film, which has been observed in certain films in the literature [Liu et al 1996]. The similar maxima have been observed in the case of DLC (diamond like carbon) film as well, which was related to the phase transformation of DLC to a low shear strength graphite-like phase by a sp^3 to sp^2 phase transition [Tambe and Bhushan 2005]. In the case of hydrophobic SAMs, the friction force is independent of the sliding velocity because of absence of the capillary

action due to negligible adsorption of water [Liu and Bhushan 2003 (b)]. Finally, Figure 7.7 also supports that the Si/APTMS/PE shows very low coefficient of friction when compared to Si/APTMS/PS at all sliding velocities.

Figure 7.8 shows the sliding wear test results for bare Si, Si/OTS, Si/APTMS, Si/APTMS/PE and Si/APTMS/PS. The dynamic coefficient of friction during sliding as a function of the number of cycles is shown in Figure 7.8 (a) whereas the average wear durability values are shown in Figure 7.8 (b).

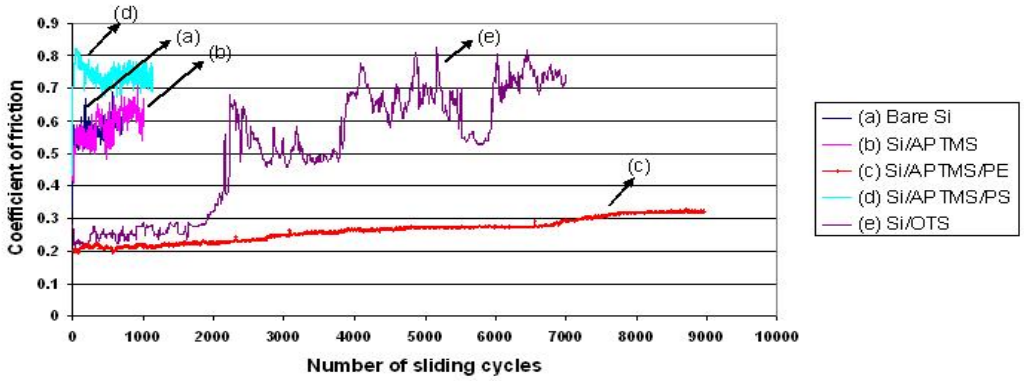

(a)

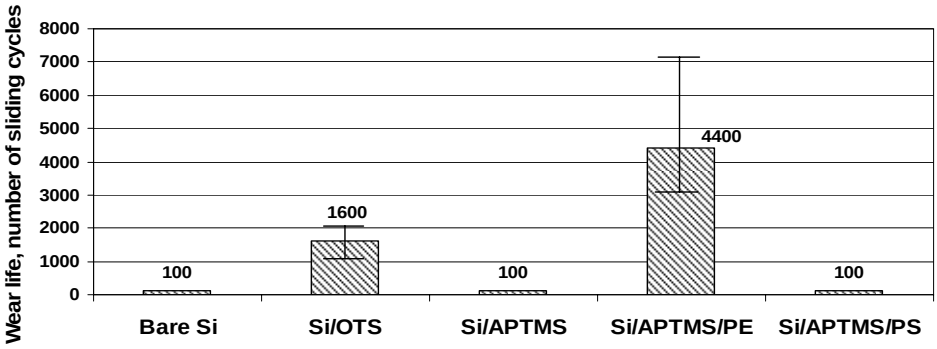

(b)

***Figure 7.8**: (a) Variation of coefficient of friction with respect to number of sliding cycles and (b) Average wear life (number of cycles after which the film failed) of bare Si, Si/OTS, Si/APTMS, Si/APTMS/PE and Si/APTMS/PS samples, obtained in ball-on-disk tests against 4 mm Si_3N_4 ball at a normal load of 5 g and sliding velocity of 0.021 m s^{-1}.*

Both bare Si and APTMS SAM surfaces have failed within few tens of cycles after beginning of the sliding. Among the two polymer films tested for molecular structure effect, Si/APTMS/PE has shown greater wear life (~4400 cycles) (which is ~2.5 times that of traditional OTS SAM (~1600cycles)), whereas Si/APTMS/PS film failed below 100 cycles of sliding, which is identical to that of bare Si and Si/APTMS. In the case of Si/APTMS/PS, the coefficient of friction was high from the beginning of the test and a clear distinct wear track appeared within few tens of cycles of sliding.

The SEM micrograph of the wear track of Si/APTMS/PS, after ~100 cycles of sliding and EDS analysis, inside and outside the wear track region are shown in Figure 7.9. The SEM image of the wear track of Si/APTMS/PS, after 100 cycles of sliding (Figure 7.9 (a)) shows severely worn polymer region and Si surface. The intensity of the C peak as shown in the EDS spectrum on the polymer surface (other than wear track region) is very small which is attributed to the low thickness of the polymer film. Figure 7.9 (c) shows the EDS spectrum inside the wear track, which contains very less intense C peak and more intense Si peak than that outside the wear track. This supports the wear durability result concluded from the coefficient of friction data during sliding test [Figure 7.8]. For Si/APTMS/PE, severely damaged wear track appeared after ~7000 cycles and EDS analysis also has shown a distinct Si peak inside the wear track after ~7000 cycles of sliding (data is not included). Therefore, SEM/EDS analysis of the worn surfaces also supports the quantitative wear durability data reported in Figure 7.7 and confirms that Si/APTMS/PE has much better tribological performance than Si/APTMS/PS.

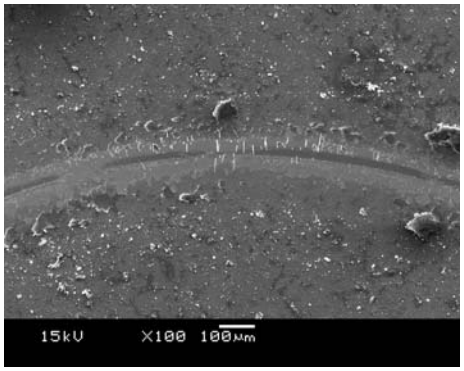

(a)

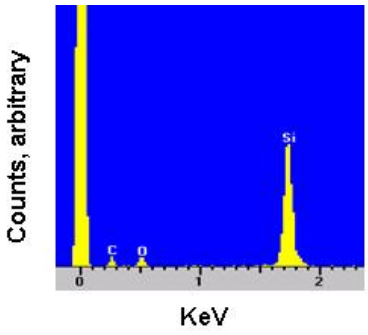

(b)

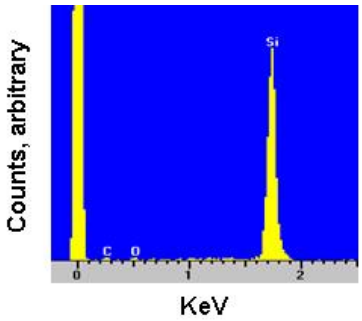

(c)

***Figure 7.9**: (a) SEM image of the wear track after tribological test, (b) EDX spectrum outside the wear track and (c) EDX spectrum inside the wear track for Si/APTMS/PS after 100 cycles of sliding at 5g and 0.021 ms^{-1} velocity.*

7.6 Discussion

As explained in Chapter 2, there is no systematic data on the effect of molecular structure of the polymer film on their tribological properties despite some studies involving the tribological characterization of ultra-thin polymer films. Among the two polymer films selected, PE has shown lower coefficient of friction and high wear durability than PS film. The low coefficient of friction and high wear durability of PE film is attributed to its linear and flexible backbone chain which offers little resistance to the sliding whereas PS molecule contains bulky benzene groups which offer higher resistance to the sliding (restricts the movement of molecular chains) and hence has resulted in higher friction and high wear. This concept has been observed in the case of bulk polymers [Pooley and Tabor 1972] and the present results conclude that same mechanism also apply for similar ultra-thin polymer films. Thomas [1996] has reported that the flow characteristics (or rheological characteristics) of the polymer films are better for the flexible molecular chains than complex rigid molecular chains, because the flexible molecular chain has low shear strength and hence offers lower resistance to the shearing/sliding resulting in lower friction. This also must have lead to the high wear in the case of Si/APTMS/PS, where the polymer molecule contains bulky benzene groups.

The mechanical properties of the polymer films also influence the anti-wear properties, besides the resistance to the shearing action, as explained above. In the bulk form, PE has very high % elongation (plastic) at failure, low ultimate tensile strength and tensile modulus than those of PS and moreover, PS is a brittle polymer whereas PE is a ductile polymer [Nielsen 1974]. Therefore, the ductile nature of PE with higher % elongation restricts the generation of wear particles because of effective plastic

deformation by shear and hence shows higher wear durability. PS shows low wear durability because of its brittle nature which leads to easy generation of wear debris by crazing and cracking phenomena under a sliding contact. The frictional energy for PE is easily dissipated by extensive plastic deformation within a thin layer close to the interface. This thin layer can shear to a great extent and relax easily before being sheared again in a dynamic situation. The excellent flexibility of the linear thermoplastic molecules gives very low strain or strain rate hardening effect as the polymer easily relaxes after being deformed. Thus, the brittle fracture processes of crazing and cracking is largely minimized for PE and similar polymers.

Therefore, the present study demonstrates that the molecular structure of the polymer film is one of the primary factors to be considered when proposing certain polymer films for tribological properties. For polymers (film or bulk) sliding against a hard counterface, the necessary condition for high wear resistance is its large elongation before failure coupled with good strength.

7.7 Conclusions

In the present study, polyethylene and polystyrene (functionalized with maleic anhydride groups) were coated as ultra-thin films onto Si, by utilizing APTMS as an intermediate reactive SAM. A micro-tribometer was used to investigate the coefficient of friction and wear durability of the polymer films sliding against 4 mm diameter Si_3N_4 ball.

Following conclusions can be drawn from the present study:

1. Si/APTMS/PE and Si/APTMS/PS have shown water contact angle values of 97^{o} and 80^{o} respectively, which are consistent with the water contact angle values of the similar bulk polymers.

2. For all the films studied, frictional force varies linearly with the normal load applied. The coefficient of friction of Si/APTMS/PE (0.08) was lower than that of Si/APTMS/PS (0.4).

3. Si/APTMS/PE has very high wear durability when compared to Si/APTMS/PS which also reflects their behaviors in bulk form. Polyethylene film has resulted in a wear durability of ~4,400 cycles whereas polystyrene film has worn out below ~100 cycles.

The present results clearly infer that the molecular structure of the polymer film greatly influences their tribological properties. The polymer films that contain linear chains with less bulky side groups may lead to low friction and wear during sliding.

The present results will help in the development of new ultra-thin polymer films with exceptional high wear durability.

Chapter 8

Conclusions

The primary objective of this thesis was to deposit and investigate the tribological properties of organic ultra-thin films (such as SAMs and polymer films) on Si surface. As Si surface itself shows high friction, adhesion and wear, we designed and tested several films which significantly reduced the friction, adhesion and wear. Some of the proposed films or lubrication mechanisms may find applications in improving the performance of components made from Si (for example MEMS).

The specific ultra-thin films that have been developed in the present research are, (1) PFPE (a top mobile layer) overcoated SAMs, (2) UHMWPE films on Si (development of coating procedure and further enhancement in tribological properties by overcoating with PFPE), (3) Addition of CNT as a filler material to PI films and (4) PE and PS films chemisorbed onto Si surface through a reactive SAM surface. Even though the underlying common objective behind the development of these films is the same (to obtain an ultra-thin film on Si with very low friction, adhesion and high wear durability), each set of films was developed with some specific objectives in order to understand the mechanisms responsible for high wear durability and low friction of certain films. The thickness of these films ranges between few nanometers to several microns.

The following conclusions are drawn from the present research:

I *PFPE overcoated SAMs*

- PFPE coating onto SAMs has made the surface more hydrophobic and the extent of increase in water contact angle values was different for different SAMs which was attributed to the specific interactions between the PFPE and SAM molecules.

- AFM imaging has shown that the surface became very smooth after overcoating the SAMs with PFPE.
- When PFPE was coated onto a SAM surface, a fraction was present as a bonded layer whereas remaining fraction was present as a mobile layer.
- PFPE overcoating has reduced the coefficient of friction of SAMs and increased their wear durability to a great extent.
- The extent of improvement in wear durability was different for different SAMs which was attributed to the SAM surface properties such as wettability, chemical interactions between SAM and PFPE molecules, molecular packing density and order in the SAM molecules. The extent of improvement in wear durability was higher when PFPE was coated onto SAMs with polar terminal groups (such as APTMS and epoxy SAMs) than with non-polar terminal groups (OTS) and this behavior was attributed to the beneficial effect from the strong chemical interactions between the PFPE and reactive SAMs.
- Post thermal treatment has influenced the chemical interactions between the PFPE and SAMs and hence affected the wear durability characteristics.
- Overall, Si/epoxy SAM/PFPE-as lubricated and Si/APTMS/PFPE-thermally treated have shown very high wear durability among several samples studied.

Finally, the primary outcome from this study is summarized as: we need an ultra-thin layer such as PFPE in addition to the chemically bound SAMs to obtain low friction, adhesion and high wear durability. Also, we need an optimum combination of strong chemical bonding between PFPE and SAM molecules and an optimum amount of mobile PFPE for better tribological properties in the case of PFPE coated SAMs.

II *UHMWPE films on Si surface*

- UHMWPE films with thicknesses in the range of few to several micrometers were obtained using a simple dip-coating technique.
- FTIR study has shown that the chemical nature of the UHMWPE film was similar to its bulk counterpart.
- The UHMWPE film was mechanically stable, very hydrophobic and has shown very low coefficient of friction and good wear durability (~10 times that of OTS SAM).
- The dual layer film (Si/UHMWPE/PFPE) has shown very high wear durability which was attributed to the lubrication nature of individual polymers and also the effect of the surface features of UHMWPE film which might have helped in trapping the PFPE molecules. The present dual layer film has protected the Si surface without any wear for many thousands of sliding cycles (> 100,000 cycles).

III *Addition of CNTs as a filler material to enhance the wear durability of PI film*

- We observed that the addition of CNTs to the polyimide film has shown good improvement in wear durability of the polyimide film.
- Nanoindentation tests have shown that there was good improvement in the mechanical properties (hardness and elastic modulus) when CNTs were added to polyimide film.
- The increase in the wear durability was attributed to the good mechanical properties after CNTs addition and good bonding between CNTs and the polymer.

IV *PE and PS films chemisorbed onto Si through reactive SAM*

- The tribological studies have shown that PE film demonstrates low coefficient of friction and good wear durability whereas PS has shown high coefficient of friction and very low wear durability (same as that of bare Si).
- The main conclusion from this study was that the molecular structure of the polymer film greatly influences the tribological properties and hence, the molecular structure must be considered as a design parameter when developing ultra-thin polymer films for lubrication purposes.
- Moreover, a polymer film with very linear molecule chains without any bulky side groups provides low friction and high wear durability.

The wear-life data of all the novel films developed in the present thesis are listed in Table 8.1, for easy reference and quick comparison. Below are some specific comparisons between various films, for better understanding of the differences in the wear lives of various films.

SAMs/PFPE vs UHMWPE/PFPE:

The extent of improvement in wear durability is very large when PFPE over-coated onto UHMWPE when compared to SAM surfaces. The primary reason could be the entrapment of PFPE molecules into the valleys present on UHMWPE film. The trapped PFPE is expected to diffuse into the contact regions during sliding and provides extended lubrication whereas in the cases of SAMs, there is very little or no entrapment of PFPE and hence once the layer of PFPE is removed from the surface there is no extra benefit

from the entrapped PFPE. Therefore, it is concluded that a textured surface produces greater improvement in wear durability after over-coating with liquid lubricants such as PFPE.

Table 8.1*: Coefficient of friction and wear lives of selected films developed in the present thesis. Contact pressure used during the tribological tests is also included.*

Material	Contact pressure used during tribological test, MPa	Coefficient of friction	Wear life, number of cycles
Bare Si	330	0.60	<100
Si/OTS	"	0.19	1600
Si/APTMS	"	0.50	<100
Si/epoxy SAM	"	0.60	<100
Si/PFPE	"	0.17	5000
Si/OTS/PFPE	"	0.15	2500
Si/APTMS/PFPE	"	0.20	5400
Si/epoxy SAM/PFPE	"	0.10	6800
Si/UHMWPE	370	0.09	12000
Si/UHMWPE/PFPE	"	0.08	> 100,000
Si/PI	"	0.10	3000
Si/PI+CNTs	"	0.12	7200
Si/APTMS/PE	330	0.08	4400
Si/APTMS/PS	"	0.40	100

SAMs/PFPE vs SAMs/PE or PS:

PFPE coating onto APTMS SAM has shown slightly higher wear durability when compared to PE film chemisorbed onto APTMS SAM. A fraction of PFPE present as bonded layer whereas the remaining fraction present as mobile layer. The presence of the mobile PFPE layer is expected to show high wear durability in the case of APTMS/PFPE than APTMS/PE because the later does not contact any mobile layer. Therefore, in the

case of APTMS/PE, once wear starts the PE and/or the SAM molecules are removed there will not be any replenishment and hence it further lead to severe wear. Hence, APTMS/PFPE has shown high wear durability when compared to APTMS/PE. The primary conclusion from this comparison is the importance of the presence of the mobile layer for high wear durability coatings.

Chapter 9

Future Recommendations

Below listed are the recommendations for future study:

I *PFPE overcoated SAMs*

Below are the suggestions for further studies based on PFPE overcoating onto SAMs

1. Several other liquid lubricants in addition to PFPE have to be studied for the possibility of further improvement in wear durability

2. The end group chemistry of PFPE will also influence the tribological properties and further studies are needed to elucidate this effect

3. Further studies are needed to identify the individual contributions of the bonded and mobile fractions of PFPE towards the wear durability

II *UHMWPE films on Si surface*

1. The procedures have to be developed to coat ultra-thin films from other wear-resistant polymers such as PEEK.

2. Other liquid lubricants in addition to PFPE can be tested for the possibility of further improvement in tribological properties.

III *Addition of CNT as a filler material to enhance the wear durability of PI film*

1. From the present study, it is not clear that whether similar improvement can be obtained when CNTs are added to other polymer films and further studies are needed to clarify this behavior.

2. Several other filler materials can be tested for the possibility of improvement in wear durability of polymer thin films.

IV *PE and PS films chemisorbed onto Si through reactive SAM*

The present work can be extended to other polymers of different molecular structure (such as PMMA [Sakata et al 2005], PDMS [Liu et al 2002] etc) to understand further details into the effect of molecular structure of the polymer film on tribological properties.

Future studies must also focus on interpreting the wear data with the analytical models available or may be able to generate some new models to better explain the experimental data. Further, investigation and in-depth analysis of the mechanical properties of the presently developed films could be interesting and stimulating.

References

Abe, T., Messner, W. C. and Reed, M. L. Effects of elevated temperature treatments in microsctructure release procedures. Journal of Microelectromechanical Systems, 4, pp. 66-75, 1995.

Adamson, A. W. Physical Chemistry of Surfaces. 5th edition, Wiley, New York, 1990.

Advincula, R. C., Brittain, W. J., Caster, K. C. and Ruhe, J. Polymer Brushes: Synthesis, Characterization and Applications. Wiley-VCH Verlag GmbH & Co., 2004.

Agarwal, M., de Guire, M. R. and Heuer, A. H. Synthesis of ZrO_2 and Y_2O_3-doped ZrO_2 thin films using self-assembled monolayers. Journal of American Ceramic Society, 80, pp. 2967-2981, 1997.

Ahn, H-S., Julthongpiput, D., Kim, D-I. and Tsukruk, V. V. Dramatic enhancement of wear stability in oil-enriched polymer gel nanolayers. Wear, 255, pp. 801-807, 2003.

Aldrich®, Handbook of chemicals and laboratory equipment, 2006.

Alley, R. L., Mai, P., Komvopoulos, K. and Howe, R. T. Surface roughness modification of interfacial contacts in polysilicon microstructures. Proceedings of the 7th International Conference on Solid-State Sensors and Actuators, Transducers '93, pp. 288-291, 1993.

Alley, R. L., Howe, R. T. and Komvopoulos, K. Method of applying a monolayer lubricant to micromachines. USA Patent, 5403665, 1995.

Alves, A. L. S., Nascimento, L. F. C. and Suarez, J. C. M. Influence of weathering and gamma irradiation on the mechanical and ballistic behavior of UHMWPE composite armor. Polymer Testing, 24, pp. 104-113, 2005.

Ando, E., Goto, Y., Morimoto, K., Ariga, K. and Okahata Y. Frictional properties of monomolecular layers of silane compounds. Thin Solid Films, 180, pp. 287-291, 1989.

Archard, J. F. Contact and rubbing of flat surfaces. Journal of Applied Physics, 24, pp. 981, 1953.

Ashurst, W. R., Yau, C., Carraro, C., Maboudian, R. and Dugger, M. T. Dichlorodimethylsilane as an anti-stiction monolayer for MEMS: A comparison to the octadecyltrichlorosilane self-assembled monolayer. Journal of Microelectromechanical Systems, 10, pp. 41-49, 2001 (a).

Ashurst, W. R., Yau, C., Carraro, C., Lee, C., Kluth, G. J., Howe, R. T. and Maboudian, R. Alkene based monolayer films as anti-stiction coatings for polysilicon MEMS. Sensors and Actuators A, 91, pp. 239-248, 2001 (b).

Ashurst, W. R., Carraro, C. and Maboudian, R. Vapor phase anti-stiction coatings for MEMS. IEEE transactions on device and materials reliability, 3, pp. 173-178, 2003.

Bailey, A. I. and Pratt, J. S. C. The area of real contact and the shear strength of monomolecular layers of a boundary lubricant. Proceedings of the Royal Society of London A, 227, pp. 500-515, 1955.

Baker, S. E., Cai, W., Lasseter, T. L., Weidkamp, K. P. and Hamers, R. J. Covalently bonded adducts of deoxyribonucleic acid (DNA) oligonucleotides with single-wall-carbon nanotubes: synthesis and hybridization. Nano Letters, 2, pp. 1413-1417, 2002.

Bao, Y., Zhang, T. and Gawne, D. T. Influence of composition and process parameters on the thermal spray deposition of UHMWPE coatings. Journal of Materials Science, 40, pp. 77-85, 2005.

Beake, B. D. and Leggett, G. J. Variation of frictional forces in air with the compositions of heterogeneous organic surfaces. Langmuir, 16, pp. 735-739, 2000.

Bernstein, J., Cho, S., King, A. T., Kourepenis, A., Maciel, P. and Weinberg, M. A micromachined comb-drive tuning fork rate gyroscope. Micro Electro Mechanical Systems, Fort Lauderdale, FL, USA, 1993.

Bhushan, B. Handbook of Micro/Nano Tribology. Boca Raton, Fl, CRC Press, 1991.

Bhushan, B., Israelachvili, J. N. and Landman, U. Nanotribology: friction, wear and lubrication at the atomic scale. Nature, 374, pp. 607-616, 1995 (a).

Bhushan, B., Kulkarni, A. V., Koinkar, V. N., Boehm, M., Odoni, L., Martelet, C. and Belin, M. Microtribological characterization of self-assembled and Langmuir-Blodgett monolayers by atomic and friction force microscopy. Langmuir, 11, pp. 3189-3198, 1995 (b).

Bhushan, B. Tribology and Mechanics of Magnetic Storage Devices. 2nd Edition, Springer Verlag, New York, 1996.

Bhushan, B. Micro/nanotribology: state of the art and its applications. In Bhushan B, Editor, Tribology Issues and Opportunities in MEMS, pp. 229-246, Dordrecht, Netherlands, Kluwer Academic Publishers , 1998.

Bhushan, B. and Dandavate, C. Thin-film friction and adhesion studies using atomic force microscopy. Journal of Applied Physics, 87, pp. 1201-1211, 2000.

Bhushan, B. and Liu, H. Nanotribological properties and mechanisms of alkylthiol and biphenyl thiol self-assembled monolayers studied by atomic force microscopy. Physical Review B, 63, pp. 245412-1-245412-11, 2001.

Bhushan, B. Self-assembled monolayers for controlling adhesion, friction and wear, Springer Handbook of Nanotechnology. Edited by B. Bhushan, Springer, Germany, pp. 831-860, 2004 (a).

Bhushan, B., Liu, H. and Hsu, S. M. Adhesion and friction studies of silicon and hydrophobic and low friction films and investigation of scale effects. Journal of Tribology, 126, pp. 583-590, 2004 (b).

Binnig, G., Quate, C. F. and Gerber, Ch. Atomic force microscope, Physical Review Letters, 56, pp. 930-934, 1986.

Blackman, G. S., Mate, C. M. and Philpott, M. R. Interaction forces of a sharp tungsten tip with molecular films on silicon surfaces. Physical Review Letters, 65, pp. 2270-2273, 1990.

Bliznyuk, V. N., Everson, M. P. and Tsukruk, V. V. Nanotribological properties of organic boundary lubricants: Langmuir films versus self-assembled monolayers. Journal of Tribology, 120, pp. 489-495, 1998.

Bouhacina, T., Aime, J. P., Gauthier, S. and Michel, D. Tribological behavior of a polymer grafted on silanized silica probed with a nanotip. Physical Review B, 56, pp. 7694-7703, 1997.

Bowden, F. P. and Tabor, D. The Friction and Lubrication of Solids. Clarendon Press, Oxford, 1986.

Braun, H. G., and Meyer, E. Thin microstructured polymer films by surface-directed film formation. Thin Solid Films, 345, pp. 222-228, 1999.

Briscoe, B. J., Pogosian, A. K. And Tabor, D. The friction and wear of high density polyethylene: The action of lead oxide and copper oxide fillers. Wear, 27, pp. 19-34, 1974.

Briscoe, B. J. Wear of polymers: An essay on fundamental aspects. Tribology International, pp. 231-243, 1981.

Briscoe, B. J. and Evans, D. C. B. The shear properties of Langmuir-Blodgett layers. Proceedings of the Royal Society of London A, 380, pp. 389-407, 1982.

Briscoe, B. J., Fiori, L. and Pelillo, E. Nano-indentation of polymeric surfaces. Journal of Physics D: Applied Physics, 31, pp. 2395-2405, 1998 (a).

Briscoe, B. J., Chateauminois, A., Lindley, T. C. and Parsonage, D. Fretting wear behaviour of polymethylmethacrylate under linear motions and torsional contact conditions. Tribology International, 31, pp. 701-711, 1998 (b).

Briscoe, B. J. and Sinha, S. K. Tribology of polymeric solids and their composites, in Wear- Materials, Mechanism and Practice, (ed. G. Stachowiak), John Wiley & Sons, Chichester, England, pp. 223-267, 2005.

Bryzek, J., Petersen, K. and McCulley, W. Micromachines on the march. IEEE Spectrum, 31, pp. 20-31, 1994.

Cai, H., Yan, F. and Xue, Q. Investigation of tribological properties of polyimide/carbon nanotube nanocomposites. Materials Science and Engineering A, 364, pp. 94-100, 2004.

Cadek, M., Coleman, J. N., Barron, V., Hedicke, K. and Blau, W. J. Morphological and mechanical properties of carbon-nanotube-reinforced semicrystalline and amorphous polymer composites. Applied Physics Letters, 81, pp. 5123-5125, 2002.

Callister, W. D. Materials Science and Engineering: An Introduction. John Wiley & Sons (Asia) Pte Ltd, 7th Edition, 2006.

Cant, N. E., Critchley, K., Zhang, H-L. and Evans, S. D. Surface functionalization for the self-assembly of nanoparticle/polymer multilayer films. Thin Solid Films, 426, pp. 31-39, 2003.

Cao, L., Mantell, S. and Polla, D. Design and simulation of an implantable medical drug delivery system using microelectromechanical systems technology. Sensors and Actuators A- Physical, 94, pp. 117, 2001.

Cappella, B. and Dietler, G. Force-distance curves by atomic force microscopy. Surface Science Reports, 34, pp. 1-104, 1999.

Cha, K-H. and Kim, D-E. Investigation of the tribological behavior of octadecyltrichlorosilane deposited on silicon. Wear, 251, pp. 1169-1176, 2001.

Chau, K. H. L. and Sulouff, R. E. Technology for the high-volume manufacturing of integrated surface-micromachined accelerometer products. Microelectronics Journal, 29, pp. 579, 1998.

Chen, C-Y., Bogy, D. and Bhatia, C. S. Effect of lubricant bonding fraction at the head-disk interface. Tribology Letters, 10, pp. 195-202, 2001.

Chitsaz-Zadeh, M. R. and Eiss, N. S. Jr. Friction and wear of polyimide thin films, Wear, 110, pp. 359-368, 1986.

Choi, J. and Kato, T. Development of the mixed nanolubricant system by FDTS islands and PFPE mobile phase. IEEE Transactions on magnetics, 39, pp. 2444-2446, 2003.

Choi, J., Morishita, H. and Kato, T. Frictional properties of bilayered mixed lubricant films on an amorphous carbon surface: effect of alkyl chain length and SAM/PFPE portion. Applied Surface Science, 228, pp. 191-200, 2004.

Clear, S. C. and Nealey, P. F. Lateral force microscopy study of the frictional behavior of self-assembled monolayers of octadecyltrichlorosilane on silicon/silicon dioxide immersed in n-alcohols. Landmuir, 17, pp. 720-732, 2001.

Cleveland, J. P., Manne, S., Bocek, B. and Hansma, P. K. A non-destructive method for determining the spring constant of cantilevers for scanning force microscopy. Review of Scientific Instruments, 64, pp. 403-405, 1993.

Colton, R. J. Forum on new ideas in tribology. Langmuir, 12, pp. 4574-4582, 1996.

De Boer, M. P. and Mayer, T. M. Tribology of MEMS. MRS Bulletin, 26, pp. 302-304, 2001.

De Guzman, M. S., Neubauer, G., Flinn, P. and Nix, W. D. The role of indentation depth on the measured hardness of materials. Materials Research Symposium Proceedings, 308, pp. 613-618, 1993.

Deligoz, H., Ozgumus, S., Yalcinyuva, T., Yildirim, S., Deger, D. and Ulutas, K. A novel cross-linked polyimide film: synthesis and dielectric properties. Polymer, 46, pp. 3720-3729, 2005.

Deng, K., Collins, R. J., Mehregeng, M. and Sukenik, C. N. Performance impact of monolayer coating of polysilicon micromotors. Journal of Electrochemical Society, 142, pp. 1278-1285, 1993.

Deng, K., Collins, R. J., Mehregany, M. and Sukenik, C. N. Performance impact of monolayer coating of polysilicon micromotors. Proceedings of IEEE Micro Electro Mechanical Systems Workshop, pp.368-373, 1995.

DePalma, V. and Tillman, N. Friction and wear of self-assembled trichlorosilane monolayer films on silicon. Langmuir, 5, pp. 868-872, 1989.

Digital Instruments MultiMode™ Instruction Manual, Version 4.22 ce, 1997.

Dong, H., Bell, T., Blawert, C. and Mordike, B. L. Plasma immersion ion implantation of UHMWPE. Journal of Materials Science Letters, 19, pp. 1147-1149, 2000.

Dowson, D. History of Tribology. Longmans, London, 1979.

Dresselhaus, M. S., Dresselhaus, G. and Avouris, Ph. (Editors). Carbon nanotubes: synthesis, structure, properties and applications. Topics in Applied Physics, 80, pp. 406, Springer, Germany, 2001.

Dugger, M. T., Senft, D. C. and Nelson, G. C. Friction and durability of chemisorbed organic lubricants for microelectromechanical systems. ACS Symposium Series, 741, pp. 455-473, 2000.

Dyck, C. W., Smith, J. H., Miller, S. L., Russick, E. M. and Adkins, C. L. J. Supercritical carbon dioxide solvent extraction from surface-micromachined micromechanical structures. Proceedings of the SPIE conference on micromachining and microfabrication, Austin, TX (USA), 14-15 Oct'1996, Report Number: SAND--96-0708C, CONF-961086--2.

Eapen, K. C., Patton, S. T. and Zabinski, J. S. Lubrication of microelectromechanical systems (MEMS) using bound and mobile phases of Fomblin Zdol®, Tribology Letters, 12, pp. 35-41, 2002.

Eapen, K. C., Patton, S. T., Smallwood, S. A., Phillips, B. S. and Zabinski, J. S. MEMS Lubricants based on bound and mobile phases of hydrocarbon compounds: film deposition and performance evaluation. Journal of Microelectromechanical systems, 14, pp. 954-960, 2005.

Eapen, K. C., Smallwood, S. A. and Zabinski, J. S. Lubrication of MEMS under vacuum. Surface and Coatings Technology, 201, pp. 2960-2969, 2006.

Egitto, F. D. Plasma etching and modification of organic polymers. Pure and applied Chemistry, 62, pp. 1699-1708, 1990.

Elender, G., Kuhner, M. and Sackmann, E. Functionalization of Si/SiO_2 and glass surfaces with ultrathin dextran films and deposition of lipid bilayers. Biosensors and Bioelectronics, 11, pp. 565-577, 1996.

Elliott, A. Infra-red Spectra and Structure of Organic Long-chain Polymers, Edward Amold (Publishers) Ltd., pp. 48, 1969.

Ellis, B. The kinetics of cure and network formations. In Chemistry and Technology of Epoxy Resins. Edited by Bryan Ellis, Blackie Academic & Professional, New York, pp. 72-116, 1993.

Falvo, M. R., Taylor II, R. M., Helser, A., Chi, V., Brooks Jr, F. P., Washburn, S. and Superfine, R. Nanometer-scale rolling and sliding of carbon nanotubes. Nature, 397, pp. 236-238, 1999.

Flater, E. E., Corwin, A. D., de Boer, M. P. and Carpick, R. W. In situ wear studies of surface micromachined interfaces subject to controlled loading. Wear, 260, pp. 580-593, 2006.

Fleer, G. J., Chen-Stuart, M. A., Scheutjens, J. M. H. M., Cosgrove, T. and Vincent, B. Polymers at Interfaces, Chapman and Hall, London, 1993.

Forsen, E., Davis, Z. J., Dong, M., Nilsson, S. G., Montelius, L. and Boisen, A. Dry release of suspended nanostructures. Microelectronic Engineering, 73-74, pp. 487-490, 2004.

Fowkes, F. M. and Harkins, W. D. The State of monolayers adsorbed at the interface solid-aqueous solution. J.Am.Chem.Soc., 62, pp. 3377-3386, 1940.

Friedrich, K., Reinicke, R. and Zhang, Z. Wear of polymer composites. Proceedings of the Institution of Mechanical Engineering-J, Journal of Engineering Tribology, 216, pp. 415-426, 2002.

Fukushima, K., Ikeda, Y., Hayashi, T., Kikuchi, N., Kusano, E. and Kinbara, A. Imidized organic thin films deposited on glass substrates. Thin Solid Films, 392, pp. 254-257, 2001.

Fusaro, R. L. Tribological properties of polymer films and solid bodies in a vacuum environment. NASA Technical Memorandum 88966, 1987.

Gardos, M. N. Advantages and limitations of silicon as a bearing material for MEMS applications. Tribology Issues and Opportunities in MEMS, edited by Bhushan, B., Boston, Kluwer Academic, pp. 341-366, 1998.

Gorlach, B. and Holweger, W. Future polyimide coatings used in high loaded bearings. Industrial Lubrication and Tribology, 57, pp. 197-201, 2005.

Gotoh, K., Togawa, M., Ohmae, N., Kinoshita, H. and Tagawa, M. Surface characterization of atomic oxygen beam exposed polyimide films using contact angle measurements. Colloid Polymer Science, 279, pp. 214-220, 2001.

Guckel, H., Sniegowski, J. J., Christenson, T. R. and Raissi, F. The application of fine-grained, tensile polysilicon to mechanically resonant transducers. Sensors and Actuators A, 21, pp. 346-351, 1990.

Guo, L-Y. and Zhao, Y-P. Effect of chain length of self-assembled monolayers on adhesion force measurement by AFM. Journal of Adhesion Science and Technology, 20, pp. 1281-1293, 2006.

Hayashi, K., Sugimura, H. and Takai, O. Force microscopy contrasts due to adhesion force difference between organosilane self-assembled monolayers. Applied Surface Science, 188, pp. 513-518, 2002.

Henck, S. A. Lubrication of digital micromirror devices™. Tribology Letters, 3, pp. 239-247, 1997.

Horiuchi, S., Matchariyakul, N., Yase, K., Kitano, T., Choi, H. K. and Lee, Y. M. Compatibilizing effect of maleic anhydride functionalized SEBS triblock elastomer through a reaction induced phase formation in the blends of polyamide 6 and polycarbonate: 2. Mechanical properties. Polymer, 38, pp. 59-78, 1997.

Hornbeck, L. J. Digital light processing update: status and future applications. Proceedings of the Society of Photo-optical Engineering, 3634, Projection Displays V, pp. 158-170, 1999.

Horrison, J. A. and Perry, S. S. Friction in the presence of molecular lubricants and solid/hard coatings. MRS Bulletin, 23, pp. 27, 1998.

Horsley, D. A., Cohn, M. B., Singh, A., Horowitz, R. and Pisano, A. P. Design and fabrication of an angular microactuato for magnetic disk drives. Journal of Microelectromechanical Systems, 7, pp. 141, 1998.

Houston, M. R., Maboudian, R. and Howe, R. T. Ammonium fluoride anti-stiction treatments for polysilicon microstructures. Transducers '95, pp. 210-213, 1995.

Houston, M. R., Howe, R. T. and Maboudian, R. Effect of hydrogen termination on the work of adhesion between rough polycrystalline silicon surfaces. Journal of Applied Physics, 81, pp. 3474-3483, 1997.

Howe, R. T. Surface micromachining for microsensors and microactuators. Journal of Vacuum Science and Technology B, 6, pp. 1809-1813, 1988.

Hur, S., Hong, S. I., Lee, H. J., Han, S. W., Kim, J. H., Kang, J. Y., Choi, B. I. and Oh, C. S. Measurements of mechanical properties of thin polymer films by nanoindentation technique. Key Engineering Materials, 270-273, pp. 1107-1112, 2004.

Iijima, S. Helical microtubules of graphitic carbon. Nature, 354, pp. 56-58, 1991.

Israelachvili, J. N. and Tabor, D. The measurement of Van der waals dispersion forces in the range 1.5 to 130nm. Proceedings of the Royal Society of London A, 331, pp. 19-38, 1972.

Israelachvili, J. N. Intermolecular and Surface Forces. Academic Press, USA, 1991.

Jang, D-S. and Kim, D-E. Optimum film thickness of thin metallic coatings on silicon substrates for low load sliding applications. Tribology International, 29, pp. 345-356, 1996.

Jia, Z., Tyng, G. S., Ling, A. H. and Srinivasan, M. P. Langmuir-Blodgett film fabricated with soluble imidized polyimide. Colloids and Surfaces A: Physicochem. Eng. Aspects, 257-258, pp. 451-456, 2005.

Jiang, X. and Hammond, P. T. Selective deposition in layer-by-layer assembly: functional graft copolymers as molecular templates. Langmuir, 16, pp. 8501-8509, 2000.

Johnson, K. L., Kendall, K. and Roberts, A. Surface energy and contact of elastic solids. Proceedings of the Royal Society of London A, 324, pp. 301-313, 1971.

Julthongpiput, D., Ahn, H-S., Kim, D-I. and Tsukruk, V. V. Tribological behavior of grafted polymer gel nanocoatings. Tribology Letters, 13, pp. 35-40, 2002.

Julthongpiput, D. Design of nanocomposite polymer coatings for MEMS applications. PhD thesis, Iowa State University, 2003 (a).

Julthongpiput, D., LeMieux, M. and Tsukruk, V. V. Micromechanical properties of glassy and rubbery polymer brush layers as probed by atomic force microscopy. Polymer, 44, pp. 4557-4562, 2003 (b).

Jung, Y. C. and Bhushan, B. Contact angle, adhesion and friction properties of micro- and nanopatterned polymers for superhydrophobicity. Nanotechnology, 17, pp. 4970-4980, 2006.

Kang, P. H. and Nho, Y. C. The effect of γ-irradiation on ultra-high molecular weight polyethylene recrystallized under different cooling conditions. Radiation Physics and Chemistry, 60, pp. 79-87, 2001.

Karamancheva, I., Stefov, V., Soptrajanov, B., Danev, G., Spasova, E. and Assa, J. FTIR spectroscopy and FTIR microscopy of vacuum-evaporated polyimide thin films. Vibrational Spectroscopy, 19, pp. 369-374, 1999.

Katano, T., Oka, M., Nakazawa, S., Aramaki, T. and Kusakawa, K. Characteristics of dual lubricant layers. IEEE Transaction on Magnetics, 39, pp. 2489-2491, 2003.

Kim, H. I., Koini, T., Lee, T. R. and Perry, S. S. Systematic studies of the frictional properties of fluorinated monolayers with atomic force microscopy: comparison of CF_3- and CH_3- terminated films. Langmuir, 13, pp. 7192-7196, 1997.

Kim, H. I., Graupe, M., Oloba, O, Koini, T., Imaduddin, S., Lee, T. R. and Perry, S. S. Molecular specific studies of the frictional properties of monolayer films: a systematic comparison of CF_3-, $(CH_3)_2CH$-, and CH_3-terminated films. Langmuir, 15, pp. 3179-3185, 1999.

Kim, B. H., Chung, T. D., Oh, C. H. and Chun, K. A New organic modifier for anti-stiction. Journal of Microelectromechanical Systems, 10, pp. 33-41, 2001.

Kim, J. T., Park, J. K. and Lee, D. C. Surface modification of polyimide film by ion implantation. Polymer International, 51, pp. 1063-1065, 2002.

Kinbara, A., Hayashi, T., Wakahara, K., Kikuchi, N., Kusano, E. and Nanto, H. Polyimide-based organic thin films prepared by rf magnetron sputtering. Thin Solid Films, 433, pp. 274-276, 2003.

Kitoh, M. and Honda, Y. Preparation and tribological properties of sputtered polyimide film. Thin Solid Films, 271, pp. 92-95, 1995.

Komvopoulos, K. Surface engineering and microtribology for microelectromechanical systems. Wear, 200, pp. 305-327, 1996.

Kozlowski, F., Lindmair, N., Scheiter, T., Hierold, C. and Lang, W. A novel method to avoid sticking of surface micromachined structures. Proceedings of 8th International Conference on Solid State Sensors and Actuators-Transducers'95, pp. 220-223, 1995.

Kuypers, L. C., Decraemer, W. F., Dirckx, J. J. J. and Timmermans. A procedure to determine the correct thickness of an object with confocal microscopy in case of refractive index mismatch. Journal of Microscopy, 218, pp. 68-78, 2005.

Lancaster, J. K. Relationship between the wear of polymers and their mechanical properties. Tribology Conv. 1969, Institution of Mechanical Engineers, London, pp. 100-108, 1969.

Lander, L. M., Brittain, W. J., DePalma V. A. and Girolmo, S. R. Friction and wear of surface-immobilized C_{60} monolayers. Chemistry of Materials, 7, pp. 1437-1439, 1995.

Lee, T. R., Carey, R. I., Biebuyck, H. A. and Whitesides, G. M. The Wetting of monolayer films exposing ionizable acids and bases. Langmuir, 10, pp. 741-749, 1994.

Lee, Y., Han, S., Lee, J-H., Yoon, J-H., Lim, H. E. and Kim, K-J. Surface studies of plasma ion implantation treated polystyrene. Journal of vacuum science and technology, 16, pp. 1710-1715, 1998.

Lehr, H. A., Doppler, J., Ehrfeld, W., Hagemanna, B., Kampel, K. P., Michel, F., Schulz, Ch. And Thurigen, Ch. Microactuators as driving units for microbotic systems. Proceedings of Microrobotics: Components and Applications (Edited by Sulzmann, A), 2906, pp. 202, 1996.

Li, X., Gao, H., Serivens, W. A., Fei, D., Xu, X., Sutton, M. A., Reynolds, A. P. and Myrick, M. L. Nanomechanical characterization of single-walled carbon nanotube reinforced epoxy composites. Nanotechnology, 15, pp. 1416-1423, 2004.

Lio, A., Charych, D. H. and Salmeron, M. Comparative atomic force microscopy study of the chain length dependence of frictional properties of alkanethiols on gold and alkylsilanes on mica. Journal of Physical Chemistry B, 101, pp. 3800-3805, 1997.

Liu, Y., Evans, D. F., Song, Q. and Grainger, D. W. Structure and frictional properties of self-assembled surfactant monolayers. Langmuir, 12, pp. 1235-1244, 1996.

Liu, H., Bhushan, B., Eck, W. and Stadler, V. Investigation of the adhesion, friction, and wear properties of biphenyl thiol self-assembled monolayers by atomic force microscopy. Journal of Vacuum Science and Technology A, 19, pp. 1234-1240, 2001 (a).

Liu, H., Ahmed, S. I-U. and Scherge, M. Microtribological properties of silicon and silicon coated with diamond like carbon, octadecyltrichlorosilane and stearic acid cadmium salt films: A comparative study. Thin Solid Films, 381, pp. 135-142, 2001 (b).

Liu, W., Zhou, F., Yu, L., Chen, M., Li, B. and Zhao, G. Preparation and tribological investigation of thin silicone films. Journal of Materials Research, 17, pp. 2357-2362, 2002.

Liu, H. and Bhushan, B. Nanotribological characterization of molecularly thick lubricant films for applications to MEMS/NEMS by AFM. Ultramicroscopy, 97, pp. 321-340, 2003 (a).

Liu, H and Bhushan, B. Adhesion and friction studies of microelectromechanical systems/nanoelectromechanical systems materials using a novel microtriboapparatus. Journal of Vacuum Science and Technology A, 21, pp. 1528-1538, 2003 (b).

Lourie, O. and Wagner, H. D. Transmission electron microscopy observations of fracture of single-wall carbon nanotubes under axial tension. Applied Physics Letters, 73, pp. 3527-3529, 1998.

Lumbantobing, A., Kogut, L. and Komvopoulos, K. Electrical contact resistance as a diagnostic tool for MEMS contact interfaces. Journal of Microelectromechanical Systems, 13, pp. 977-987, 2004.

Luzinov, I., Julthongpiput, D., Liebmann-Vinson, A., Cregger, T., Foster, M. D. and Tsukruk, V. V. Epoxy-terminated self-assembled monolayers: Molecular glues for polymer layers. Langmuir, 16, pp. 504-516, 2000.

Luzinov, I., Julthongpiput, D., Gorbunov, V. and Tsukruk, V. V. Nanotribological behavior of tethered reinforced polymer nanolayer coatings. Tribology International, 34, pp. 327-333, 2001.

Ma, Q. and Clarke, D. R. Size dependent hardness in silver single crystals. Journal of Materials Research, 10, pp. 853-863, 1995.

Maas, J. H., Cohen Stuart, M. A. and Fleer, G. J. Thin block copolymers films: film formation and corrugation under an AFM tip. Thin Solid Films, 358, pp. 234-240, 2000.

Maboudian, R. Surface processes in MEMS technology. Surface Science Reports, 30, pp. 207-269, 1998.

Maboudian, R. and Howe, R. T. Critical review: Adhesion in surface micromechanical structures. Journal of Vacuum Science and Technology B, 15, pp. 1-20, 1997.

Maboudian, R., Ashurst, W. R. and Carraro, C. Tribological challenges in micromechanical systems. Tribology Letters, 12, pp. 95-100, 2002.

Madou, M. J. Fundamentals of Microfabrication. CRC Press, Boca Raton, 1997.

Major, R. C., Kim, H. I., Houston, J. E. and Zhu, X.-Y. Tribological properties of alkoxyl monolayers on oxide terminated silicon. Tribology Letters, 14, pp. 237-244, 2003.

Makkonen, L. Friction as a result of surface tension. 27th Annual Meeting of the Adhesion Society, Wilmington, NC, USA, pp.399-341, 2004.

Man, P. F., Gogoi, B. P. and Mastrangelo, C. H. Elimination of post-release adhesion in microstructures using conformal uorocarbon coatings. J. Microelectromechanical Systems, 6, pp. 25-34, 1997.

Marti, A., Hahner, G. and Spencer, N. D. Sensitivity of frictional forces to pH on a nanometer scale: A lateral force microscopy study. Langmuir, 11, pp. 4632-4635, 1995.

Mastrangelo, C. H. and Saloka, G. S. A dry-release method based on polymer columns for microstructure fabrication. Proceedings of IEEE Microelectromechanical Systems Workshop, Ft. Lauderdale, FL, pp. 77-81, 1993.

Mastrangelo, C. H. Adhesion-related failure mechanisms in micromechanical devices, Tribology Letters, 3, pp. 223-238, 1997.

Mate, C. M., McClelland, G. M., Erlandsson, R. and Chiang, S. Atomic-scale friction of a tungsten tip on a graphite surface. Physical Review Letters, 59, pp. 1942-1945, 1987.

Mate, C. M. Atomic-force-microscope study of polymer lubricants on silicon surfaces. Physical Review Letters, 68, pp. 3323-3326, 1992.

Mehregany, M., Gabriel, K. J. and Trimmer, W. S. N. Integrated fabrication of polysilicon mechanisms. IEEE Transactions on Electron Devices, 35, pp. 719, 1988.

Miller, S., Sniegowski, J. J., LaVigne, G. and McWorther, P. J. Friction in surface micromachined microengines. Proc. SPIE Smart Electronics and MEMS, 2722, pp. 197-204, 1996.

Mino, N., Ogawa, K., Minoda, T., Takatsuka, M., Sha, S. and Moriizumi, T. Thin film characteristics of fluorine-substituted monolayers prepared by chemical adsorption from solution. Thin Solid Films, 230, pp. 209-216, 1993.

Miwa, M., Nakajima, A., Fujishima, A., Hashimoto, K. and Watanabe, T. Effects of the surface roughness on sliding angles of water droplets on superhydrophobic surfaces. Langmuir, 16, pp. 5754-5760, 2000.

Morcos, I. Surface tension of stress-annealed pyrolytic graphite. Journal of Chemical Physics, 57, pp. 1801-1802, 1972.

Moulder, J. F., Stickle, W. F., Sobol, P. E. and Bomben, K. D. Handbook of X-ray Photoelectron Spectroscopy. Perkin-Elmer Corporation, Eden Prairie, 1992.

Mulhern, G. T., Soane, D. S. and Howe, R. T. Supercritical carbon dioxide drying of microsctructures. Proceedings of 7th International Conference on Solid-State Sensors and Actuators-Transducers'93, Yokohama, Japan, pp. 296-300, 1993.

Muller, R. S. Microdynamics. Sensors and Actuators A, 21, pp. 1-8, 1990.

Muller, R. S., Howe, R. T., Senturia, S. D., Smith, R. L. and White, R. M. Microsensors, IEEE Press, New York, 1990.

Muller, M., Lee, S., Spikes, H. A. and Spencer, N. D. The influence of molecular architecture on the macroscopic lubrication properties of the brush-like co-polyelectrolyte poly(L-lysine)-g-poly(ethylene glycol) (PLL-g-PEG) adsorbed on oxide surfaces. Tribology Letters, 15, pp. 395-405, 2003.

Nakano, M., Ishida, T., Numata, T., Ando, Y. and Sasaki, S. Alkyl chain length effect on tribological behavior of alkanethiol self-assembled monolayers on Au. Japanese Journal of Applied Physics, 42, pp. 4734-4738, 2003.

Narayanan Unni, K. N., Seignon, S. D. and Nunzi, J-M. Improved performance of pentacene field-effect transistors using a polyimide gate dielectric layer. Journal of Physics D: Applied Physics, 38, pp. 1148-1151, 2005.

Nielsen, L. E. Mechanical properties of polymers and composites. Marcel Dekker, New York, 1974.

Novotny, V. and Swalen, J. D. Tribology of Langmuir-Blodgett layers. Langmuir, 5, pp. 485-489, 1989.

Noy, A., Frisbie, C. D., Rozsnyal, L. F., Wrighton, M. S. and Lieber, C. M. Chemical force microscopy: Exploiting chemically-modified tips to quantify adhesion, friction, and functional group distributions in molecular assemblies. Journal of American Chemical Society, 117, pp. 7943-7951, 1995.

Nuzzo, R. G. and Allara, D. L. Adsorption of bifunctional organic disulfides on gold surfaces. Journal of the American Chemical Society, 105, pp. 4481-4483, 1983.

Oiseth, S. K., Krozer, A., Kasemo, B. and Lausmaa, J. Surface modification of spin-coated high-density polyethylene films by argon and oxygen glow discharge plasma treatments. Applied Surface Science, 202, pp. 92-103, 2002.

Oliver, W. C. and Pharr, G. M. An improved technique for determining hardness and elastic modulus using load and displacement sensing indentation experiments. Journal of Materials Research, 7, pp. 1564, 1992.

Oliver, W. C. and Pharr, G. M. Measurement of hardness and elastic modulus by instrumented indentation: Advances in understanding and refinements to methodology. Journal of Materials Research, 19, pp. 3-20, 2004.

Orpana, M. and Korhonen, A. O. Control of residual stress of polysilicon thin films by heavy doping in surface micromachining. Proceedings of the 6th International Conference on Solid-State Sensors and Actuators, Transducers'91, pp. 957-960, 1991.

Osawa, S., Yabe, M., Miyamura, M. and Mizuno, K. Preparation of super-hydrophobic surface on biodegradable polymer by transcribing microscopic pattern of water-repellant leaf. Polymer, 47, pp. 3711-3714, 2006.

Parikh, A. N., Allara, D. L., Azouz, I. B. and Rondelez, F. An intrinsic relationship between molecular structure in self-assembled n-alkylsiloxane monolayers and deposition temperature. Journal of Physical Chemistry, 98, pp. 7577-7590, 1994.

Patton, S. T., Cowan, W. D., Eapen, K. C. and Zabinski, J. S. Effect of surface chemistry on the tribological performance of a MEMS electrostatic lateral output motor. Tribology Letters, 9, pp. 199-209, 2000.

Patton, S. T. and Zabinski, J. S. Failure mechanisms of a MEMS actuator in very high vacuum. Tribology International, 35, pp. 373-379, 2002.

Pavoor, P. V., Gearing, B. P., Gorga, R. E. and Cohen, R. E. Engineering the friction-and-wear behavior of polyelectrolyte multilayer nanoassemblies through block copolymer surface capping, metallic nanoparticles, and multiwall carbon nanotubes. Journal of Applied Polymer Science, 92, pp. 439-448, 2004.

Petersen, K. Silicon as a mechanical material, Proceedings of IEEE Electron Devices, 70, pp. 420-457, 1982.

Pettersson, U. and Jacobson, S. Influence of surface texture on boundary lubricated sliding contacts. Tribology International, 36, pp. 857-864, 2003.

Pooley, C. M. and Tabor, D. Friction and molecular structure: The behavior of some thermoplastics. Proceedings of the Royal Society of London A, 329, pp. 251-274, 1972.

Pratt, G. C. Recent developments in polytetrafluoroethylene-based dry bearing materials and treatments. Transactions of the Plastics Institution, 32, pp. 255-271, 1964.

Pronjoto, H. and Denton, D. D. Graviometric measurements of steady state moisture uptake in spin-coated polyimide films. Journal of Applied polymer Science, 42, pp. 75-83, 1991.

Prucker, O. and Ruhe, J. Synthesis of poly (styrene) monolayers attached to high surface area silica gels through self-assembled monolayers of azo initiators. Macromolecules, 31, pp. 592-601, 1998.

Rabinowicz, E. and Tabor, D. Metallic transfer between sliding metals: An autoradiographic study. Proceedings of the Royal Society of London A, 208, pp. 455-475, 1951.

Ratner, S. N., Farberoua, I. I., Radyukeuich, O. V. and Lure, E. G. Correlation between wear resistance of plastics and other mechanical properties. Soviet Plastics, 7, pp. 37-45, 1964.

Ren, S., Yang, S., Zhao, Y., Zhou, J., Xu, T. and Liu, W. Friction and wear studies of octadecyltrichlorosilane SAM on silicon. Tribology Letters, 13, PP. 233-239, 2002.

Ren, S., Yang, S. and Zhao, Y. Micro- and macro- tribological study on a self-assembled dual-layer film. Langmuir, 19, pp. 2763-2767, 2003.

Ren, S-L., Yang, S-R., Wang, J-Q., Liu, W-M. and Zhao, Y-P. Preparation and tribological studies of stearic acid self-assembled monolayers on polymer-coated silicon surface. Chemistry of Materials, 16, pp. 428-434, 2004.

Robertson, J. K. and Wise, K. D. A low pressure micromachined flow modulator. Sensors and Actuators A, 71, pp. 98-106, 1998.

Ruhe, J., Novotny, V. J., Kanazawa, K. K., Clarke, T. and Street, G. B. Structure and tribological properties of ultrathin alkylsilane films chemisorbed to solid surfaces. Langmuir, 9, pp. 2383-2388, 1993.

Ruhe, J., Blackman, G., Novotny, V. J., Clarke, T., Street, G. B. and Kuan, S. Terminal attachment of perfluorinated polymers to solid surfaces, Journal of Applied Polymer Science, 53, pp. 825-836, 1994.

Ruhe, J., Novotny, V., Clarke, T. and Street, G. B. Ultrathin perfluoropolyether films-influence of anchoring and mobility of polymers on the tribological properties. Journal of Tribology, 118, pp. 663-668, 1996.

Rymuza, Z. Control tribological and mechanical properties of MEMS surfaces. Part 1: critical review. Microsystem Technologies, 5, pp. 173-180, 1999.

Sakata, H., Kobayashi, M., Otsuka, H. and Takahara, A. Tribological properties of poly (methyl methacrylate) brushes prepared by surface-initiated atom transfer radical polymerization. Polymer Journal, 37, pp. 767-775, 2005.

Sandler, J., Shaffer, M. S. P., Prasse, T., Banhofer, W., Schutte, K. and Windk, A. H. Development of a dispersion process for carbon nanotube in an epoxy matrix and the resulting electrical properties. Polymer, 40, pp. 5967-5971, 1999.

Satyanarayana, N., Sinha, S. K. and Srinivasan, M. P. Wear-life evaluations of silane-based self-assembled monolayers in "Life Cycle Tribology" (Edited by D.Dowson, M.Priest, G.Dalmaz and A.A.Lubrecht). Tribology and Interface Engineering Series, No. 48, Elsevier Publishers, pp. 821-826, 2004 (a).

Satyanarayana, N., Chen, C. H., Sinha, S. K. Influence of bonding type of self-assembled monolayers with silicon substrate on tribological properties. Proceedings of

the 1st International Conference in Advanced Tribology (iCAT 2004), Singapore, 1st-3rd Dec'2004 (b).

Satyanarayana, N. and Sinha, S. K. Tribology of PFPE overcoated self-assembled monolayers deposited on Si surface. Journal of Physics D: Applied Physics D, 38, pp. 3512-3522, 2005.

Satyanarayana, N., Sinha, S. K. and Ong, B. H. Tribology of a novel UHMWPE/PFPE dual-film coated onto Si surface. Sensors and Actuators A, 128, pp. 98-108, 2006.

Satyanaryana, N., Gosvami, N., Sinha, S. K. and Srinivasan, M. P. Friction, adhesion and wear durability studies of ultra-thin PFPE overcoated 3-Glycidoxypropyltrimethoxy silane SAM on Si surface. Philosophical Magazine, 87, pp. 3209-3227, 2007 (a).

Satyanarayana, N., Skandesh Rajan, K. S., Sinha, S. K. and Shen, L. Carbon nanotube reinforced polyimide thin-film for high wear durability. Tribology Letters, 27, pp. 181-188, 2007 (b).

Satyanarayana, N., Sinha, S. K. and Shen, L. Effect of molecular structure on friction and wear of polymer thin films deposited on Si surface. Tribology Letters, 28, pp. 71-80, 2007 (c).

Scherge, M. and Gorb, S. Biological Micro and Nanotribology: Nature's Solutions. Springer, Germany, 2001.

Schreiber, F. Self-assembled monolayers: from 'simple' model systems to biofunctionalized interfaces. Journal of Physics: Condensed Matter, 16, pp.R1-R20, 2004.

Senft, D. C. and Dugger, M. T. Friction and wear in surface micromachined tribological test devices. SPIE, 3224, pp. 31-38, 1997.

Shen, L. and Zeng, K. Comparison of mechanical properties of porous and non-porous low-*k* dielectric films. Microelectronic Engineering, 71, pp. 221-228, 2004.

Shipway, P. H. and Ngao, N. K. Microscale abrasive wear of polymeric materials. Wear, 255, pp. 742-750, 2003.

Sidorenko, A., Ahn, H. S., Kim, D. I., Yang, H. and Tsukruk, V. V. Wear stability of polymer nanocomposite coatings with trilayer architecture. Wear, 252, pp. 946-955, 2002.

Sidorov, V., Shai, A., Ritter, D. and Paz, Y. Polyimide coating on non-planar microelectronic devices: characterization of vacuum drying effects by a new 'flip-paste' back-etching method. Surface and Coatings Technology, 122, pp. 214-218, 1999.

Singh, R. A., Yoon, E-S., Han, H-G. and Kond, H. Frictional behavior of chemical vapor deposited self-assembled monolayers on silicon wafer. Wear, 262, pp. 130-137, 2007.

Sinha, S. K. Wear failures of plastics. ASM International Handbook, Vol. 11, ASM International, Ohio, pp. 1019-1027, 2002.

Sinha, S. K., Kawaguchi, M., Kato, T. and Kennedy, F. E. Wear durability studies of ultra-thin perfluoropolyether lubricant on magnetic hard disks. Tribology International, 36, pp. 217-225, 2003.

Sira, M., Trunec, D., Stahel, P., Bursikova, V., Navratil, Z. and Bursik, J. Surface modification of polyethylene and polypropylene in atmospheric pressure glow discharge. Journal of Physics D: Applied Physics, 38, pp. 621-627, 2005.

Skrovanek, D. J., Howe, S. E., Painter, P. C. and Coleman, M. M. Hydrogen bonding in polymers: Infrared temperature studies of an amorphous polyamide. Macromolecules, 18, pp. 1676-1683, 1985.

Srinivasan, U., Houston, M. R., Howe, R. T. and Maboudian, R. Self-assembled fluorocarbon films for enhanced stiction reduction. Proceedings of the 9th International Conference on Solid-State Sensors and Actuators, pp.210-213, Transducers' 97.

Srinivasan, U., Houston, M. R., Howe, R. T. and Maboudian, R. Alkyltrichlorosilane-based self-assembled monolayer films for stiction reduction in silicon micromachines. Journal of Microelectromechanical systems, 7, pp. 252-260, 1998 (a).

Srinivasan, U., Foster, J. D., Habib, U., Howe, R. T., Maboudian, R., Senft, D. C. and Dugger, M. T. Lubrication of polysilicon micromechanisms with self-assembled monolayers. Technical Digest, Proceedings of the 1998 Solid-State Sensor and Actuator Workshop, Hilton Head '98, pages 156-161, 1998 (b).

Stolarski, T. A. Tribology of polyetheretherketone. Wear, 158, pp. 71-78, 1992.

Stolarski, T. A. Rolling contact fatigue of polymers and polymer composites, Advances in Composite Tribology (ed K. Friedrich), Elsevier Science Publishers B. V., Amsterdam, pp. 629-667, 1993.

Suh, H., Bharathi, P., Beebe, D. J. and Moore, J. S. Dendritic material as a dry-release sacrificial layer. Journal of Microelectromechanical Systems, 9, pp. 198-205, 2000.

Sun, C., Zhou, F., Shi, L., Yu, B., Gao, P., Zhang, J. and Liu, W. Tribological properties of chemically bonded polyimide films on silicon with polyglycidyl methacrylate brush as adhesive layer. Applied Surface Science, 253, pp. 1729-1735, 2006.

Sung, I-H., Yang, J-C., Kim, D-E. and Shin, B-S. Micro/nano-tribological characteristics of self-assembled monolayer and its application in nano-structure fabrication. Wear, 255, pp. 808-818, 2003.

Sze, S. M. Semiconductor Sensors, Wiley, New York, 1994.

Tabor, D. and Winterton, R. H. S. The direct measurement of normal and retarted van der Waals forces. Proceedings of the Royal Society of London A, 312, pp. 435-450, 1969.

Tai, Y. C., Fan, L. S. and Muller, R. S. IC-processed micro-motors: Design, technology and testing. Proceedings of IEEE Microelectromechanical systems, pp. 1, 1989.

Tambe, N. S. and Bhushan, B. Nanoscale friction-induced phase transformation of diamond-like carbon. Scripta Materialia, 52, pp. 751-755, 2005.

Tang, X. C., Pikal, M. J. and Taylor, L. S. The effect of temperature on hydrogen bonding in crystalline and amorphous phases in dihydropyrine calcium channel blockers. Pharmaceutical Research, 19, pp. 484-490, 2002.

Tani, H. and Matsumoto, M. Spreading mechanism of PFPE lubricant on the Magnetic Disks. Journal of Tribology, 123, pp. 533-540, 2001.

Tanner, D. M., Miller, W. M., Peterson, K. A., Dugger, M. T., Eaton, W. P., Irwin, L. W., Senft, D. C., Smith, N. F., Tangyunyong, P. and Miller, S. L. Frequency dependence of the lifetime of a surface micromachined microengine driving a load. Microelectronics Reliability, 39, pp. 401-414, 1999 (a).

Tanner, D. M., Walraven, J. A., Irwin, L. W., Dugger, M. T., Smith, N. F., Eaton, W. P., Miller, W. M. and Miller, S. L. The effect of humidity on the reliability of a

surface micromachined microengine. Proceedings of the 37th Annual International Reliability Physics Symposium, San Diego, California, pp. 189-197, 1999 (b).

Tas, N., Sonnenberg, T., Jansen, H., Legtenberg, R. and Elwenspoek, M. Stiction in surface micromachining. Journal of Micromechanics and Microengineering, 6, pp. 385-397, 1996.

Thomas, P. S. Dependence of the friction process on the molecular structure and architecture of thin polymer films. Tribology International, 29, pp. 631-637, 1996.

Tompkins, H. G. A User's Guide to Ellipsometry. Academic Press Inc, London, 1993.

Tsukruk, V. V., Everson, M. P., Lander, L. M. and Brittain, W. J. Nanotribological properties of composite molecular films: C_{60} anchored to a self-assembled monolayer. Langmuir, 12, pp. 3905-3911, 1996.

Tsukruk, V. V., Nguyen, T., Lemieux, M., Hazel, W. H., Schevchenko, V. V., Klimenko, N. and Sheludko, E. Tribological properties of modified MEMS surfaces. In Tribology Issues and Opportunities in MEMS (Ed., Bhushan, B), Kluwer, Dordrecht, The Netherlands, pp. 607-614, 1998.

Tsukruk, V. V., Ahn, H.-S., Kim, D. and Sidorenko, A. Triplex molecular layers with nonlinear nanomechanical response. Applied Physics Letters, 80, pp. 4825-4827, 2002 (a).

Tsukruk, V. V., Sidorenko, A. and Yang, H. Polymer nanocomposite coatings with non-linear elastic response. Polymer, 43, pp. 1695-1699, 2002 (b).

Ulman, A. An Introduction to Ultra Thin Organic Films: From Langmuir-Blodgett to Self-assembly. Academic Press, San Diego, CA, 1991.

Ulman, A. Formation and structure of self-assembled monolayers. Chemical Reviews 96, pp. 1533-1554, 1996.

Unal, H. and Mimaroglu, A. Friction and wear behavior of unfilled engineering thermoplastics. Materials and Design, 24, pp. 183-187, 2003.

Vincent, L., Berthier, Y., Dobourg, M. C. and Godet, M. Mechanics and materials in fretting. Wear, 153, pp. 135-148, 1992.

Volinsky, A. A. and Gerberich, W. W. Nanoindentation techniques for assessing mechanical reliability at the nanoscale. Microelectronic Engineering, 69, pp. 519-527, 2003.

Wallace, R. M., Henck, S. A. and Webb, D. A. PFPE coatings for micromechanical devices. US Patent, 5512374, 1996.

Wang, Y. Q. and Li. J. Sliding wear behavior and mechanism of ultra-high molecular weight polyethylene. Materials Science and Engineering A, 266, pp. 155-160, 1999.

Wang, A., Essner, A., Polineni, V. K., Stark, C. Dumbleton, J. H. Lubrication and wear of ultra-high molecular weight polyethylene in total joint replacements. Tribology International, 31, pp. 17-33, 1998.

Wang, W. Y., Wang, Y. L., Bao, H. F., Xiong, B. and Bao, M. H. Friction and wear properties in MEMS. Sensors and Actuators, 97-98, pp. 486-491, 2002.

Webb, D. A. Polymeric coatings for micromechanical devices. US Patent, 5447600, 2005.

Wei, C., Cho, K. and Srivastava, D. Chemical bonding of polymer on carbon nanotube. Mat. Res. Soc. Symp. Proc., 675, pp. W.4.7.1-W.4.7.5, 2001.

Weisenhorn, A. L., Hansma, P. K., Albrecht, T. R. and Quate, C. F. Forces in atomic force microscopy in air and water. Applied Physics Letters, 54, pp. 2651-2653, 1989.

Wiesendanger, R. Scanning probe microscopy and spectroscopy- methods and applications. Cambridge University Press, New York, 1994.

Williams, J. A. Engineering Tribology.Oxford University Press, Oxford, 1994.

Williams, J. A. Friction and wear of rotating pivots in MEMS and other small scale devices. Wear, 250, pp. 965-972, 2001.

Williams, J. A. and Le, H. R. Tribology and MEMS. Journal of Physics D: Applied Physics, 39, pp. R201-R214, 2006.

Wong, E. W., Sheehan, P. E. and Lieber, C. M. Nanobeam mechanics: Elasticity, strength, and toughness of nanorods and nanotubes. Science, 277, pp. 1971-1975, 1997.

Xiao, X., Hu, J., Charych, D. H. and Salmeron, M. Chain length dependence of the frictional properties of alkylsilane molecules self-assembled on mica studied by atomic force microscopy. Langmuir, 12, pp. 235-237, 1996.

Xu, X. and Coleman, M. R. Atomic force microscopy images of ion-implanted 6FDA-PMDA polyimide films. Journal of Applied Polymer Science, 66, pp. 459-469, 1997.

Yamada, Y., Tanaka, K. and Saito, K. Friction and damage of coatings formed by sputtering polytetrafluoroethylene and polyimide. Surface and Coatings Technology, 43-44, pp. 618-628, 1990.

Yang, Z., Xu, H., Li, M-K., Shi, Y-L., Huang, Y. and Li, H-L. Preparation and properties of Ni/P/single-walled carbon nanotubes composite coatings by means of electroless plating. Thin Solid Films, 466, pp. 86-91, 2004.

Yang, Z., Dong, B., Huang, Y., Liu, L., Yan, F-Y. and Li, H-L. Enhanced wear resistance and micro-hardness of polystyrene nanocomposites by carbon Nanotubes. Materials Chemistry and Physics, 94, pp. 109-113, 2005.

Yeow, T. W., Law, K. L. E. and Goldenberg, A. MEMS optical switches. IEEE Communications Magazine, 39, pp. 158, 2001.

Yerushalmi-Rozen, R., Klein, J. and Fetters, L. J. Suppression of rupture in thin, nonwetting liquid films. Science, 263, pp. 793-795, 1994.

Zarrad, H., Chovelon, J. M., Clechet, P., Jaffrezic-Renault, N., Martelet, C., Belin, M., Perez, H. and Chevalier, Y. Optimization of lubricants for silica micromotors. Sensors and Actuators A: Physical, 46-47, pp. 598-600, 1995.

Zeng, X. M., Weng, L. T., Li, L., Chan, C. M., Liu, S. Y. and Jiang, M. ToF-SIMS study of the surface morphology of blends of polystyrene and poly (N-vinyl-2-pyrrolidone) compatibilized by poly (styrene-co-4-vinylphenol). Surface and Interface Analysis, 31, pp. 421-428, 2001.

Zhang, F and Srinivasan, M. P. Self-assembled molecular films of aminosilanes and their immobilization capacities. Langmuir, 20, pp. 2309-2314, 2004.

Zhu, X. Y. and Houston, J. E. Molecular lubricants for silicon-based microelectromechanical systems (MEMS): a novel assembly strategy. Tribology Letters, 7, pp. 87-90, 1999.

Zhu, L., Zhang, J., Liew, T. and Ye, K. D. Chemical bonding of perfluoropolyether with carbon underlying layer induced by visible laser light. Journal of Vacuum Science and Technology A, 21, pp. 1087-1091, 2003

Zoo, Y-S., Ahn, J-W., Lim, D-P. and Lim, D-S. Effect of carbon nanotube addition on tribological behavior of UHMWPE. Tribology Letters, 16, pp. 305-309, 2004

Appendix A

Effect of thermal treatment temperature of Si/UHMWPE film on mechanical and tribological properties

A.1 Background

The results presented in Section 5.1 correspond to UHMWPE film post-heated at 100^{o}C. To study the influence of the post-heating temperature on the film properties, a second heat treatment temperature close to the melting point of UHMWPE (130^{o}C) is selected and the results are presented in this Appendix. The results of the film heated at 130^{o}C are compared with the results of the film heated at 100^{o}C (Section 5.1).

A.2 Results and Discussion

A.2.1 Surface features observed using SEM and AFM

Figure A.1 shows the surface features of UHMWPE film heated at 130^{o}C observed using SEM. It shows the island structure with nearly uniform size. There are some valleys with very low depth especially when compared to very deep valleys in the case of UHMWPE film heated at 100^{o}C (Figure 5.1).

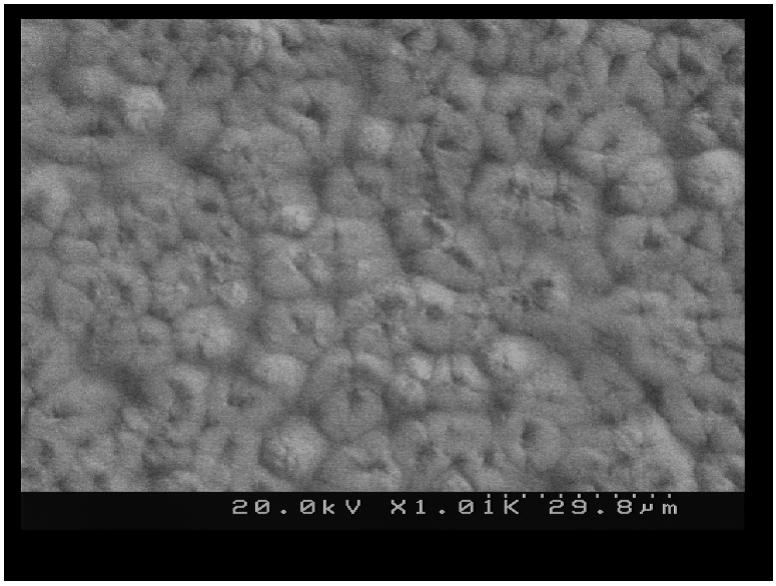

Figure A.1: *SEM morphology of the UHMWPE film on Si surface post heated at 130^{o}C for 20 h immediately after dip-coating.*

Figure A.2 shows AFM topography of UHMWPE film post-heated at 130^{o}C. It has very flat surface with a roughness of 81 nm which is very small when compared to that of the film heated at 100^{o}C (~550 nm).

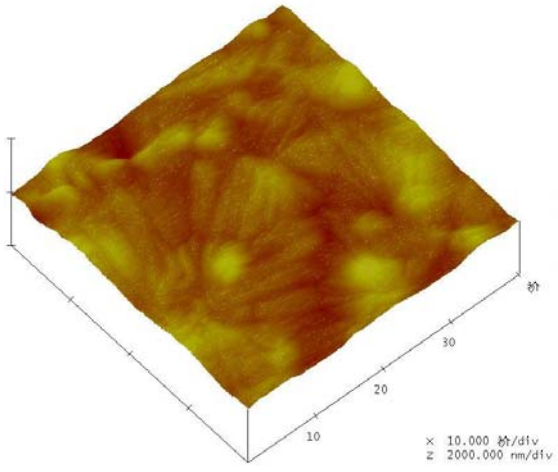

Figure A.2: *AFM image of the Si/UHMWPE film (post heated at 130^{o}C after dip-coating) with a scan size of 40 µm x 40 µm. The vertical scale is 2 µm.*

A.2.2 Chemical characterization

The FTIR spectrum of UHMWPE film post-heated at 130^{o}C is identical to that post-heated at 100^{o}C and hence it is concluded that the chemical nature of both the films is the same and the post-heating temperature did not influence the chemical nature in any observable way.

A.2.3 Tribological characterization

Figure A.3 shows the coefficient of friction versus number of cycles curve for UHMWPE film post-heated at 130^{o}C. The film has shown an initial coefficient of friction of 0.4 and it gradually increases as the sliding progresses. The tests are not continued until large number of cycles as the initial coefficient of friction itself is high (0.4). Therefore, the UHMWPE film post-heated at 130^{o}C has shown lower wear life when compared to that heated at 100^{o}C.

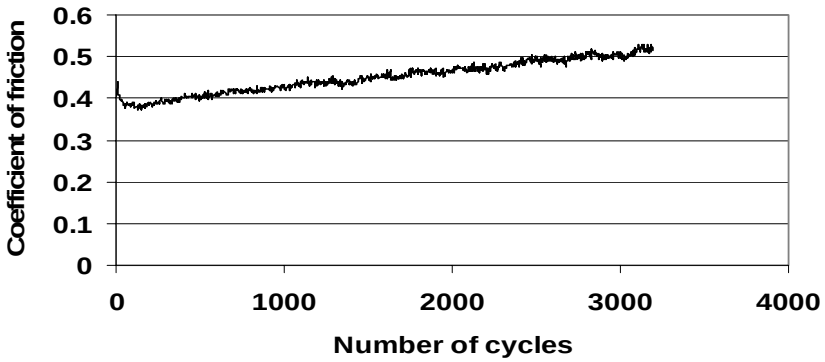

Figure A.3: *Coefficient of friction versus number of sliding cycles for Si/UHMWPE (post heated at 130^{o}C for 20 h after dip-coating) tested at 370 MPa and 0.04-0.08 m s^{-1} sliding velocities.*

A.2.4 Nano-scratch characteristics

Figure A.4 shows the SEM images of scratches of UHMWPE films post-heated at two different temperatures and Figure A.5 shows the variation of penetration depth versus scratching distance during ramp-load scratch testing. The two different films have shown very different scratch resistance. The film post-heated at 130^{o}C is peeled off completely at the beginning of the scratching itself and carried until the end along with the scratching tip; the film is partly delaminated. This is not observed in the case of the film post-heated at a temperature of 100^{o}C. There is a progressive penetration of the tip in the case of the film post-heated at 100^{o}C.

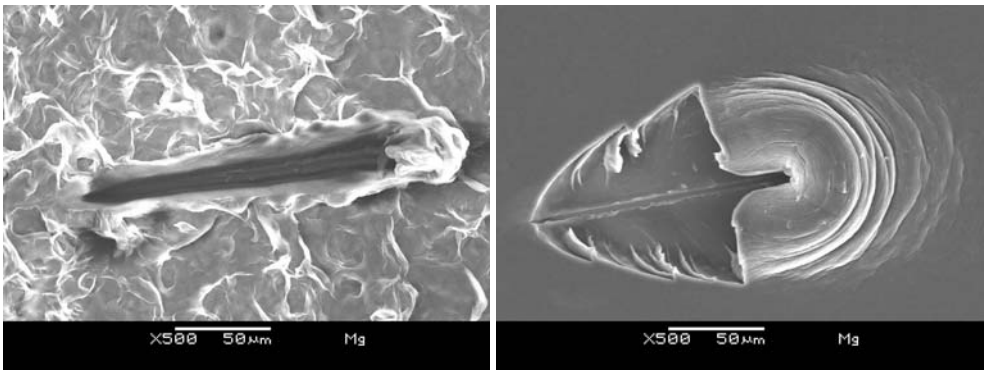

Figure A.4: *SEM images of the ramp load scratches of UHMWPE films post heated at (a) 100^{o}C and (b) 130^{o}C, made using nano-scratch tester.*

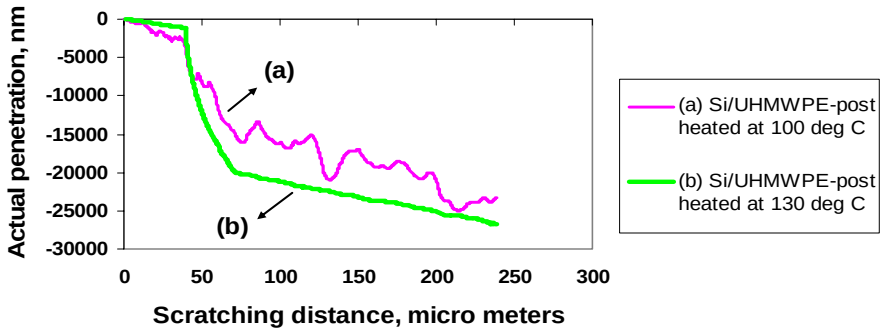

Figure A.5: *Penetration depth versus scratching distance for UHMWPE films post-heated at two different temperatures obtained using nano-scratch tests.*

The nano-scratch results suggest that the film heated at 100^{o}C has better scratch resistance and is more adherent to the Si surface when compared to the one post-heated at 130^{o}C. One possible reason for the less adherence in the case of the film post-heated at 130^{o}C is the de-wetting of the film and weaker bonding with the substrate due to the heating at higher temperature.

A.2.5 Nano-mechanical properties using nano-indentation

Figure A.6 shows a typical load versus displacement curve in a nano-indentation test for UHMWPE film post-heated at 130^{o}C and the average elastic modulus and hardness values are listed in the Table A.1 along with the data corresponding to the film post-heated at 100^{o}C.

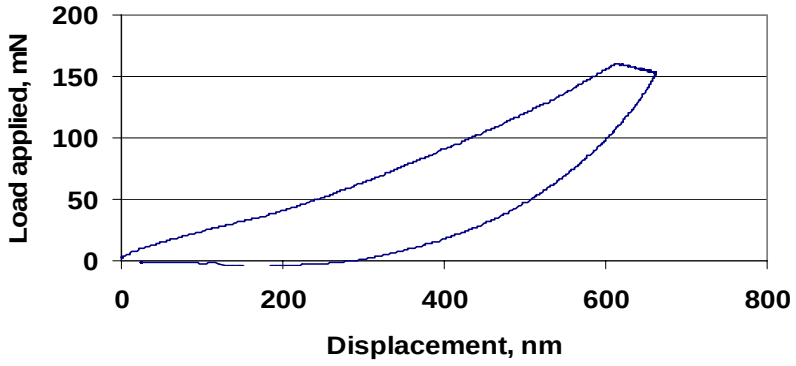

Figure A.6: *A typical load versus displacement curve for Si/UHMWPE heated at 130^{o}C obtained during nano-indentation at a load of 250 µN.*

Table A.1: *Elastic modulus and hardness of the UHMWPE films heated at two different temperatures obtained using nano-indentation characterization.*

Sample	Elastic modulus, GPa	Hardness, GPa
UHMWPE, post-heated at 100^{o}C	3.7	0.3
UHMWPE, post-heated at 130^{o}C	0.12	0.02

Figure A.7 compares the loading curves for both films post-heated at two different temperatures. The data presented in Table A.1 and Figure A.7 suggests that the film heated at 130^{o}C is softer and very complaint when compared to the one heated at 100^{o}C. As we are close to the melting point in the case of 130^{o}C heating, many of the bonds between various molecules might have melted and hence the film became softer and compliant.

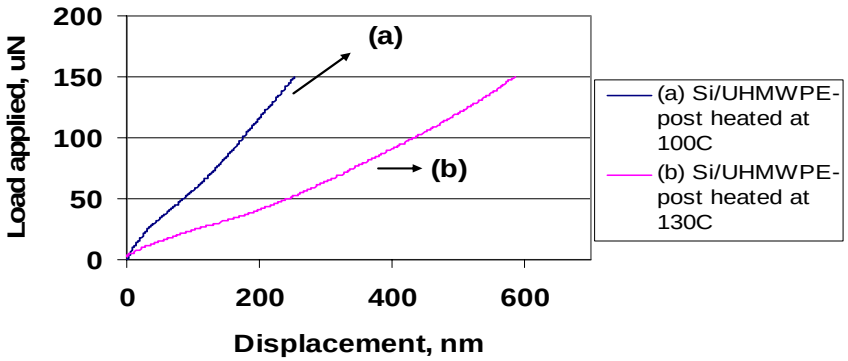

Figure A.7: *Comparison of loading curves for UHMWPE films heated at two different temperatures after dip-coating obtained during nano-indentation at a load of 250 μN.*

As the film heated at 130^{o}C became softer, it has shown high coefficient of friction (Figure A.3) because of an increase in the contact area and more material transfer to the counterface [Bowden and Tabor 1950]. As a result of high coefficient of friction and early generation of the wear debris, the film heated at 130^{o}C has shown lower wear life when compared to that heated at 100^{o}C. The less compliance of the film heated at 130^{o}C also explains the lower scratch resistance (Figure A.5).

A.3 Conclusions

Below are the conclusions from the present study:

1. Post heating temperature after UHMWPE film coating has great influence on the physical, mechanical and tribological properties of the film.

2. A post-heat treatment temperature of 100^{o}C has shown a surface with deep valleys, high scratch resistance, better mechanical properties (high Elastic modulus and hardness) and better tribological properties (low coefficient of friction and high wear durability) when compared to the post-heating temperature of 130^{o}C.

Curriculum vitae

Personal Information

Name:	Satyanarayana Nalam
Nationality:	Indian
Date of birth:	April 14, 1978
Present Address:	Materials Science Division, Department of Mechanical Engineering, National University of Singapore, Singapore-117576
Permanent Address:	Bollavaram (Post), Muppalla (Mandal), Guntur (Dist), Andhra Pradesh, India-522403
E-amil:	g0203714@nus.edu.sg, nsatyam2001@gmail.com

Education

1992-1993:	Secondary School Certificate in Zilla Praza Parishadh High School, Madala, AP, India
1994-1997:	Diploma in Metallurgical Engineering, Government Polytechnic, Visakhapatnam, AP, India
1998-2002:	B. Tech in Metallurgical Engineering, National Institute of Technology (NIT), Warangal, AP, India
2003-2007:	PhD in Department of Mechanical Engineering, NUS, Singapore

Languages

Telugu (native Indian language); English (fluent, both spoken and written)